Wheat improvement for heat and drought stress tolerance

by

Anju Giri

B.S., Tribhuwan University, 2011
M.S., University of Toledo, 2013

AN ABSTRACT OF A DISSERTATION

submitted in partial fulfillment of the requirements for the degree

DOCTOR OF PHILOSOPHY

Department of Agronomy
College of Agriculture

KANSAS STATE UNIVERSITY
Manhattan, Kansas

2019

Abstract

Heat and drought are the major abiotic factors that limit wheat production worldwide. Wheat is one of the important staple crops, so, the production decline due to these factors faces a major challenge in addressing food security. Grain filling in wheat occurs when the temperature is rising, and soil moisture is declining in most wheat growing environment, so there is high demand in breeding wheat for post anthesis heat and drought stress tolerance. However, limited genetic variability in wheat cultivars possess a challenge. The objective of the first study was to screen wild emmer wheat (*Triticum dicoccoides*) for post anthesis heat tolerance and measure physiological traits and yield trait associated with the tolerance. Twenty-one accessions of *Triticum dicoccoides* and four check varieties were screened at optimum temperature (25/19 ^{o}C day/night) and high temperature (35/29 ^{o}C day/night). High temperature decreased flag leaf survival duration, chlorophyll content, and chlorophyll fluorescence more in the wild accessions than in the checks. A few wild accessions were found to be heat tolerant based on the lower heat susceptibility index (HSI) value in seed weight. Therefore, there is a potential for utilizing this genetic variability from the accessions to improve post anthesis heat tolerance in wheat. The maintenance in seed weight might be coming from the mobilization of stored reserve in the stem. The stem reserves are commonly called water-soluble carbohydrates (WSC). WSC accumulated during the vegetative stage, pre-flowering, or right after flowering can be mobilized to assist grain filling when assimilate supply is limited under stress. The second chapter is about the physiological and genetic basis of water-soluble carbohydrates (WSC) concentration during mid-grainfilling stage in wheat. We evaluated 400 diverse winter wheat breeding lines and 30 released varieties in different environments ranging from irrigated to rainfed for WSC concentration. WSC concentration was significantly and positively correlated with the seed

weight, whereas the height was mostly negatively correlated, and we didn't see any relation with heading date. Less decline in grain yield under simulated terminal drought stress was observed in varieties with high WSC content. Further, we identified six significant SNP markers in 7D region significantly associated with the WSC concentration, and each marker explained 4-5% of the variation. On running several genomic selection prediction models on WSC using ridge regression, partial least squares, elastic net, and random forest models and different training population sizes (20%, 40%, 60%, and 80%), the prediction accuracy increased from 0.2 to 0.6. The accuracy increased as a large amount of data was available to train the model, and overall the highest accuracy was observed with the random forest and average of all four models. The accuracy can be further increased with the inclusion of a large number of samples, and multi-year and location testing on WSC. Higher genetic variation, high heritability, and significant positive relation with seed weight make WSC an important trait for selection under post anthesis drought.

In the third study, aerial phenotyping using UAV with a multispectral camera was used to capture the images in three different wave bands: red, green, and near infrared. Normalized Difference Vegetative Index (NDVI) was calculated from red and near infrared bands. NDVI calculated from the aerial imaging during reproductive stages were more correlated with the grain yield than a visual screening of percentage greenness. NDVI measurement during grain filling had the highest significant correlation and explained more than 50% variation in the yield. Lodging was another factor impacting yield explaining about 60% variability in yield. With its wide applicability, aerial phenotyping has the potential for assisting breeders in selecting diverse genotypes and can outperform visual selection.

Wheat improvement for heat and drought stress tolerance

by

Anju Giri

B.S., Tribhuwan University, 2011
M.S., University of Toledo, 2013

A DISSERTATION

submitted in partial fulfillment of the requirements for the degree

DOCTOR OF PHILOSOPHY

Department of Agronomy
College of Agriculture

KANSAS STATE UNIVERSITY
Manhattan, Kansas

2019

Approved by:

Major Professor
Dr. Allan K. Fritz

Copyright

Abstract

Heat and drought are the major abiotic factors that limit wheat production worldwide. Wheat is one of the important staple crops, so, the production decline due to these factors faces a major challenge in addressing food security. Grain filling in wheat occurs when the temperature is rising, and soil moisture is declining in most wheat growing environment, so there is high demand in breeding wheat for post anthesis heat and drought stress tolerance. However, limited genetic variability in wheat cultivars possess a challenge. The objective of the first study was to screen wild emmer wheat (*Triticum dicoccoides*) for post anthesis heat tolerance and measure physiological traits and yield trait associated with the tolerance. Twenty-one accessions of *Triticum dicoccoides* and four check varieties were screened at optimum temperature (25/19 ^{o}C day/night) and high temperature (35/29 ^{o}C day/night). High temperature decreased flag leaf survival duration, chlorophyll content, and chlorophyll fluorescence more in the wild accessions than in the checks. A few wild accessions were found to be heat tolerant based on the lower heat susceptibility index (HSI) value in seed weight. Therefore, there is a potential for utilizing this genetic variability from the accessions to improve post anthesis heat tolerance in wheat. The maintenance in seed weight might be coming from the mobilization of stored reserve in the stem. The stem reserves are commonly called water-soluble carbohydrates (WSC). WSC accumulated during the vegetative stage, pre-flowering, or right after flowering can be mobilized to assist grain filling when assimilate supply is limited under stress. The second chapter is about the physiological and genetic basis of water-soluble carbohydrates (WSC) concentration during mid-grainfilling stage in wheat. We evaluated 400 diverse winter wheat breeding lines and 30 released varieties in different environments ranging from irrigated to rainfed for WSC concentration. WSC concentration was significantly and positively correlated with the seed

weight, whereas the height was mostly negatively correlated, and we didn't see any relation with heading date. Less decline in grain yield under simulated terminal drought stress was observed in varieties with high WSC content. Further, we identified six significant SNP markers in 7D region significantly associated with the WSC concentration, and each marker explained 4-5% of the variation. On running several genomic selection prediction models on WSC using ridge regression, partial least squares, elastic net, and random forest models and different training population sizes (20%, 40%, 60%, and 80%), the prediction accuracy increased from 0.2 to 0.6. The accuracy increased as a large amount of data was available to train the model, and overall the highest accuracy was observed with the random forest and average of all four models. The accuracy can be further increased with the inclusion of a large number of samples, and multi-year and location testing on WSC. Higher genetic variation, high heritability, and significant positive relation with seed weight make WSC an important trait for selection under post anthesis drought.

In the third study, aerial phenotyping using UAV with a multispectral camera was used to capture the images in three different wave bands: red, green, and near infrared. Normalized Difference Vegetative Index (NDVI) was calculated from red and near infrared bands. NDVI calculated from the aerial imaging during reproductive stages were more correlated with the grain yield than a visual screening of percentage greenness. NDVI measurement during grain filling had the highest significant correlation and explained more than 50% variation in the yield. Lodging was another factor impacting yield explaining about 60% variability in yield. With its wide applicability, aerial phenotyping has the potential for assisting breeders in selecting diverse genotypes and can outperform visual selection.

Table of Contents

List of Figures

List of Tables

Acknowledgements

First, my sincere gratitude and appreciation goes to my major advisor Dr. Allan K Fritz for all what he has done for me. His kind and warm gesture always inspire confidence within myself and without his advice and encouragement, I wouldn't be where I am today. Dr. Fritz has been an outstanding mentor and a very motivating person, I am very fortunate to work under his guidance. I am also very grateful to my committee members Drs. Rob Aiken, Krishna Jagadish and Jesse Poland for constant communication, valuable feedback, critical comments, and guidance on my work. Thank you for encouraging me to think creatively. Dr. Aiken's help was phenomenal on working through the aerial imaging chapter.

I feel blessed and thankful to be the part of the K-State Wheat breeding team. Everyone in the team deserves my sincere appreciation for what they have done to complete my work. Shaun Winnie, Andy Auld, Angie Matthews, Marshall Clinesmith, Dr. Cristiano Lemes, Seth Filbert, and all student helpers in Manhattan, Dr. Guorong Zhang and Clayton Seaman from Hays for their constant help on field, lab, and/or greenhouse works. I am also thankful to Ray Duffey and Raenette Martin from NWREC for their help in managing field work in Colby, aerial imagery collection and data extraction. My sincere thanks Dr. Floyd Dowell for his valuable guidance on the NIR part and Tim Todd for the help on the statistical data analysis.

I am forever indebted to my MS advisor Dr. Scott Heckathorn for the motivation he has provided to do better science and the help I have been getting along the way. His encouraging words were instrumental for me to keep moving forward.

Finally, my special appreciation goes to my family and friends abroad and home.

Dedication

I dedicate this work to my family. My proud parents Bharat and Renuka Giri, my sister Sujata and brother Sudip for believing in me and encouraging me every day. Dear Avyn, my son, you are my inspiration to work harder and be better every day. My husband for his constant companionship and support. Although my name is written in the diploma, it's a joint accomplishment of me and my husband, Abhishes Lamsal.

Chapter 1 - Introduction

Origin of Wheat

Modern wheat is an allohexaploid species originating from two independent hybridization events. The first event is thought to have happened 300,000-500,000 years ago between *Triticum uratu* Thumanjan ex Gandilyan (A genome donor) and a relative of *Aegilops speltoides* Tausch (B genome donor) producing a stable and fertile tetraploid species known as *Triticum turgidum* L. (AABB; 2n = 4x = 28) or Emmer wheat. The second hybridization event happened around 9,000 years ago between tetraploid *T. turgidum* and diploid *Aegilops tauschii* Coss. (DD; 2n = 2x = 14) or Goat grass, resulting in modern hexaploid wheat (*Triticum aestivum* L. (AABBDD)) (Curtis et al., 2002; Dvorak et al., 1998; Marcussen et al., 2014). Due to its wide adaptation, higher yield, ease of growing, harvesting and storage, wheat is popular and grown worldwide.

Importance of Wheat

Wheat is the third largest cereal crop after maize and rice in global cereal production (USDA, 2017). With the highest acreage planted in the world, global wheat production was projected to be at 740 million metric tons in 2017 (USDA, 2017). It can be used as a primary food and feed for both human and animal consumption. Wheat is a staple diet for 35% of the population and is a major source of carbohydrate, provides more protein than any other companion crops, and is also an important source of minerals and vitamins. Global wheat consumption per capita is 65 kg/year, supplying nearly 20% of calories and protein (FAOSTAT).

World population is expected to reach 9 billion by 2050 (Gerland et al., 2014). World food production has to be doubled, including cereals, as cereal demand is predicted to increase by 50%. With the current available technologies, the demand is more likely to exceed the

production (FAO, 2002). The two main ways to meet the demand is to expand the area under production or increase production per unit area (Curtis et al., 2002). Most of the world's cultivable land is already in production, the current estimate shows that the 85% increase should be from the land already in cultivation (Borlaug and Dowswell, 2003).

It's clear from past that the increase in production comes from advances in breeding (Curtis et al., 2002). Some of these have already been demonstrated during the green revolution, such as a reduced height, which significantly improved production (Gale et al., 1985). There is a possibility of increasing yield potential, however, it comes as a trade off with tolerance to biotic or abiotic stress (Tack et al., 2014). In most wheat growing areas, grain filling happens around the time the temperature in the atmosphere is rising, and moisture in the soils are declining, therefore, production is impacted mainly by these two abiotic stresses. The effect of heat and drought stress is further exacerbated by the disease pressure during or after flowering, however biotic stresses are beyond the scope of this dissertation. Therefore, we will focus mainly on two abiotic stress after during grain filling, terminal heat, and terminal drought.

Heat and Drought Stress in Wheat

High temperature and low moisture affect wheat in all growing stages, but the effect is more severe and irreversible during reproductive stages, resulting in a large decline in yield (Prasad et al., 2008). Kernel abortion or reduction in kernel growth are the two main reasons for yield decline under stress, as wheat yield is dependent on the number of plants per meter square, seed number per plant, and individual seed weight.

Boyer (1982) analyzed crop insurance usage for several reasons of crop loss and found that there was an 87% decline in US grown wheat, where 94% was due to abiotic stress, mainly heat and drought. In a recent modeling study, Tack et al. (2014) showed a 22% yield reduction

by drought and 11% by warming. Heat and drought stress are hard to distinguish as a stress signal because these are typically confounded, and defense mechanism are very closely related (Reynolds et al., 2007). Heat stress is accompanied by drought stress, and vice versa, in most field environments. The effect of one is usually exacerbated by the other, impacting growth, development, and ultimately yield.

Heat stress and drought stress during mid-grain filling is likely to decrease the seed weight by decreasing grain filling duration, whereas the stress during pollination or fertilization causes abortion of recently fertilized embryos resulting in a decline in seed number (Pradhan et al., 2012; Prasad et al., 2008). The decrease in grain filling duration lowers starch accumulation in grains, reducing the seed size, as starch is the main component in the grain. Though the decreased grain filling duration under stress is generally accompanied by an increase in the rate of grain filling, it cannot compensate for the loss in grain yield (Prasad et al., 2008; Streck, 2005; Yin et al., 2009). In a controlled chamber study by Yin et al. (2009), grain filling duration decreased more than 30%, whereas, the rate increased only 20%, and was therefore unable to ameliorate the loss. Adverse effects of high temperature on grain filling duration have also been reported by Streck (2005), where he showed that even 1^{o}C rise in temperature above 20^{o}C decreases grain filling by more than three days. This leads to the expectation that the average life cycle of the crop could decrease as a result of rising temperatures predicted by IPCC (Allen et al., 2014).

Outline of the Dissertation

Plant breeding over the years has focused on selecting for yield. As a result, modern varieties are high yielding but are less tolerant to heat and drought stress (Tack et al., 2014). Some effects can be partially mitigated by environmental manipulation like irrigation and

fertilizer application. However, these are not practical and possess several economic and ecological limitations, therefore, the genetic resistance/tolerance needs to be identified (Curtis et al., 2002).

The narrow genetic base in modern cultivated wheat is due to an evolutionary bottleneck followed by extensive selection and breeding. Only a few individuals of the donor species are involved in the evolution of modern wheat. Most of the genetic variation in the tetraploid emmer wheat and diploid *Aegilops* is not present in hexaploid wheat. This bottleneck likely resulted in alleles for tolerance being excluded from the common wheat gene pool and variation has likely been further reduced through targeted selection (Haudry et al., 2007). The second chapter of this dissertation highlights the importance of widening genetic diversity. It's is focused on the identification of novel sources of heat stress tolerance from the tetraploid progenitor of wheat. The chapter discusses how these genetic resources could be used to deepen the gene pool of cultivated wheats for greater tolerance to heat stress. This chapter discusses on the source of heat tolerance as well as a physiological mechanism to target for selection.

The third chapter focuses on stem reserves as a potential contributor to grain fill under drought stress. Stem reserves were measured as water-soluble carbohydrates (WSC), and their potential contribution to yield and seed weight under diverse environments are discussed. A simple method of using near infrared spectroscopy, as opposed to the lab analysis of mass samples is presented. Along with the relation of WSC with yield and yield components in diverse varieties, the genetic basis of its accumulation is studied in a set of 400 winter wheat breeding lines. The QTLs significantly associated with the WSC accumulation are identified using association mapping. The pros and cons of genome wide association studies on a trait like WSC

are discussed along with the application of modern plant breeding tool genomic selection to predict WSC based on the genomic data only.

The fourth chapter studies the applicability of aerial phenotyping in the breeding program. The aerial phenotyping platform using a UAV connected with multispectral cameras is presented as an important tool in assisting plant breeders in making selections and predicting yield. The analysis is based on image captured at various growth stages. The appropriate stage(s) that can explain most of the variability in yield are discussed. Along with yield, the study attempts to predict lodging and studies its relation to yield. Superiority of imaging to capture minute variation, as opposed to visual assessment, is discussed in the context of an irrigated environment.

Overall, this dissertation provides the basis for improving wheat for heat and drought stress tolerance. With the need for increasing productivity per unit area of land, this study identified some physiological traits that can be targeted for selection within the ecological and economical limitations. Wheat being a C3 crop, efficient water use should be one of the major targets to address in the future wheat breeding for drought tolerance, and some additional research in increasing canopy productivity on a large-scale need to be addressed in the future.

References

Allen, M.R., Barros, V.R., Broome, J., Cramer, W., Christ, R., Church, J.A., Clarke, L., Dahe, Q., Dasgupta, P., Dubash, N.K., 2014. IPCC fifth assessment synthesis report-climate change 2014 synthesis report.

Borlaug, N.E., Dowswell, C.R., 2003. Feeding a world of ten billion people: a 21st century challenge, in: Proceedings of the International Congress in the Wake of the Double Helix: From the Green Revolution to the Gene Revolution. Citeseer, p. 31.

Boyer, J.S., 1982. Plant productivity and environment. Science 218, 443–448.

Curtis, B.C., Rajaram, S., Gómez, M., 2002. Bread wheat: improvement and production. Food and Agriculture Organization of the United Nations (FAO).

Dvorak, J., Luo, M.-C., Yang, Z.-L., Zhang, H.-B., 1998. The structure of the Aegilops tauschii genepool and the evolution of hexaploid wheat. Theor. Appl. Genet. 97, 657–670. https://doi.org/10.1007/s001220050942

Gale, M. D., Youssefian, S., & Russell, G. E. (1985). Dwarfing genes in wheat. *Progress in plant breeding*, *1*, 1-35.

Gerland, P., Raftery, A.E., Ševčíková, H., Li, N., Gu, D., Spoorenberg, T., Alkema, L., Fosdick, B.K., Chunn, J., Lalic, N., Bay, G., Buettner, T., Heilig, G.K., Wilmoth, J., 2014. World population stabilization unlikely this century. Science 346, 234–237. https://doi.org/10.1126/science.1257469

Haudry, A., Cenci, A., Ravel, C., Bataillon, T., Brunel, D., Poncet, C., Hochu, I., Poirier, S., Santoni, S., Glémin, S., David, J., 2007. Grinding up Wheat: A Massive Loss of Nucleotide Diversity Since Domestication. Mol. Biol. Evol. 24, 1506–1517. https://doi.org/10.1093/molbev/msm077

Marcussen, T., Sandve, S.R., Heier, L., Spannagl, M., Pfeifer, M., Jakobsen, K.S., Wulff, B.B., Steuernagel, B., Mayer, K.F., Olsen, O.-A., 2014. Ancient hybridizations among the ancestral genomes of bread wheat. science 345, 1250092.

Pradhan, G.P., Prasad, P.V.V., Fritz, A.K., Kirkham, M.B., Gill, B.S., 2012. High temperature tolerance in Aegilops species and its potential transfer to wheat. Crop Sci. 52, 292–304.

Prasad, P.V.V., Staggenborg, S.A., Ristic, Z., 2008. Impacts of drought and/or heat stress on physiological, developmental, growth, and yield processes of crop plants. Response Crops Ltd. Water Underst. Model. Water Stress Eff. Plant Growth Process. 301–355.

Reynolds, M.P., Pierre, C.S., Saad, A.S., Vargas, M., Condon, A.G., 2007. Evaluating potential genetic gains in wheat associated with stress-adaptive trait expression in elite genetic resources under drought and heat stress. Crop Sci. 47, 172–189.

Streck, N.A., 2005. Climate change and agroecosystems: the effect of elevated atmospheric CO2 and temperature on crop growth, development, and yield. Ciênc. Rural 35, 730–740. https://doi.org/10.1590/S0103-84782005000300041

Tack, J., Barkley, A., Nalley, L.L., 2014. Heterogeneous effects of warming and drought on selected wheat variety yields. Clim. Change 125, 489–500. https://doi.org/10.1007/s10584-014-1185-1

USDA (2017) World Agricultural Supply and Demand Estimates Report (WASDE). United States Department of Agriculture.

Yin, X., Guo, W., Spiertz, J.H., 2009. A quantitative approach to characterize sink–source relationships during grain filling in contrasting wheat genotypes. Field Crops Res. 114, 119–126. https://doi.org/10.1016/j.fcr.2009.07.013

Chapter 2 - Heat Tolerance Screening of Wild Tetraploid Wheat *Triticum dicoccoides*

Introduction

High temperature is one of the main abiotic stresses limiting wheat production worldwide. Wheat is a temperate cereal, so the rise in temperature affects wheat negatively during all growth stages, impacting yield and yield components (Ferris et al., 1998; Pimentel et al., 2015; Pradhan et al., 2012; Slafer and Rawson, 1994). Porter and Gawith (1999) reviewed 65 articles on the mean minimum, maximum lethal temperatures, base and optimal temperatures for both vegetative and reproductive growth and development and they acknowledged that the temperature range depend on cultivar sensitivity, heat/cold hardening, and other environmental condition. The set of cardinal temperature is different at all growth stages, but the overall growing season cardinal temperature is considered 0^{o}C as minimum temperature, 20-25^{o}C optimum temperature, and 37^{o}C as maximum temperature, beyond which growth ceases (Farooq et al., 2014; Porter and Gawith, 1999 and reference therein). Temperatures above 32^{o}C are likely to cause heat shock at any growth stage, resulting in a severe decline in yield (Cossani and Reynolds, 2012; Djanaguiraman and Prasad, 2014; Tack et al., 2014).

Yield loss during heat stress mainly happens due to decline in seed number by abortion of recently fertilized embryos or reduced seed weight from lower starch accumulation in grain. Heat stress during mid-grain filling is likely to decrease the seed weight by decreasing grain filling duration, whereas the stress during early grain filling (during lag phase) and pollination results in a decline in seed number (Djanaguiraman and Prasad, 2014; Mohammadi, 2012; Pradhan et al., 2012; Prasad et al., 2008a; Stratonovitch and Semenov, 2015). The decreased duration of grain fill under stress is also accompanied by an increase in the rate of grain filling. However, in most

cases, it cannot compensate for the loss (Streck, 2005; Yin et al., 2009). With a 1°C increase in mean temperature, maturity shortens by seven days, grain filling rate increases from 0.9 to 1 mg per day, leading to 15% or more decline in seed weight (Mohammadi, 2012). In a controlled chamber study by Yin et al. (2009), grain filling duration decreased by more than 30%, where the increase in the rate of grain fill was only 20%. The adverse effect of high temperature on grain filling duration has also been reported Streck (2005), where he showed that even 1°C rise in temperature above 20°C decreases grain filling by more than three days. Although, the rise in temperature in the Great Plains might have reduced the risk of late spring freeze damage, the overall effect of warming is negative with an 11% reduction in yield (Tack et al., 2014). With the projected increase in temperature by IPCC (Allen et al., 2014), the average life cycle of the crop could decrease in the future.

Early leaf senescence (mainly flag leaf) is the first sign of damage under terminal heat stress. The flag leaf is an important source for maximum light reception and can contribute 30-50% of the assimilate used for grain fill (Al-Tahir, 2014). Leaf senescence is first initiated by structural change, followed by loss of chlorophyll. Because the chlorophylls are housed in thylakoids, the damage to the thylakoid membrane leads to the decline in chlorophyll pigments (Prasad et al., 2008b; Ristic et al., 2007; Schreiber and Berry, 1977; Talukder, 2013). Since chlorophyll pigments are the main light receptor for assimilation, damage negatively affects light interception. The injury to these receptors can be assessed by the fluorescence emitted by these pigments. When the leaf is exposed to a saturating flash of light, it increases the fluorescence from a ground state (F_o) to a maximum value (F_m). During this period, it completely shuts down the electron accepting mechanism of photosystem II (PSII). The difference in F_m and F_o is known as variable fluorescence (F_v), and the ratio between F_v and F_m can be used to assess the

status of PSII. A lower value of F_v/F_m indicates the damage to the PSII reaction centers (Moffatt et al., 1990).

Plants with the ability to stay green have lower expression of senescence related genes and are more likely to maintain yield under heat stress (Cossani and Reynolds, 2012; Reynolds et al., 2007; Ristic et al., 2007). Chlorophyll content and fluorescence are found to be highly associated, so they can be used for assessing thermotolerance (Djanaguiraman et al., 2010; Ristic et al., 2007). There is a significant body of research in this area targeting wheat cultivars, but only a few studies have focused on wild accessions (Bergkamp, 2016; Green, 2016; McGowan, 2016; Pradhan et al., 2012).

The narrow genetic base in modern cultivated wheat is due to an evolutionary bottleneck. This bottleneck likely resulted in alleles for tolerance being excluded from the common wheat gene pool and variation has likely been further reduced through targeted and controlled breeding (Waines, 1994). Tack et al. (2014) also suggested a tradeoff between high temperature tolerance and yield potential that could negatively affect the level of high temperature tolerance of wheat cultivars in the Great Plains. Additionally, heat tolerance appears to be governed by several genes of small effect, which complicates marker assisted selection (Mason et al., 2011; Talukder et al., 2014; Vijayalakshmi et al., 2010). Lower genetic diversity, coupled with the quantitative nature of this trait, poses a great challenge for wheat improvement for heat stress tolerance.

Genetic diversity can be broadened by exploiting naturally existing variation in wild species (Tanksley and McCouch, 1997). Wild emmer wheat, *Triticum dicoccoides* (2n=4x=28, genome AABB) is the progenitor of both common bread wheat and durum wheat. It has the same genome formula as durum wheat and carries two of the three genomes of modern bread wheat (2n=6x=42, genome AABBDD). It, therefore, serves a central role in wheat evolution and

domestication (Dvorak et al., 1998; Peng et al., 2011). Favorable genetic resources for variety improvement in emmer wheat have been documented in some earlier studies (Çakmak et al., 2004; Khan et al., 2000; Nevo, 2001; Nevo et al., 2013; Xie and Nevo, 2008). It possesses several beneficial traits to humans like high protein content and superior baking quality, disease resistance (yellow stripe rust, stem rust, powdery mildew), abiotic stress tolerance (salinity and drought), nutrient content, herbicide tolerance, wider adaptation, and higher yield (Çakmak et al., 2004; Ji et al., 2008; Marais et al., 2005; Nevo, 2001; Uauy et al., 2005, 2006). Peng et al. (2003) mapped 70 QTLs for 11 domestication traits in a mapping population developed from a cross between T. *dicoccoides* and T. *durum* and found that 18 (24%) of the QTLs were agriculturally beneficial. These favorable alleles, along with other resistance genes in emmer wheat, could make an important contribution to modern wheat improvement.

The wild accessions collected from areas that are prone to high temperature may possess the natural ability to withstand heat stress. Plants adapted to the Mediterranean type of climate are more likely to have tolerance to terminal heat stress (Asseng et al., 2015), which can be exploited in breeding wheat for high-temperature tolerance. Some studies have been carried out in the *Aegilops* species for their ability to tolerate heat stress during reproductive stages (Green, 2016; Pradhan et al., 2012). Pradhan et al. (2012) screened accessions of five different species of *Aegilops* and found some heat tolerant accessions among *Aegilops speltoids* and *Aegilops geniculata*. Green (2016) screened accessions of *Aegilops kotschyi* and *Aegilops peregrina* and identified some accessions that could carry useful genetic variation of high temperature tolerance. However, very few studies have been conducted in emmer wheat to evaluate post anthesis heat stress tolerance (Nevo, 2001; Waines, 1994). In this study, we evaluated heat tolerance of 21 wild emmer wheats of diverse origin and four common wheat varieties for post

anthesis heat tolerance. Chlorophyll content, the efficiency of photosystem II, flag leaf duration, and individual kernel weight were measured for all entries under both stress and optimal conditions. Tolerance was evaluated based on the ability to retain chlorophyll content, stability of photosystem II, and heat susceptibility index for individual grain weight.

Materials and Methods

Plant materials and experimental condition

Twenty-one accessions of *Triticum dicoccoides* chosen based on diverse geographic origin and four check varieties were used in the study (Table 2-1). The seeds of T. *dicoccoides* were obtained from National Plant Germplasm Collection. Among the four check varieties used in the experiment, Ventnor and Jefimija were considered to be highly tolerant (Narayanan et al., 2015; Ristic et al., 2007; Yang et al., 2002a) and U1275 and Jagger were intermediate (Talukder et al., 2014). The pedigree for U1275, Jagger, and Jefimija are TAM-107 *3/TA 2460 (*Aegilops tauschii*), KS82W418/Stephens and Sremka-1/Proteinka[4361]; NS-63-25/NS-3722[3578] respectively. The pedigree of Ventnor is not known. These four checks were also included in the study by Green (2016).

Seeds were sown in 4-cm-deep trays containing Sunshine Metro Mix 360 potting soil (Hummert International, Topeka, KS) and placed on a greenhouse bench maintained at 21/15°C (day/night). After two weeks, the seedlings were moved to a chamber maintained at 4°C and 8 h photoperiod and vernalized for 6 weeks. Following vernalization, two seedlings of each genotype were transplanted into twelve 24cm long, 10cm wide, 1.6-L volume pots (Stuewe and Sons, Corvallis, OR) using commercial growing mix Sunshine Metro Mix 360 potting soil (Hummert International, Topeka, KS). After seedling establishment, seedlings were thinned to one plant per pot, and each pot was treated with Marathon systemic granular insecticide (1% imidacloprid, 1–

[(6–Chloro– 3–pyridinyl)methyl]–N–nitro–2–imidazolidinimine)] (Hummert International, Topeka, KS) at a rate of 1.2 g per pot to control sucking insect infestation. After 25 days, each pot was fertilized with 100ml of Peters professional plant starter 9:45:15 (Hummert International, Earth City, MO) diluted at the rate of 1 tablespoon per gallon. Two weeks after first application, plants were supplemented with fertilizer solution containing a mixture of Peters professional mix 20:20:20 (Hummert International, Earth city, MO) and urea to maintain 250 ppm of N, 200 ppm P, and 200 ppm K. Two subsequent applications of this solution were applied at two weeks' interval after the first application. Ambient light in the green house was supplemented with artificial lights that is approximately 200 µM $m^{-2}s^{-1}$. Pots were arranged in completely randomized design and rotated every two weeks to minimize positional effects. Plants were well-watered to avoid water-stress and supported by a bamboo stake to avoid lodging at jointing stage (Feekes 6) (Large, 1954). Anthesis date was determined when the anther extrudes from the ear in the main tiller. The main tiller was tagged for all physiological measurements.

Ten days after anthesis (DAA), three pots of each genotype were randomly transferred to two sets of growth chambers (Conviron PGR15 chambers with CMP 6050 controllers) maintained at high temperature (HT) 35/29 °C (day/night) or optimum temperature (OT) 25/19 °C (day/night). The temperature treatment was similar to the treatment adopted in Green (2016) and Pradhan et al (2012). The photoperiod was 16 h, and photon flux density (400 to 700 nm) provided by cool fluorescent lamps was around 600 µmol $m^{-2}s^{-1}$ at the top of the plant canopy in both chambers. The light and temperature were increased in a sinusoidal fashion with the maximum lasting for six hours during the treatment period. The lights were turned on at 6 am in the morning to 12.5% of the maximum for two hours and hourly increased to 25%, 50%, 75%

and finally to 100% of the full photon flux density by 12 pm until 6pm, after which it was reduced to 75% and decreased in the same fashion. Plants were grown in condition mentioned above for 15 days and moved back to the greenhouse on the 16th day. All heads of T. *dicoccoides* were covered with lightweight waxy crossing bag (Hummert International, Topeka, KS) during mid grain fill to prevent loss of spikelet due to shattering.

Chlorophyll content and chlorophyll fluorescence

Chlorophyll content and chlorophyll fluorescence were measured on the same recently fully expanded flag leaf of the main tiller between 11:00 and 16:00 h. Measurements were taken before transferring them to the temperature treatment and continued every alternate day until the death of flag leaf. Chlorophyll content was measured using a self-calibrating chlorophyll meter SPAD (Soil Plant Analytical Device) (Konica-Minolta SPAD 502 Plus) in three different parts of the leaves: base, midpoint, and tip of the adaxial surface of the flag leaf and the values were averaged together. The average value was used for further comparison and slope was calculated every alternate day measurement using the value. The days to minimum slope was expressed as senescence. Chlorophyll fluorescence parameters were measured at the base of the same leaf, near the culm, using a hand-held fluorimeter (Optisciences OS-30P, Hudson, New Hampshire, USA). The minimum fluorescence (F_o) and maximum fluorescence (F_m) were measured after 15-20 minutes of dark adaptation by placing insulated clips on the base of the leaf. The maximum quantum yield of PSII was calculated as the photochemical efficiency of photosystem II given by the ratio of variable fluorescence, F_v (the difference between F_m and F_o) to maximum fluorescence, F_m.

Flag leaf duration under heat stress (FLD)

The flag leaf of wheat is the main source of assimilates, contributing 30-50% of photosynthesis. Therefore, flag leaf survival is important to produce enough assimilate to support grain filling. Days of flag leaf survival under heat stress was calculated as the total number of days from the temperature treatment (10 DAA) to flag leaf death (the point at which no physiological measurement can be taken). The flag leaf death was determined from the visual observation further confirmed with the SPAD reading less than 20.

Heat susceptibility index (HSI) on individual kernel weight

Individual Kernel weight (IKW) was calculated by dividing the total kernel weight by the number of kernels in each plant. Heat Susceptibility Index for IKW was calculated using the formula by Fischer and Maurer (1978):

$$HSI = \frac{\left(1 - \frac{Y_h}{Y_o}\right)}{\left(1 - \frac{X_h}{X_o}\right)}$$

Where,

Y_h = average kernel weight of each genotype under heat stress

Y_o = average kernel weight of each genotype under optimum temperature

X_h = average kernel weight of all genotypes under heat stress

X_o = average kernel weight of all genotypes under optimum temperature

Statistical analysis

The experimental design was a completely randomized split-plot design, where the temperature was the main plot factor and genotype was the subplot factor. The growth chambers were the experimental unit for temperature treatment with two replicates of each temperature treatment. Each chamber had three replicate plants per genotype. Genotype, temperature

treatment, and their interaction were analyzed as fixed effects. All analysis was performed in SAS 9.4 (SAS Institute) using proc mixed and significance at 0.05 level of probability.

Results and Discussion

Flag leaf survival under heat stress: Flag leaf duration (FLD)

The flag leaf duration is the number of days the flag leaf of the main tiller survived after the onset of treatment at 10 DAA. The flag leaf of all the wild accessions died before the completion of treatment, even in optimum temperature, which could be related to the shorter life cycle of these accessions. The short life cycle at the reproductive stage may be due to hot and dry weather that characterizes the native habitat of these accessions. Overall, the survival duration ranged from 12-24 days after anthesis. It is possible these genotypes had already assimilated the carbohydrate required by leaf at that time. The excess of carbohydrates synthesized in the leaves are stored various plant parts, but mainly on the stem, collectively known as stem reserve or water-soluble carbohydrates (Blum, 1998). Further studies to evaluate water-soluble carbohydrate concentrations would be required to address this question.

The ANOVA result showed significant interaction between genotype and treatment on FLD (Table 2-2). The significant interaction suggests a differential response of genotypes to the temperature treatment, i.e., the effect of temperature on FLD depends on the genotypes and vice versa. Only four genotypes, PI 467005, 470978, 479777, and 466962 were able to maintain similar FLD under heat stress relative to their companion control plants (Table 2-3). In addition, PI 470978 and 479777 had the highest duration of flag leaf survival among wild accessions at approximately 24 days after anthesis. The flag leaves of PI 538699 and PI 466953 also survived for 24 days after anthesis in control but died significantly earlier under stress conditions. Only

the flag leaf of two tolerant checks, Ventnor and Jefimija, survived the entire duration of treatment and showed no significant difference between the two treatments.

Chlorophyll content and chlorophyll fluorescence (F_v/F_m)

The fluorescence (F_v/F_m) and chlorophyll content were used as an indirect measure of photosynthetic efficiency in wheat. These two measurements were found to be highly and significantly correlated in wheat with the highest correlation after four days of heat stress (Table 2-4 and Figure 2-1). High significant correlation between fluorescence and chlorophyll content means that SPAD measurement can be an effective surrogate for variable fluorescence. SPAD measurements are quick and easy compared to the fluorescence measurement that requires application of clip to the leaf to provide dark adaptation of leaf for 20 minutes, which limits the number of plants screened in the given duration. SPAD can, therefore, be used for screening large sets of material evaluated in a breeding program. Similar results were also observed in wheat cultivars by Ristic et al. (2007), but has not been reported in wild genotypes. One important consideration when working with wild genotypes is that they often have much smaller leaves. This trait makes more difficult to use the clips for variable fluorescence measurements and results in SPAD measurement being of greater practical value (Green, 2016; Pradhan et al., 2012). The high correlation between SPAD and F_v/F_m suggests similar genetic and physiological control for both of these traits (Ristic et al., 2007; Talukder et al., 2014).

Heat stress resulted in a decline in both chlorophyll content and chlorophyll fluorescence, however, the decline was greater on wild accessions compared to the checks (Figure 2-2). The checks were able to maintain chlorophyll for a longer duration compared to the wild accessions in both treatments. The result on the check varieties is presented separately in Figure 2-3. Both the chlorophyll content and chlorophyll fluorescence were significantly lower

in Jagger compared to the other three checks in the study. Jagger was found to be more heat susceptible than the variety Ventnor also in reported in Green (2016) and Talukder (2014).

Since the flag leaf of more than 30% of the wild accessions died before ten days of heat stress, the effect was analyzed for five days after heat stress (Table 2-5). The wild accessions behaved differently than the selected varieties, so the results were analyzed for wild accessions only. Most of the accessions were able to maintain leaf chlorophyll content as high as optimum condition after five days of heat stress except for three accessions PI 470978, PI 538656, and PI 538719. However, the fluorescence significantly declined in eight accessions under heat stress. The flag leaf of accession number 470986 died after two to four days of transferring to the chamber in both treatments, so it was eliminated from the analysis.

The differential response of genotypes suggests the presence of genetic variation for tolerance to heat stress among these genotypes. The genotypes able to retain chlorophyll content for longer duration were the same genotypes with longer duration of flag leaf survival under heat stress. The Chlorophyll content reached maximal decline at or around the time of flag leaf death, as shown in the higher and significant positive correlation between the maximum negative slope and the time of the death of flag leaf in Figure 2-4. None of the wild accessions were superior to heat tolerant checks for green leaf characteristics such as flag leaf survival duration, chlorophyll content and fluorescence measurement under heat stress and control. This suggests the wild genotypes are programmed for earlier senescence. Some accessions retained green leaf area under stress for nearly as long as under optimal conditions. It is likely the short grain fill period of these materials is an evolutionary adaptation to their native environment. They might have a shorter life cycle to avoid or escape the heat stress later in the growing season as heat escape is one way to avoid post anthesis heat tolerance in plants in Mediterranean environments

(Shavrukov et al., 2017). It is unclear how well any green leaf duration traits from *T. dicoccoides* will function when transferred to *T. aestivum*. This would largely depend on whether the genes responsible for maintaining a full grain fill cycle under heat stress also influence phenology. It is speculative, but it seems likely that accessions of *T. dicoccoides* that retain photosynthetic capacity under heat stress conditions could be useful genetic resources for germplasm development in *T. aestivum*.

Individual kernel weight (IKW) and heat susceptibility index (HSI)

Kernel weight was used to calculate HSI as a measure of heat tolerance. The genotypes with HSI less than 1 were considered heat tolerant, where the genotypes with HSI<0.5 were highly tolerant and 0.5-1 were considered moderately tolerant. HSI not only accounts for the variation of genotypes in the trait measured, it also indicates the performance of genotypes under heat stress. It represents a relative decline in seed weight under post anthesis high temperature (Cao et al., 2015). Therefore, it can be used to measure relative stress injury between genotypes. HSI is widely used to assess heat tolerance screening in wheat cultivars as well as wild accessions (Cao et al., 2015; Pradhan et al., 2012; Viswanathan and Khanna-Chopra, 2001; Yang et al., 2002b).

Along with FLD, we observed a significant interaction of genotypes and treatment for IKW (Table 2-2). Further slicing the temperature effect by genotype, only six genotypes (PI 466977, PI 466953, PI 467024, PI 538699, PI 554584 and PI 538719) were able to maintain kernel weight under heat stress with no significant difference between two treatments (Table 2-3). These six genotypes were also considered to be relatively heat tolerant based on the lower HSI values as presented in the same table, for this set of germplasm.

HSI ranged from 0.018 to 1.744. The low and high HSI values were observed for PI 466977 and PI 466998, respectively (Table 2-6 and Figure 2-5). Interestingly, both of these genotypes were collected from the same geographical location (Table 2-1). Overall, the correlation between HSI and altitude at which the accession was collected was not significant. We had hypothesized that accessions collected at lower altitude may be more likely to be heat tolerant as these environments should be relatively warmer. It is possible that the failure to identify a correlation between heat tolerance and altitude of origin is due to the relatively few genotypes used in the study. We do note that all tolerant and moderately tolerant genotypes, based on HSI values, were collected below 74m altitude, with the exception of PI 470978 (HSI of 0.99).

Three genotypes PI 466977, PI 466953, PI 467024, were found to be highly heat tolerant based on their HSI values of less than 0.5. These genotypes also had no significant difference in IKW between heat stress and control treatments. Similarly, nine genotypes PI 538699, PI 466962, PI 538681, PI 467005, PI 554584, PI 479781, PI 538719, PI 466969, and PI 470978 were found to be moderately tolerant with HSI values ranging from 0.5 to 1. Among these moderately tolerant genotypes, only three genotypes PI 554584, PI 538699 and PI 538719 didn't have significant differences in IKW between the two treatments. The kernel weights for all three of these accessions were very low (less than 20mg) (Table 2-6). The kernel weight significantly declined in all four checks used in the experiment with HSI values close to 1 or higher than 1.

HSI of individual kernel weight was used to compare genotypic differences as well as the stability of the genotypic performance under heat stress. While HSI is an important tool to screen heat tolerance among similar kinds of species but care must be used in the interpretation of HSI. HSI only accounts for the performance under heat stress, but it doesn't account for the relative

kernel size of the genotypes. The IKW for T. *dicoccoides* accessions ranged from 0.015 to 0.044g under control condition. The three control checks Jefimija, U1275, and Ventnor, had similar kernel weights of 0.044, 0.044 and 0.046 grams, respectively. Their HSI values also fell in a close range at 1.180, 1.113 and 1.077, respectively. On the other hand, Jagger had a lower kernel size at 0.036 g and a relatively lower HSI 0.975 compared to three other checks. The genotypes with smaller seeds will have less to lose under heat stress compared to the genotypes with larger seed. Also, the smaller seeded genotypes require less assimilates to fill small seeds so lower impact from heat might have been observed in these genotypes. Therefore, HSI can be used as a tool but should also be interpreted in the context of the experiment. In the context of this experiment, larger kernels are generally preferred to smaller ones. Among the three highly tolerant genotypes, based on the kernel size PI 467024 may be of more value for heat tolerance compared to PI466977 or PI466953, even though they have a comparatively lower HSI value.

Heat tolerance as an integrated measure

Generally, the genotypes able to maintain chlorophyll content under longer duration are expected to maintain higher yield under heat stress as discussed in Reynolds et al. (2007). However, in our study, the genotypes able to maintain flag leaf characteristic of the main tiller and those with favorable HSI for kernel weight were mostly mutually exclusive except for three genotypes (PI466962, PI467005, and PI470978). These three genotypes were moderately tolerant based on the HSI value of 0.5-1, and were able to maintain FLD, F_v/F_m, and/or chlorophyll content. However, the highly tolerant genotypes were not able to maintain the flag leaf characteristics, therefore, greater focus on stay green may cause one to dismiss genotypes that maintain higher yield due to stem reserve translocation. Reserve translocation process depends on the complex relation between carbohydrate synthesized by green leaves (source

strength) *vs* the grain filling requirement (sink strength) (Shi et al., 2016). Blum (1998) showed that the reserves in the stem could contribute up to 60% of the grainfill under the stressful condition and 20% under normal condition. Therefore, plants with longer duration of green leaf may not always lead to higher grain weight. Grain fill is a complex process. Maintenance of the ability to photosynthesize is important, but it is also known that starch synthesis in wheat is temperature sensitive (Keeling et al., 1993; Prakash et al., 2009; Tian et al., 2018). These traits should, therefore, be viewed as important components of heat tolerance and should not be thought of in isolation from the entire grain fill process. It may be those lines with superior HSI for kernel weight are better as translocation and deposition of resources in the grain. These lines may be candidates for having more heat stable forms of soluble starch synthase. Stay green has been the primary focal point of most published reports on heat tolerance of wheat and its relatives but reliance solely on green leaf traits may not provide a comprehensive understanding of the mechanisms necessary to develop wheat varieties with robust tolerance to heat stress. In the context of this experiment, further research with a large number of genotypes and more replicates is required before reaching a definitive conclusion.

Lower survival of flag leaf and higher maintenance of kernel characteristics in most of these wild accessions suggests that these wild genotypes are putting more effort in seed fill than the green leaf duration or green leaf characteristics. The higher fluorescence and chlorophyll measurements are often not resulting in stable seed weight means that some other mechanisms are at play beyond simple maintenance of chlorophyll content. These accessions are wild species and were not exposed to artificial selection. Therefore, they are likely well adapted to produce viable seed rather than maximize production of grain. These genotypes, when exposed to high temperature, might have genetic ability to utilize stored reserves that might lead to more stable

kernel weight, leading to lower heat susceptibility index values. This is more relevant when we are looking at the post-anthesis heat tolerance since most wheat growing areas are likely to experience post anthesis heat stress. The stem reserve accumulation is mostly a genetic characteristic. Most accumulation occurs before anthesis and can buffer grain filling under stress (Rebetzke et al., 2008; Ruuska et al., 2006). Our results also showed that some wild accessions might have the good buffering capacity. However, more research is required to understand the storage and translocation of water-soluble carbohydrates in these materials before reaching a solid conclusion. Testing the more promising materials under field conditions is warranted as direct translation from growth chamber to field results is not guaranteed.

High temperature stress negatively impacted flag leaf characteristics and yield components. Both the day and night temperature in our high temperature treatment are higher than the optimum temperature. Therefore, the effect could be due to high day time temperature, night time temperature or both. Along with day time temperature, night time temperatures are projected to increase in the future. Further, the minimum night temperature is likely to increase much faster than the maximum day time temperature (Alexander et al., 2006; Sillmann et al., 2013). Both high day and night temperature produce the similar effect on yield and physiological traits, but the effects could be more pronounced and detrimental under high day and night temperature. The higher rate of reduction in photosynthesis, increase in respiration rate and carbon loss has been reported in wheat and other species (Giri et al., 2017; Heckathorn et al., 2013; Impa et al., 2018). Therefore, its crucial to take an account of both high day and night temperature for breeding for high temperature tolerance.

Summary and Conclusions

Assessment of post-anthesis heat tolerance was carried out in 21 wild accessions of emmer wheat. Post-anthesis heat stress, also known as terminal heat stress is more likely to happen in wheat growing areas in the world and it's one of the main limiting factors in wheat production. Incorporation of wild accessions will contribute to breeding for terminal heat stress tolerance and also contribute towards widening the genetic diversity in the crossing material.

Triticum dicoccoides shares the A and B genomes with modern cultivated common wheat, so high-temperature tolerance characteristics identified in this study could be utilized in the wheat breeding program to develop high yielding cultivars with improved heat tolerance. Three accessions (PI 466977, PI 466953, PI 467024) were identified as highly tolerant based on HSI values of less than 0.5 for kernel weight. Three moderately tolerant genotypes (PI466962, PI467005, and PI470978) were also able to maintain flag leaf under heat stress. The lines satisfying the criteria are check marked in the Table 2-7. The highly tolerant genotypes will be used in a germplasm development program to assess the value of these materials to contribute to greater heat tolerance in elite wheat varieties. Further research with a large number of genotypes is also warranted to determine if there are accessions more tolerant than the accessions used in this study.

References

Alexander, L.V., Zhang, X., Peterson, T.C., Caesar, J., Gleason, B., Tank, A.M.G.K., Haylock, M., Collins, D., Trewin, B., Rahimzadeh, F., Tagipour, A., Kumar, K.R., Revadekar, J., Griffiths, G., Vincent, L., Stephenson, D.B., Burn, J., Aguilar, E., Brunet, M., Taylor, M., New, M., Zhai, P., Rusticucci, M., Vazquez-Aguirre, J.L., 2006. Global observed changes in daily climate extremes of temperature and precipitation. J. Geophys. Res. Atmospheres 111. https://doi.org/10.1029/2005JD006290

Allen, M.R., Barros, V.R., Broome, J., Cramer, W., Christ, R., Church, J.A., Clarke, L., Dahe, Q., Dasgupta, P., Dubash, N.K., 2014. IPCC fifth assessment synthesis report-climate change 2014 synthesis report.

Al-Tahir, F.M., 2014. Flag leaf characteristics and relationship with grain yield and grain protein percentage for three cereals. J. Med. Plants Stud. 2, 01–07.

Asseng, S., Ewert, F., Martre, P., Rötter, R.P., Lobell, D.B., Cammarano, D., Kimball, B.A., Ottman, M.J., Wall, G.W., White, J.W., 2015. Rising temperatures reduce global wheat production. Nat. Clim. Change 5, 143.

Bergkamp, B.L., 2016. Physiological and agronomic characterization of post-flowering heat stress in winter wheat. Kansas State University.

Blum, A., 1998. Improving wheat grain filling under stress by stem reserve mobilisation. Euphytica 100, 77–83.

Cao, X., Mondal, S., Cheng, D., Wang, C., Liu, A., Song, J., Li, H., Zhao, Z., Liu, J., 2015. Evaluation of agronomic and physiological traits associated with high temperature stress tolerance in the winter wheat cultivars. Acta Physiol. Plant. 37, 90.

Cossani, C.M., Reynolds, M.P., 2012. Physiological traits for improving heat tolerance in wheat. Plant Physiol. 160, 1710–1718.

Djanaguiraman, M., Prasad, P.V., 2014. High temperature stress, in: Plant Genetic Resources and Climate Change (CABI). pp. 201–220.

Djanaguiraman, M., Prasad, P.V., Seppanen, M., 2010. Selenium protects sorghum leaves from oxidative damage under high temperature stress by enhancing antioxidant defense system. Plant Physiol. Biochem. 48, 999–1007.

Dvorak, J., Luo, M.-C., Yang, Z.-L., Zhang, H.-B., 1998. The structure of the Aegilops tauschii genepool and the evolution of hexaploid wheat. Theor. Appl. Genet. 97, 657–670. https://doi.org/10.1007/s001220050942

Farooq, M., Hussain, M., Siddique, K.H., 2014. Drought stress in wheat during flowering and grain-filling periods. Crit. Rev. Plant Sci. 33, 331–349.

Ferris, R., Ellis, R.H., Wheeler, T.R., Hadley, P., 1998. Effect of high temperature stress at anthesis on grain yield and biomass of field-grown crops of wheat. Ann. Bot. 82, 631–639.

Fischer, R.A., Maurer, R., 1978. Drought resistance in spring wheat cultivars. I. Grain yield responses. Aust. J. Agric. Res. 29, 897–912.

Giri, A., Heckathorn, S., Mishra, S., Krause, C., 2017. Heat stress decreases levels of nutrient-uptake and-assimilation proteins in tomato roots. Plants 6, 6.

Green, A.J., 2016. Abiotic stress tolerance from the tertiary gene pool of common wheat (PhD Thesis). Kansas State University.

Heckathorn, S.A., Giri, A., Mishra, S., Bista, D., 2013. Heat stress and roots. Clim. Change Plant Abiotic Stress Toler. 109–136.

Impa, S.M., Sunoj, V.S.J., Krassovskaya, I., Bheemanahalli, R., Obata, T., Jagadish, S.V.K., 2018. Carbon balance and source-sink metabolic changes in winter wheat exposed to high night-time temperature. Plant Cell Environ. https://doi.org/10.1111/pce.13488

Keeling, P.L., Bacon, P.J., Holt, D.C., 1993. Elevated temperature reduces starch deposition in wheat endosperm by reducing the activity of soluble starch synthase. Planta 191, 342–348. https://doi.org/10.1007/BF00195691

Large, E.C., 1954. Growth stages in cereals illustration of the Feekes scale. Plant Pathol. 3, 128–129.

Mason, R.E., Mondal, S., Beecher, F.W., Hays, D.B., 2011. Genetic loci linking improved heat tolerance in wheat (Triticum aestivum L.) to lower leaf and spike temperatures under controlled conditions. Euphytica 180, 181–194.

McGowan, J., 2016. Generation of T. aestivum x Ae. speltoides doubled amphiploids for future use in heat tolerance research, and analysis of their clonality (Thesis). Kansas State University.

Moffatt, J.M., Sears, R.G., Paulsen, G.M., 1990. Wheat High Temperature Tolerance during Reproductive Growth. I. Evaluation by Chlorophyll Fluorescence. Crop Sci. 30, 881–885. https://doi.org/10.2135/cropsci1990.0011183X003000040024x

Mohammadi, M., 2012. Effects of kernel weight and source-limitation on wheat grain yield under heat stress. Afr. J. Biotechnol. 11, 2931–2937.

Narayanan, S., Tamura, P.J., Roth, M.R., Prasad, P.V.V., Welti, R., 2015. Wheat leaf lipids during heat stress: I. High day and night temperatures result in major lipid alterations. Plant Cell Environ. 39, 787–803. https://doi.org/10.1111/pce.12649

Nevo, E., 2001. Genetic resources of wild emmer, Triticum dicoccoides, for wheat improvement in the third millennium. Isr. J. Plant Sci. 49, 77–92.

Peng, J., Ronin, Y., Fahima, T., Röder, M.S., Li, Y., Nevo, E., Korol, A., 2003. Domestication quantitative trait loci in Triticum dicoccoides, the progenitor of wheat. Proc. Natl. Acad. Sci. 100, 2489–2494.

Peng, J., Sun, D., Nevo, E., 2011. Wild emmer wheat,'Triticum dicoccoides', occupies a pivotal position in wheat domestication process. Aust. J. Crop Sci. 5, 1127.

Pimentel, A.J.B., Rocha, J.R. do A.S., Souza, M.A. de, Ribeiro, G., Silva, C.R., Oliveira, I.C.M., 2015. Characterization of heat tolerance in wheat cultivars and effects on production components. Rev. Ceres 62, 191–198.

Porter, J.R., Gawith, M., 1999. Temperatures and the growth and development of wheat: a review. Eur. J. Agron. 10, 23–36.

Pradhan, G.P., Prasad, P.V.V., Fritz, A.K., Kirkham, M.B., Gill, B.S., 2012. High temperature tolerance in Aegilops species and its potential transfer to wheat. Crop Sci. 52, 292–304.

Prakash, P., Kumari, A., Singh, D.V., Pandey, R., Sharma-Natu, P., Ghildiyal, M.C., 2009. Starch synthase activity and grain growth in wheat cultivars under elevated temperature: a comparison of responses. Indian J Plant Physiol 14, 364–369.

Prasad, P.V.V., Pisipati, S.R., Ristic, Z., Bukovnik, U., Fritz, A.K., 2008a. Impact of nighttime temperature on physiology and growth of spring wheat. Crop Sci. 48, 2372–2380.

Prasad, P.V.V., Staggenborg, S.A., Ristic, Z., 2008b. Impacts of drought and/or heat stress on physiological, developmental, growth, and yield processes of crop plants. Response Crops Ltd. Water Underst. Model. Water Stress Eff. Plant Growth Process. 301–355.

Rebetzke, G.J., Van Herwaarden, A.F., Jenkins, C., Weiss, M., Lewis, D., Ruuska, S., Tabe, L., Fettell, N.A., Richards, R.A., 2008. Quantitative trait loci for water-soluble carbohydrates and associations with agronomic traits in wheat. Aust. J. Agric. Res. 59, 891–905.

Reynolds, M.P., Pierre, C.S., Saad, A.S., Vargas, M., Condon, A.G., 2007. Evaluating potential genetic gains in wheat associated with stress-adaptive trait expression in elite genetic resources under drought and heat stress. Crop Sci. 47, S–172.

Ristic, Z., Bukovnik, U., Prasad, P.V., 2007. Correlation between heat stability of thylakoid membranes and loss of chlorophyll in winter wheat under heat stress. Crop Sci. 47, 2067–2073.

Ruuska, S.A., Rebetzke, G.J., Herwaarden, A.F. van, Richards, R.A., Fettell, N.A., Tabe, L., Jenkins, C.L.D., 2006. Genotypic variation in water-soluble carbohydrate accumulation in wheat. Funct. Plant Biol. 33, 799–809. https://doi.org/10.1071/FP06062

Schreiber, U., Berry, J.A., 1977. Heat-induced changes of chlorophyll fluorescence in intact leaves correlated with damage of the photosynthetic apparatus. Planta 136, 233–238.

Shavrukov, Y., Kurishbayev, A., Jatayev, S., Shvidchenko, V., Zotova, L., Koekemoer, F., de Groot, S., Soole, K., Langridge, P., 2017. Early flowering as a drought escape mechanism in plants: How can it aid wheat production? Front. Plant Sci. 8, 1950.

Shi, H., Wang, B., Yang, P., Li, Y., Miao, F., 2016. Differences in sugar accumulation and mobilization between sequential and non-sequential senescence wheat cultivars under natural and drought conditions. PLOS ONE 11, e0166155. https://doi.org/10.1371/journal.pone.0166155

Sillmann, J., Kharin, V.V., Zwiers, F.W., Zhang, X., Bronaugh, D., 2013. Climate extremes indices in the CMIP5 multimodel ensemble: Part 2. Future climate projections. J. Geophys. Res. Atmospheres 118, 2473–2493. https://doi.org/10.1002/jgrd.50188

Slafer, G.A., Rawson, H.M., 1994. Sensitivity of wheat phasic development to major environmental factors: a re-examination of some assumptions made by physiologists and modellers. Funct. Plant Biol. 21, 393–426. https://doi.org/10.1071/pp9940393

Stratonovitch, P., Semenov, M.A., 2015. Heat tolerance around flowering in wheat identified as a key trait for increased yield potential in Europe under climate change. J. Exp. Bot. 66, 3599–3609. https://doi.org/10.1093/jxb/erv070

Streck, N.A., 2005. Climate change and agroecosystems: the effect of elevated atmospheric CO2 and temperature on crop growth, development, and yield. Ciênc. Rural 35, 730–740. https://doi.org/10.1590/S0103-84782005000300041

Tack, J., Barkley, A., Nalley, L.L., 2014. Heterogeneous effects of warming and drought on selected wheat variety yields. Clim. Change 125, 489–500. https://doi.org/10.1007/s10584-014-1185-1

Talukder, S.K., 2013. Heat tolerance studies for wheat improvement. Kansas State University.

Talukder, S.K., Babar, M.A., Vijayalakshmi, K., Poland, J., Prasad, P.V.V., Bowden, R., Fritz, A., 2014. Mapping QTL for the traits associated with heat tolerance in wheat (Triticum aestivum L.). BMC Genet. 15, 97.

Tanksley, S.D., McCouch, S.R., 1997. Seed banks and molecular maps: unlocking genetic potential from the wild. Science 277, 1063–1066.

Tian, B., Talukder, S.K., Fu, J., Fritz, A.K., Trick, H.N., 2018. Expression of a rice soluble starch synthase gene in transgenic wheat improves the grain yield under heat stress conditions. Vitro Cell. Dev. Biol. - Plant 54, 216–227. https://doi.org/10.1007/s11627-018-9893-2

Vijayalakshmi, K., Fritz, A.K., Paulsen, G.M., Bai, G., Pandravada, S., Gill, B.S., 2010. Modeling and mapping QTL for senescence-related traits in winter wheat under high temperature. Mol. Breed. 26, 163–175.

Viswanathan, C., Khanna-Chopra, R., 2001. Effect of Heat Stress on Grain Growth, Starch Synthesis and Protein Synthesis in Grains of Wheat (Triticum aestivum L.) Varieties Differing in Grain Weight Stability. J. Agron. Crop Sci. 186, 1–7. https://doi.org/10.1046/j.1439-037x.2001.00432.x

Waines, J.G., 1994. High temperature stress in wild wheats and spring wheats. Funct. Plant Biol. 21, 705–715.

Yang, J., Sears, R.G., Gill, B.S., Paulsen, G.M., 2002a. Genotypic differences in utilization of assimilate sources during maturation of wheat under chronic heat and heat shock stresses. Euphytica 125, 179–188.

Yang, J., Sears, R.G., Gill, B.S., Paulsen, G.M., 2002b. Growth and senescence characteristics associated with tolerance of wheat-alien amphiploids to high temperature under controlled conditions. Euphytica 126, 185–193.

Yin, X., Guo, W., Spiertz, J.H., 2009. A quantitative approach to characterize sink–source relationships during grain filling in contrasting wheat genotypes. Field Crops Res. 114, 119–126. https://doi.org/10.1016/j.fcr.2009.07.013

Figure 2-1 Relationship between average chlorophyll content and F_v/F_m expressed as percentage of day 0 for all genotypes under heat stress treatment.

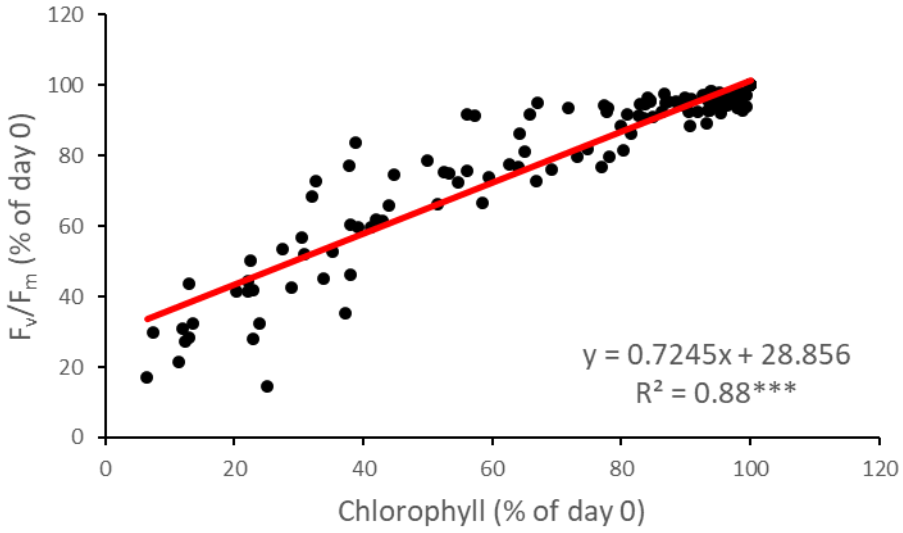

Figure 2-2 (a) Chlorophyll content and (b) chlorophyll fluorescence presented as % of day 0 (before the stress is applied) after 2, 4, 6, 8, 10, 12, 14, and 16 days of high temperature treatment (35/29 ºC (day/night)).

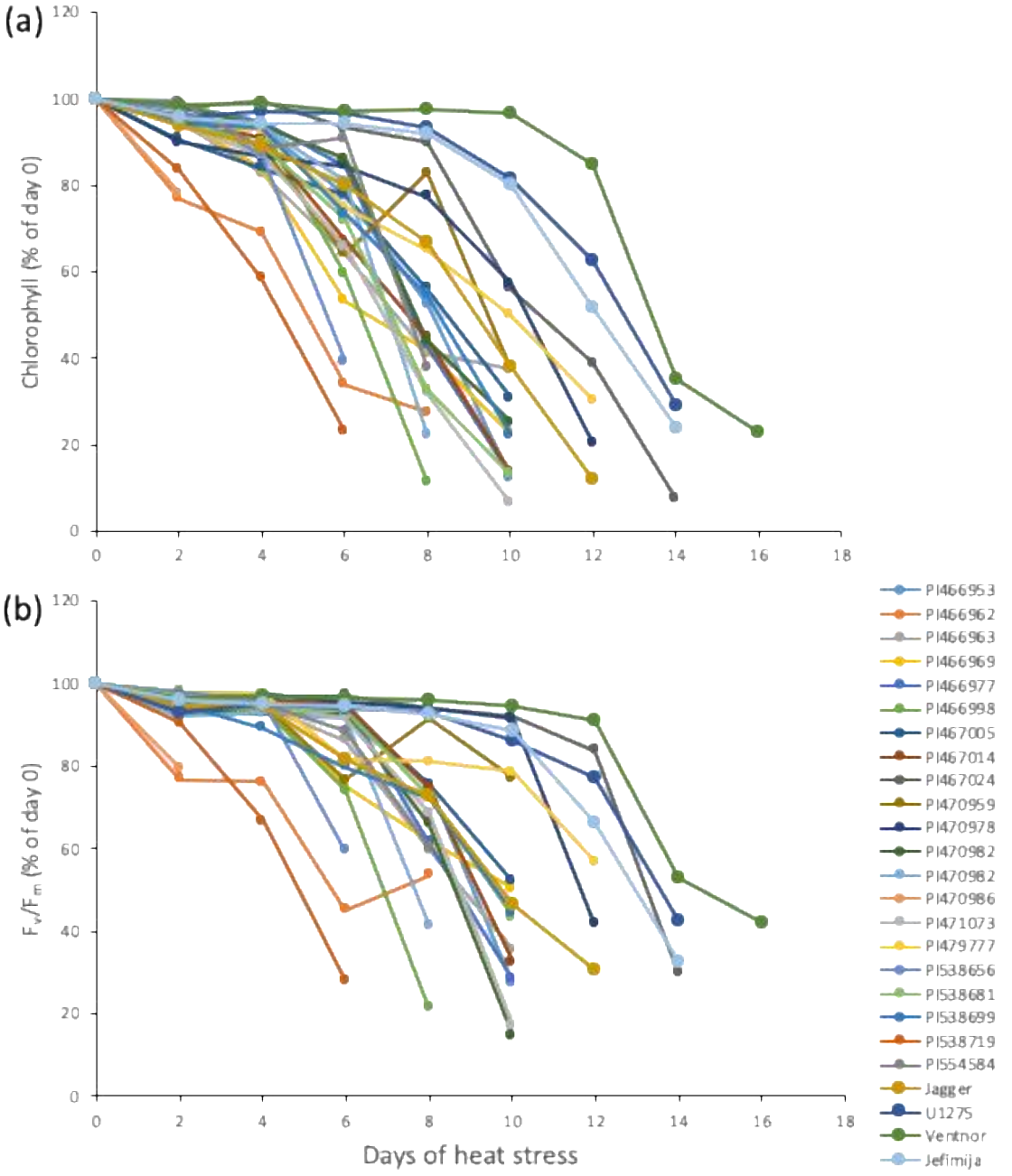

Figure 2-3 (a) Chlorophyll content and (b) chlorophyll fluorescence presented as % of day 0 (before the stress is applied) after 2, 4, 6, 8, 10, and 12 days of high temperature treatment (35/29 ºC (day/night)). Error bars are ± 1 Standard error from the mean of two chamber treatments.

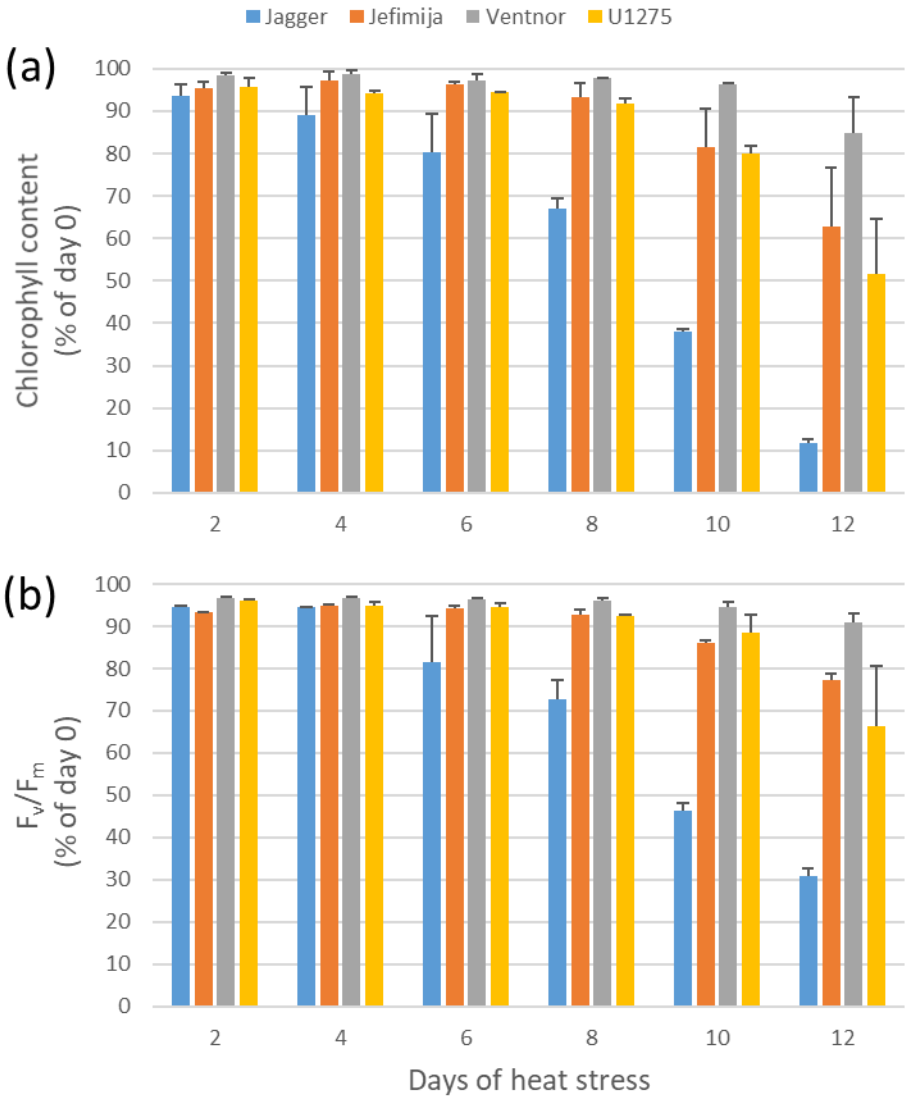

Figure 2-4. Relationship between senescence (expressed as days to minimum slope in chlorophyll values (more negative value) at two days interval measurement) and duration of flag leaf survival under heat stress treatment.

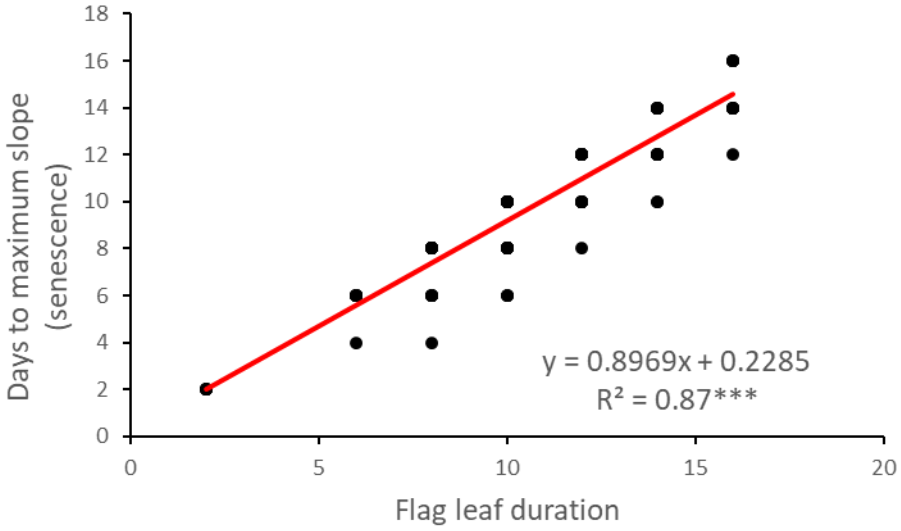

Figure 2-5 Heat Susceptibility Index (HSI) calculated from the Individual Kernel Weight (IKW) measurement under high temperature and optimum temperature for all genotypes.

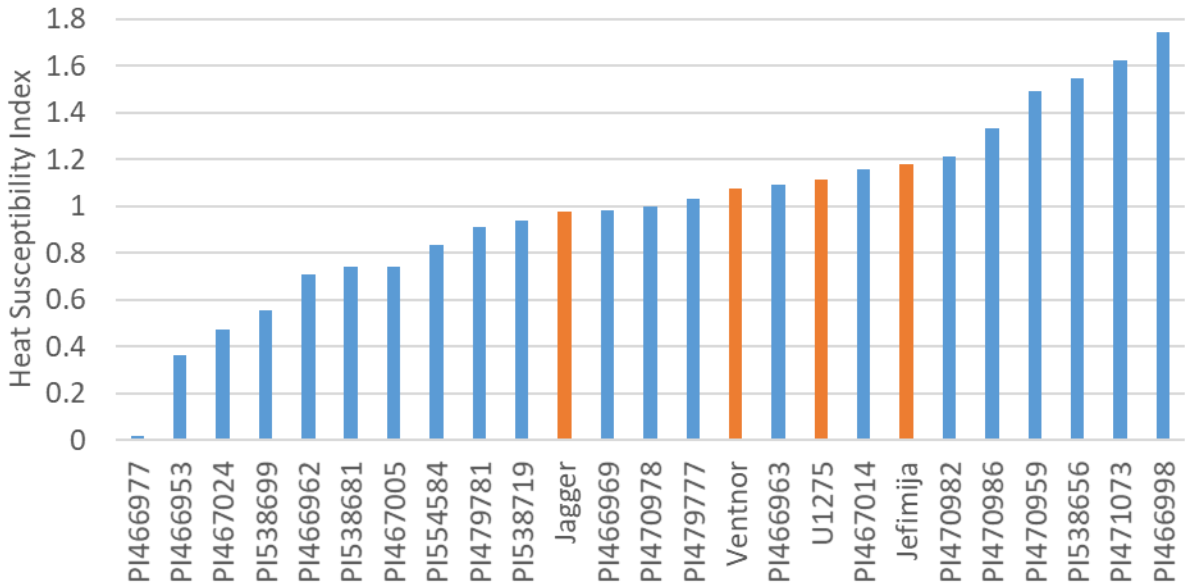

Table 2-1 Species, accession number, country of origin, and altitude for genotypes used for identifying source of post anthesis heat tolerance.

Entry No.	Genus	Species	subsp	Common name/Cultivar	Accession No.	Country of origin	Altitude (m)
1	*Triticum*	*turgidum*	*dicoccoides*	Emmer wheat	PI466953	ISRAEL	44
2	*Triticum*	*turgidum*	*dicoccoides*	Emmer wheat	PI466962	ISRAEL	74
3	*Triticum*	*turgidum*	*dicoccoides*	Emmer wheat	PI466963	ISRAEL	74
4	*Triticum*	*turgidum*	*dicoccoides*	Emmer wheat	PI466969	ISRAEL	74
5	*Triticum*	*turgidum*	*dicoccoides*	Emmer wheat	PI466977	ISRAEL	74
6	*Triticum*	*turgidum*	*dicoccoides*	Emmer wheat	PI466998	ISRAEL	75
7	*Triticum*	*turgidum*	*dicoccoides*	Emmer wheat	PI467005	ISRAEL	-202
8	*Triticum*	*turgidum*	*dicoccoides*	Emmer wheat	PI467014	ISRAEL	-202
9	*Triticum*	*turgidum*	*dicoccoides*	Emmer wheat	PI467024	ISRAEL	-202
10	*Triticum*	*turgidum*	*dicoccoides*	Emmer wheat	PI470959	ISRAEL	44
11	*Triticum*	*turgidum*	*dicoccoides*	Emmer wheat	PI470978	LEBANON	2655
12	*Triticum*	*turgidum*	*dicoccoides*	Emmer wheat	PI470982	LEBANON	2655
13	*Triticum*	*turgidum*	*dicoccoides*	Emmer wheat	PI479781	ISRAEL	12
14	*Triticum*	*turgidum*	*dicoccoides*	Emmer wheat	PI470986	LEBANON	2655
15	*Triticum*	*turgidum*	*dicoccoides*	Emmer wheat	PI471073	ISRAEL	-202
16	*Triticum*	*turgidum*	*dicoccoides*	Emmer wheat	PI479777	ISRAEL	44
17	*Triticum*	*turgidum*	*dicoccoides*	Emmer wheat	PI538656	TURKEY	1560
18	*Triticum*	*turgidum*	*dicoccoides*	Emmer wheat	PI538681	ISRAEL	-31
19	*Triticum*	*turgidum*	*dicoccoides*	Emmer wheat	PI538699	ISRAEL	-249
20	*Triticum*	*turgidum*	*dicoccoides*	Emmer wheat	PI538719	ISRAEL	-178
21	*Triticum*	*turgidum*	*dicoccoides*	Emmer wheat	PI554584	TURKEY	30
22	*Triticum*	*aestivum*		Jagger		USA	
23	*Triticum*	*aestivum*		U1275		USA	
24	*Triticum*	*aestivum*		Ventnor		AUSTRALIA	
25	*Triticum*	*aestivum*		Jefimija		SERBIA	

Table 2-2 F-values for Individual Kernel Weight (IKW) and Flag leaf duration (FLD) under two treatments. Single (*), double (**), or Triple asterisks (***) indicates the significance at 0.05, 0.01, or <0.001 level of probability.

Source of Variation	DF	IKW	FLD
Genotype	24	101***	42.37***
Treatment	1	299.87**	112.26**
Genotype*Treatment	24	3.53***	3.65***
Treatment (Chamber)	2	NS	NS

Table 2-3 Mean Flag leaf duration (FLD) of genotypes at Optimum temperature (OT) and High Temperature (HT) treatment. Individual datum is the mean of six plants from two replicate growth chamber. Single (*), double (**), or Triple asterisks (***) indicates the significance at 0.05, 0.01, or <0.001 level of probability.

Genotype	FLD OT	FLD HT
PI467005	8.7	8.7
PI470978	13.3	13.3
PI479777	14.0	13.7
Jefimija	15.7	15.3
Ventnor	16.0	15.5
U1275	15.7	14*
PI466963	11.7	10.3**
PI467024	15.3	13.3*
PI471073	12.3	10.7*
PI467014	13.3	11**
Jagger	14.7	11.5***
PI554584	12.3	9.7**
PI538681	12.0	9.3***
PI466962	8.7	6.7
PI470982	13.0	10***
PI538699	14.0	10.7**
PI470959	13.0	9.7***
PI466953	14.0	10.3***
PI538656	11.0	8***
PI466977	13.0	9.3***
PI538719	10.3	7**
PI479781	13.0	8.3**
PI466998	13.7	8.3***
PI466969	13.7	8.3***
PI470986	4.0	2***

Table 2-4 Correlation between chlorophyll content and chlorophyll fluorescence at different duration (days) of heat stress treatment. Double (**), or Triple asterisks (***) indicates that the correlation is significantly different from zero at 0.05, 0.01, or <0.001 level of probability.

Days	2	4	6	8	10	12	14	16
r	0.41***	0.73***	0.84***	0.85***	0.85***	0.86***	0.85***	0.83**

Table 2-5 Effect of high temperature stress on chlorophyll fluorescence expressed as F_v/F_m and chlorophyll content of individual genotype (genotype by treatment interaction sliced by genotype) after 5 days of heat stress. Single (*), double (**), or Triple asterisks (***) indicates that the measurement at high temperature is significantly lower at 0.05, 0.01, or <0.001 level of probability.

Genotypes	F_v/F_m		Chlorophyll	
	OT	HT	OT	HT
PI466953	0.78	0.74*	45.6	42.9
PI466962	0.77	0.72**	41.0	38.1
PI466963	0.75	0.73	45.1	39.7
PI466969	0.79	0.75*	40.5	37.0
PI466977	0.80	0.78	40.4	41.9
PI466998	0.76	0.71**	41.9	39.2
PI467005	0.74	0.76	29.0	31.3
PI467014	0.76	0.76	40.8	37.3
PI467024	0.79	0.78	43.8	44.2
PI470959	0.76	0.76	40.9	38.4
PI470978	0.74	0.77	44.6	34.4***
PI470982	0.78	0.74**	42.5	39.4
PI470986	NA	NA	NA	NA
PI471073	0.77	0.74	44.1	39.8
PI479777	0.78	0.75	45.0	49.4
PI479781	0.77	0.78	41.1	38.9
PI538656	0.73	0.72	38.1	31.5*
PI538681	0.79	0.77	43.3	39.5
PI538699	0.78	0.73**	48.6	45.7
PI538719	0.74	0.63***	41.2	28**
PI554584	0.77	0.73*	37.6	39.7

Table 2-6 Mean Individual Kernel Weight (IKW) of genotypes at Optimum temperature (OT), High Temperature (HT) treatment, and Heat Susceptibility Index (HSI) calculated from IKW. Individual datum is the mean of six plants from two replicate growth chamber. Single (*), double (**), or Triple asterisks (***) indicates the significance at 0.05, 0.01, or <0.001 level of probability.

Genotype	IKW OT (g)	IKW HT (g)	HSI
PI466977	0.031	0.031	0.018
PI466953	0.034	0.032	0.366
PI467024	0.037	0.034	0.472
PI538699	0.022	0.020	0.556
PI466962	0.035	0.032*	0.711
PI538681	0.034	0.030*	0.739
PI467005	0.035	0.031*	0.739
PI554584	0.023	0.020	0.832
PI479781	0.043	0.037***	0.913
PI538719	0.015	0.012	0.941
Jagger	0.036	0.031***	0.975
PI466969	0.034	0.029**	0.981
PI470978	0.044	0.037***	0.999
PI479777	0.043	0.036***	1.029
Ventnor	0.046	0.037***	1.077
PI466963	0.041	0.034***	1.094
U1275	0.044	0.037***	1.113
PI467014	0.044	0.036***	1.156
Jefimija	0.044	0.035***	1.180
PI470982	0.028	0.023**	1.210
PI470986	0.030	0.024***	1.334
PI470959	0.037	0.029***	1.494
PI538656	0.029	0.022***	1.544
PI471073	0.028	0.021***	1.624
PI466998	0.032	0.020***	1.744

Table 2-7 Summary table of heat tolerance based on no significant difference between FLD, F_v/F_m, Chlorophyll content, Individual Kernel Weight (IKW) under high temperature treatment (HT) and optimum temperature treatment (OT) and HSI <1. Significance was assessed at 0.05 level of probability.

	FLD	Fv/Fm	Chlorophyll	IKW	HSI<1
PI466953			□	□	□
PI466962	□		□		□
PI466963		□	□		
PI466969			□		□
PI466977		□	□	□	□
PI466998			□		
PI467005	□	□	□		□
PI467014		□	□		
PI467024		□	□	□	□
PI470959		□	□		
PI470978	□	□			□
PI470982			□		
PI470986					
PI471073		□	□		
PI479777	□	□	□		
PI479781		□	□		□
PI538656		□			
PI538681		□	□		□
PI538699			□	□	□
PI538719				□	□
PI554584			□	□	□

Chapter 3 - Physiological and Genetic Analysis of Water-soluble Carbohydrates Accumulation in Wheat Stems

Introduction

Abiotic stresses, such as drought and heat, greatly reduce productivity in wheat and many other crops. While analyzing insurance usage for crop loss, Boyer (1982) found that the 94% decline from record to average production in US grown wheat was due to abiotic stress, mainly drought. Yield loss due to drought has been reported in several studies (Boyer, 1982; Musick et al., 1994; Tack et al., 2014), and it affects both developed and developing countries (Trethowan and Pfeiffer, 2000). A recent modelling study by Tack (2014), reported that 22% of the yield reduction in US Great Plains wheat is due to drought.

Drought can be defined in several forms, but the agricultural drought is the condition when the water available in the soil is not enough for normal growth and development at a particular time (Hayes, 2010). It can happen during any growth stage, but drought during reproductive stage can be more damaging to the developing floret, hence to final yield (Ahmadi and Baker, 2001; Prasad et al., 2008). Drought 15 days after flowering can decrease grain weight by as much as 40% (Ahmadi and Baker, 2001; Wardlaw and Willenbrink, 2000). The wheat growing areas of the US Great Plains are drought prone and often experience terminal drought, which decreases yield by decreasing grain number or grain weight. The stress during early grain filling stage is more likely to lower the grain number by limiting the supply of photoassimilates to the developing grain, causing the abortion of recently fertilized ovaries (Ji et al., 2010). Stress during mid/late grain filling stages negatively impact on the kernel weight by decreasing the grain fill duration (Ji et al., 2010).

Plants deal with drought mainly by two primary mechanisms: avoidance or escape and tolerance (Blum, 2011a). Avoidance is common in areas that are likely to experience terminal drought stress and mediated by the hormone abscisic acid (ABA). ABA is primarily responsible for triggering drought responsive traits in plants like stomatal closure, leaf retardation, promotion of root growth and so on. Early maturation takes advantage of avoidance or escape from terminal drought stress, however, longer grain fill duration is beneficial for maintaining yield potential (Blum, 1998). Grain yield is a function of the biomass and harvest index. Biomass depends on a series of factors impacting ongoing photosynthesis like light interception, radiation or water use efficiency and involves several enzymatic activities in the process (Reynolds et al., 2009). Drought stress negatively impacts these processes, increases respiration and senescence, ultimately decreasing yield.

Grain filling in wheat relies on post anthesis assimilates mobilized directly to the grain or the remobilization of earlier synthesized assimilate stored in the stems and mobilized into the maturing grain. Under favorable conditions, up to 80% of the grain weight is contributed by post anthesis assimilate, but terminal drought stress limits this production resulting in a severe decline in yield (Blum, 1998; van Herwaarden et al., 2003). The assimilation rate alone cannot support the sink demand and respiration rate; therefore, mobilization of the stored reserves is crucial in maintaining yield under stress when photosynthesis is compromised (e.g., terminal heat and drought stress, diseases after flowering). These stored reserves are referred to as water-soluble carbohydrates (WSC) to distinguish them from structural cell wall carbohydrates. Studies have shown that mobilization of WSC can contribute up to 60% of the resources for yield under stress (Blum, 1998; Ehdaie et al., 2008; Plaut et al., 2004; Rattey et al., 2009; Rebetzke et al., 2008; Yang et al., 2007). Therefore, WSC is an important adaptive trait for terminal drought stress.

WSC accumulation occurs when excess assimilates are synthetized before, during, or right after anthesis. It can constitute more than 40% of stem dry weight, depending on genotype (Rebetzke et al., 2008; Ruuska et al., 2006; Schnyder, 1993). WSC can be stored in the form of hexose and sucrose but is predominantly present as fructans in wheat (Wardlaw and Willenbrink, 1994). Two main enzymes predominantly involved in fructan synthesis are sucrose sucrose fructosyl transferase (SST) and fructan fructan fructosyl transferase (FFT), and the activity of these enzymes are found to be positively correlated with the WSC accumulation (Blum, 1998; Housley et al., 1989; Xue et al., 2008). Glucose is a product of fructan synthesis, converted to sucrose, and stored as fructan by the activity of SST, but the enzymes sucrose synthatase and sucrose phosphatase are also believed to play a role during the conversion (Wardlaw and Willenbrink, 1994). Pre-anthesis drought stress decreases WSC accumulation, and this decrease has been linked to the decreased activity of these enzymes (Ji et al., 2010; Xue et al., 2008). Unlike accumulation, remobilization is dependent on demand, enzymatic activity and source availability (Blum, 1998; Plaut et al., 2004, Shi et al., 2016). The driving factor for remobilization is the rate of starch deposition in the grain, which is mainly regulated by soluble starch synthase (SSS). Given the highly thermosensitive nature of SSS enzyme in wheat (Keeling et al., 1993; Prakash et al., 2009; Tian et al., 2018), mobilization is largely dependent on the external environmental conditions.

Although there is parsimonious literature showing that the use of WSC promises increased drought tolerance, WSC is not used as a selection in the United States wheat breeding programs. The two main reasons are (i) the lack of research in diverse genotypes to understand the role of WSC, and (ii) the analysis method. The conventional method for analyzing this trait is labor intensive and time consuming, limiting its application to the large number of samples

required in breeding. Many studies in the past were based on the tedious lab method but, in recent years, the use of near infrared spectroscopy (NIRS) has also been widely adopted (Piaskowski et al., 2016; Rebetzke et al., 2008; Ruuska et al., 2006; Wang et al., 2011). NIRS is based on the measurement of the absorption of specific frequencies of light by the molecules present in the sample, therefore it needs to be calibrated to a set of laboratory-analyzed samples. NIRS is rapid, non-destructive, cost effective, and has been widely applied in predicting several compounds in agriculture research (Roberts et al., 2004). Very few studies using NIRS for predicting WSC have addressed accumulation in diverse genotypes or assessed accumulation in different parts of the plant (Piaskowski et al., 2016; Ruuska et al., 2006; Wang et al., 2011). The inclusion of data from diverse genotypes and various plant parts in the model will help widen the applicability of the model in predicting diverse genotypes in multiple environments.

Leaf desiccants like sodium or magnesium chlorate or potassium iodide have been used to simulate terminal drought stress and study the mobilization of stem reserves for grain fill (Blum, 1998). Nicholas and Turner (1993) confirmed that the desiccant application is positively and significantly correlated with terminal drought stress under field conditions. Desiccants have also been evaluated for early generation selection for drought tolerance in the breeding program (Haley and Quick, 1993). In their study, the two cycle of selection produced bulks more tolerant genotypes to desiccant application. The application of desiccant to simulate terminal drought stress is potentially a powerful tool for selection, especially when the genotype is also evaluated under sufficient moisture to more accurately assess the yield potential of that genotype.

Genomic analysis of water-soluble carbohydrates

Genomic analysis provides significant promise for the understanding and improvement of drought tolerance traits. Genome wide association studies (GWAS) uses recombination from

diverse genotypes to identify the genetic regions associated with the trait, therefore it has higher resolution compared to biparental mapping population. Also, there is no additional time, cost, and effort for population development (Bernardo, 2016). Population structure, relatedness, and covariates can also be taken in to account in the analysis (Korte and Farlow, 2013).

Marker availability and cost for genotyping used to be the major constraints for GWAS studies. Limited studies were done with SSR markers to identify genomic regions associated with WSC concentration, mainly in biparental mapping populations (McIntyre et al., 2012; Rebetzke et al., 2008; Snape et al., 2007; Yang et al., 2007). Genotyping using fixed arrays has been applied for other traits like diseases and yield but has not been used for WSC in the context of a breeding program. Genotyping by sequencing (GBS) has an unprecedented capacity to discover and utilize genome-wide SNP markers at a relatively low cost and has been widely adapted in wheat research (Poland and Rife, 2012; Thomson, 2014).

Although GWAS can be a very important tool to detect variants associated with the traits, it fails to detect rare variants and care must be taken to avoid false positives that may arise from performing a significance test at every single locus (Bernardo, 2016). Another approach, genomic selection (GS), might be more appropriate to accomplish breeding objectives (Meuwissen et al., 2001). GS is also a form of marker assisted selection but, unlike GWAS, GS uses genome wide molecular markers, to calculate genomic estimated breeding values (GEBVs), that can be used to predict the performance of another set of genotypes that have been genotyped but not phenotyped (Heffner et al., 2009). GS has been tested in wheat for several other traits such as disease resistance (Poland and Rutkoski, 2016; Rutkoski et al., 2012, 2014), yield and end use quality (Battenfield et al., 2016; Guzman et al., 2016), however, to the best of our

knowledge, there has not been any attempt to evaluate the applicability of GS using WSC as the target trait.

With the use of the GS model, superior candidates can be selected prior to phenotyping based on the GEBVs estimated from the genotypic data. GS can accelerate genetic gain through the shorter breeding cycle (Heffner et al., 2009). The gain per year from the GS breeding program is higher, even at moderate GEBV accuracy, but can increase to several fold with an increase in GEBV accuracy. GS is more important in a commercial crop with a large and complex genome and traits with moderate heritability (Jarquín et al., 2017; Poland and Rife, 2012).

Genomic selection has two primary components: training population (TP) and unknown population (UP). The training population has genotypes that have been both phenotyped and genotyped, and the unknown/target population has been genotyped, and the phenotypic value is estimated based on the GEBVs derived from the genotypic data (Heffner et al., 2009). The optimum size of the training population is always a question, as smaller TPs will have lower prediction accuracy, but the size of the TP must be balanced with the ability to obtain phenotypic data and the costs associated with data acquisition (Hayes et al., 2009).

In this experiment, we performed GWAS and GS with different training population sizes on WSC concentration using an association mapping panel of winter wheat. Given the applicability of near-infrared spectroscopy and the importance of water-soluble carbohydrate in maintaining grain yield under stress, we aimed to develop an NIRS calibration curve for rapid and accurate determination of WSC in the top and bottom part of stem in genotypes from the Kansas State wheat breeding program and the most broadly adopted varieties in the region. Predicted WSC was analyzed in relation to seed weight, grain yield, and other physiological

traits. Also, we tested a broad set of genotypes under several different environments, including control and simulated terminal drought stress conditions in each environment and analyzed the effect on yield, yield components, and quality.

Materials and Methods

Experimental details

Kansas State University maintains breeding programs based in Manhattan, KS and Hays, KS. The programs have different objectives, based on their target environments. The Manhattan program focuses primarily on central Kansas where its humid and fungal diseases are of primary importance and the Hays program is primarily focused on western Kansas where drought tolerance and resistance to viral disease are emphasized. A diverse panel of 400 winter wheat breeding lines consisting of 200 lines each from both the Manhattan and Hays programs, and 30 released varieties for Great Plains were used in the study (Table 3-1).

The experimental lines were planted in type II modified augmented design in Colby, Kansas under two environments, irrigated and limited irrigation, in 2016 and 2017. A detailed description of this type of augmented design is presented in chapter 4. In 2016, the replicates of varieties were embedded in the augmented design, allowing the varieties to be analyzed as a randomized complete block design (RCBD). In 2017, the thirty varieties were planted in a stand-alone RCBD experiment in the same environments, along with one additional rainfed location at Hays, Kansas. The soil type at both locations was silty clay loam. The planting locations for varieties in 2018 increased to five sites in Kansas. Planting and harvesting information are provided in Table 3-2.

Irrigation

No supplemental irrigation was supplied at Hays in 2017 or 2018. Pre-germination irrigation was supplied to ensure uniform seedling establishment for all experiments in Colby. The Colby Irrigated environment (COI) received supplemental irrigation in all three years. The timing and irrigation amount are presented in Table 3-2. Colby dry environment (COD) relied on the rainfall except for the pre-germination irrigation. Weather data, including monthly precipitation and maximum and minimum temperatures, as well as normal precipitation during the wheat growing season in Colby (2015/2016, 2016/2017, 2017/2018) and Hays (2016/2017, 2017/2018) are presented in Figure 3-3.

Phenotyping for water-soluble carbohydrates

Sample preparation

Twenty stems from each genotype were harvested 15 days after mid-flowering (Flowering in 50% genotypes in plot) as determined on an experiment-wide basis. Flowering date was determined to be five days after 50% of the samples headed out in plot. Immediately (within 1 hour) after sampling, stem tissue was dried in an oven set at temperature 60 ^{o}C until samples reached a constant weight. Head and leaf sheath were removed, and the stems were separated into ‘top’ and ‘bottom’ sections. The top part included the stem above an upper node (first internode) and rest were stored as the bottom part. All samples were stored in air-tight zip lock bags. The stem samples were then ground to a fine powder (<0.2 mm) using Cyclone Sample Mill (UDY Corporation, Fort Collins, CO) and stored in the same bags at room temperature.

Laboratory analysis

Approximately 10% of ground stem samples from both top and bottom sections were randomly selected each year for direct analysis of WSC. Soluble carbohydrates were extracted using a modified method by Xue et al. (2008) and glucose was used as a standard. 50-100 mg of tissue was weighed in a microfuge tube and placed in a water bath set at 80 ^{o}C with 2ml of 80% ethanol for 15 minutes. The procedure was repeated one time with ethanol and two times with water. After each extraction, the samples were cooled to room temperature and centrifuged at 10,000 rpm for 8 minutes. Supernatants from each extract were combined and distilled water was added to reach a volume of 50 ml. Two technical replications were independently performed on the first 10 samples to assess the within-sample variation. Two aliquots were removed from each extraction and the concentration of soluble carbohydrates was determined using the anthrone method with glucose as a standard (Yemm and Willis, 1954). Briefly, one part of the sample or standard solution of glucose at different concentrations was allowed to react with three parts of anthrone reagents at 100 ^{o}C for 12 minutes, and the reaction was stopped by holding at 4° C. Sugar concentration was determined by reading the absorbance at 630nm in a microplate reader and Gen5 2.0 software (Synergy H1 Hybrid Microplate Reader, BioTek, Winooski, VT). Samples from each assay were read in two wells of a microplate, and the results were averaged together to determine concentration per sample.

Near-infrared spectral calibration and validation

Near infrared spectra were taken using a high intensity contact probe (model number A122317) with a bifurcated cable (ASD-135680) that has 78,200-micron fibers from Analytical Spectral Devices (ASD Inc., Boulder, CO). The probe was held 1.5 mm above the ground sample. The same amount of sample was used in each scan by cutting and leveling along the edges in a black dish. Twenty scans were integrated per recorded spectra at wavelengths in the

350-2500 nm range at a spectral resolution of 3 nm up to 700 nm and 10nm above 700nm using LabSpec 4 Std-res spectrophotometer (ASD Inc., Boulder, CO) with RS3 software. White reference was taken every hour from the same height using a spectralon.

The lab analyzed samples were used for spectral calibration and validation using leave out one (LOO) method in partial least square (PLS) regression, a spectral decomposition technique similar to principal component regression. The PLS regression uses concentration data during the decomposition process and includes as much information as possible on the first few loading vectors (Dowell et al., 1999). The spectra from each sample were monitored before analyzing in GRAMS/32 software (Galactic Industries Corp., Salem NH) and 'pls' package in R (R core team). The data were mean-centered before analysis. The number of components in the calibration curve were chosen to yield a maximum coefficient of determination (R^2) and minimum RMSEP. The same calibration curve was developed for both the top and bottom samples to predict the remaining samples in the population. A paired t-test was conducted between actual lab measured concentration and model predicted concentration to test if the predicted values were significantly different from lab measured values.

Simulating terminal drought stress by desiccant spraying

The varieties were planted in paired plots, where one companion plot of the pair received desiccant spray 15 days after mid-flowering, immediately after the sample collection for water-soluble carbohydrates. A commercially available desiccant, defol5 (Drexel Chemical Co, Memphis, TN), was diluted to maintain 6% sodium chlorate (% by volume) in 2018 and sprayed at the rate of 187 liters $hectare^{-1}$ using a MudMaster spray unit (Bowman Manufacturing, Newport, AR). Bidirectional application was made to maximize canopy coverage. The sprayer was equipped with a hood so as not to spread the solution onto adjacent plots. In 2017, the same

chemical was diluted, as suggested on the label, to a final concentration of 12-15% sodium chlorate.

Heading date and plant height measurements

Heading and plant height data were recorded in Hays location only (2017 and 2018). Plot heading date was determined when 50% of the fully emerged heads in the plot (Zadoks et al., 1974). Experiment-wide heading dates in Colby were estimated from general observation in the plot. Plant height was measured from the ground to the peduncle, excluding awns. At maturity, grain yield from the varieties was harvested using a combine harvester to obtain the grain yield $plot^{-1}$ and moisture content. Moisture contents are harvest ranged from 9-12%.

Grain harvested from each plot was measured for test weight and protein using Perten IM 9500 Protein/oil Analyzer (Perten Instruments, PerkinElmer Company). Kernel weight measurements were performed on samples of 200 seeds counted using an automatic seed counter (The Old Mill Co, Savage, MD), and the weight was used to calculate thousand kernel weight (TKW) in kilogram (kg).

Genotyping

Leaf tissue from 3-5 two-weeks old seedlings was bulked together for DNA extraction by a modified CTAB protocol. The genotyping-by-sequencing (GBS) method was used for reduced representation library preparation and DNA sequencing, where the DNA samples were quantified, normalized, digested with two enzymes (rare cutter and common cutter), barcoded, amplified and sequenced using Illumina HiSeq equipment (Poland and Rife, 2012; Poland et al., 2012).

The Trait Analysis by Association, Evolution, and Linkage (TASSEL 5.0) software was used to call and filter single nucleotide polymorphisms (SNPs). The SNPs were aligned with the

IWGSC draft reference genome 161010_Chinese_Spring_v1.0 pseudomolecule reference (IWGSC, 2018) and ordered from the short arm to long arm of each chromosome using Bowtie 2 (Langmead and Salzberg, 2012). SNPs with more than 25% missing data across all genotypes and genotypes with more than 50% missing data across all markers were removed from the resultant SNP call because a large number of missing SNPs can hamper association analysis with an unacceptable degree producing unreliable results. Additionally, SNPs that yielded multi-allelic calls, heterozygosity higher than 10%, and minor allele frequency (MAF) of less than 1% were omitted from the analysis. The unanchored SNPs were retained in the genotypic data and assigned to an unknown chromosome, labelled as "UN" in the analysis. All bioinformatics analysis was performed on the Beocat Research Cluster at Kansas State University.

Genome-wide association analysis

Genome wide association studies (GWAS) were performed in Genome Association and Prediction Integrated Tool (GAPIT) package using enhanced mixed linear model in R (Tang et al., 2016). The threshold for significance in GAPIT is based on the Bonferroni correction. This method is highly conservative, limiting the identification of significant marker-trait associations, therefore a less stringent false discovery rate (FDR) of 10% and P-value of 0.0004 was adopted in our study. The R package 'CMplot' was used to reconstruct Manhattan plots from GWAS results.

Genomic selection

The hapmap format for SNPs was converted to numeric format as 1, -1, 0, and NA for more frequent (major) allele, less frequent (minor) allele, heterozygotes, and missing data, respectively. Loci with missing data were EM imputed with A. mat function in the rrBLUP package in R (Endelman, 2011; Rutkoski et al., 2013). Four genomic selection models, 1) ridge

regression best linear unbiased predictor (rrBLUP), 2) partial least square regression (PLSR), 3) elastic net (ELNET), and 4) random forest (RF) and an average of all four models (AVE) were tested using 'GSwGBS' package in R (Gaynor, 2015). The four models rrBLUP, PLSR, ELNET, and RF) were obtained using R packages 'rrBLUP', 'pls' (Wehrens and Mevik, 2007), 'glmnet' (Friedman et al., 2009), and 'randomForest' (Liaw and Wiener, 2002) respectively. The average prediction (AVE) was calculated using standardized values as described by (Battenfield et al., 2016) avoiding overly weighting the average towards any single model.

Among the models used in the study, rrBLUP uses a mixed linear model to solve for individual random marker effects (Endelman, 2011). These effects are then multiplied by the marker matrix to predict the line performance in the unknown population. PLSR is similar to regression based on principal components (Wehrens and Mevik, 2007). ELNET fits a generalized linear model with a penalized maximum likelihood (Friedman et al., 2009) and RF is based on the decision tree method (Breiman, 2001).

Cross validation prediction was conducted using four training population sizes (20%, 40%, 60%, and 80% of total population) to predict the remaining population, and the average value was obtained after running a 100-fold analysis. The accuracies were obtained by dividing the correlation coefficient by the average square root of broad sense heritability from the average of 100 replications (Poland and Rutkoski, 2016).

Heritability calculation

Heritability is the ratio of genetic variance to the total variance for a given trait (Acquaah, 2009).

$$h^2 = \frac{\sigma_g^2}{(\sigma_g^2 + \frac{\sigma_{ge}^2}{e} + \frac{\sigma_{error}^2}{er})}$$

Where, σ^2_g is genotypic variance; σ^2_{ge} is genotype by environment interaction; σ^2_{error} is the residual error variance; e is the number of environments, and r is a number of replications in each environment.

Broad sense heritability was calculated using 'Sommer' package in R (Covarrubias-Pazaran, 2016). Heritability was calculated using a linear mixed model by likelihood methods (REML) solving mixed model equations in R using both genotype and environment as a random effect. Since the experimental lines were not replicated across different environments, only the 30 varieties replicated in randomized complete block design were used in heritability calculations from seven different site year combinations. The variance effects were calculated as:

$$Y_{ijk} = \mu + g_i + e_j + (ge)_{ij} + b_{jk} + e_{ijk}$$

Where,

Y_{ijk} = yield of the i^{th} genotype in the j^{th} environment and k^{th} replicate

μ = overall mean

g_i = main effect of the i^{th} genotype; ~ $N(0, \sigma_g^2)$

e_j = main effect of the j^{th} environment

$(ge)_{ij}$ = ij^{th} genotype × environment interaction effect; ~ $N(0, \sigma_g^2)$

b_{jk} = k^{th} replicate/block effect in j^{th} environment

e_{ijk} = residual comprising both genotypes × location × year interaction as well as the error of a mean; ~ $N(0, \sigma_e^2)$

Results and Discussions

Near-infrared spectroscopy (NIRS) calibration, validation, and data prediction

To develop the NIRS calibration curve, approximately 10% of the sample were analyzed in the lab each year for WSC concentration using glucose as a standard. We adopted the

microplate method for high throughput analysis in the lab, where 96 wells can be read at once, as opposed to single sample reading in a conventional spectrophotometer. The standard curve of glucose was prepared in every microplate to account for plate variation, but the microplate variation was very low, as shown in Figure 3-2. The coefficient of determination, R^2 in all plates was higher than 0.98. In 2016, the calibration equation involved both experimental lines and varieties from two environments whereas the calibration curves in 2017 and 2018 involved only released varieties from all available environments. With the diverse samples being analyzed in the same calibration in 2016, the minimum and maximum range of lab measured WSC in the calibration equation was 79 to 546 mg/g, whereas for the 2018 samples, the range was between 78 and 258 mg/g. R square of calibration and validation was more than 0.81 for all years, and RMSE was 35, 20, and 19 mg/g, respectively, for 2016, 2017, and 2018. The higher RMSE in 2016 compared to 2017 and 2018 could be due to the inclusion of diverse experimental lines in the calibration equation. The calibration equation thus developed was used to predict unknown samples in the population for that given year.

Paired t-test results showed that there is no significant difference between the lab-measured and model-predicted values of WSC concentration with a P-value of 0.9 (Table 3-4). The predicted and observed values were evenly distributed around the 1:1 regression line with a R^2 of 86.1% (Figure 3-3), therefore the model is not under or over predicting the concentration. Notably, the inclusion of both top and bottom plant parts, diverse genotypes with a wide range of WSC concentrations, and representative genotypes from different environments should made the calibration model suitable for predicting WSC across the wider range of genotypes in the study.

Variation in WSC concentration across plant parts, genotypes and environments

Variation across plant parts

Overall, a higher concentration was observed in the bottom portion of the stem compared to the top (part above top node), as presented in Figure 3-4 (a). Similar to the present study, a higher WSC concentration in the basal internode was also observed in winter barley (Bonnett and Incoll, 1992). In contrast, Wardlaw and Willebrink (1994) and Daniels et al. (1982) observed a higher concentration in the peduncle and penultimate internode of wheat and barley, respectively. Gebbing (2003) observed significantly higher fructan concentration in the peduncle enclosed in leaf sheath compared to the exposed, photosynthetic part of peduncle. These differences could be due to (i) differences in genetic material used in the study, as WSC is a genetically-influenced trait (Ruuska et al., 2006; Schnyder, 1993), (ii) environmental conditions, as they can affect the activity of enzymes involved in the accumulation of WSC (Xue et al., 2008), or (iii) the stage of stem harvesting, which can be influenced by differing rates of remobilization of WSC to the grain (Wardlaw and Willenbrink, 1994). Xue et al. (2008) mentioned that differential WSC partitioning is one of the important mechanisms for genotypic variation in WSC accumulation. Earlier mobilization could have lowered the concentration in the upper stem portion, as the peduncle (carbon source) is closer to the head (sink), however we do not have enough evidence to support this hypothesis.

Though the concentration was significantly higher in the bottom of the stem, with a mean of 300 mg/g, compared to 172 mg/g in the top part of the stem (Figure 3-4 (a)). We observed a significant, positive correlation between top and bottom concentration in the stem using all 1500 plots in 2016 with the R^2 of 0.37 (Figure 3-4 (b)). From this result, it appears top (above top-node) or bottom (below top-node) sections of the sem can be used for the analysis of WSC concentration.

Variation across genotypes and environments

Similar to the lab analysis of a smaller number of genotypes, overall range of predicted WSC was higher in diverse experimental lines (Tables 3-5 and 3-6) compared to the 30 released varieties presented in Table 3-1. The average WSC concentration ranged from 51 to 417 mg/g in experimental lines, whereas the range was 124 (18 COI) to 360 mg/g (17 Hays) for varieties planted across locations for three years. The wider range could also be due to greater variation present in the larger set of experimental lines from the two K-State wheat breeding programs. Though these programs collaborate closely to breed varieties for the same state, the Hays program focuses on Western Kansas, which is relatively drier; and the Manhattan program focuses on central Kansas, which is relatively humid and less prone to drought. Therefore, these genotypes might have varying levels of drought tolerances, and phenological traits- the two major factors influencing WSC accumulation (Blum, 1998; Wardlaw and Willenbrink, 1994). Wardlaw and Willenbrink (1994), found that WSC accumulation peaks from 10 - 35 days after anthesis. We attempted to maximize the number of genotypes within this frame, however, these genotypes were not individually assigned a heading date. Therefore, some genotypes might have been beyond the period of highest accumulating, or yet to be on the peak. This may also have contributed some to a wider range observed. Nonetheless, we were still in the linear growth phase of kernel development, and previous literature also suggest the phenological differences were not likely a major factor in phenotypic variation (Ovenden et al., 2017; Salem et al., 2007).

Significant positive correlation of WSC accumulation was observed over environments in both experimental lines and varieties (Figure 3-5 and 3-6). There was not much variation in the experimental lines planted in water-limited or irrigated environments in 2016, which can be seen in the even distribution around the regression line in Figure 3-6. These lines are grown in the same location where environmental variation was primarily based on moisture regime. Higher

than normal rainfall occurred during the 2016 wheat growing season, with more than half of in-season precipitation occurring after April. The result was the materials in the field did not experience any moisture deficit from shortly after jointing through physiological maturity (Figure 3-1). In 2018, the WSC concentration levels were highest at Hays (rainfed), followed by Colby (dry) and Colby (irrigated). The two experiments at Colby were very similar in WSC concentration, suggesting moisture regime was not the most important factor influencing WSC. However, the general trend of higher WSC in drier environments in the same year, was consistent with the results of Ehdaie et al. (2008 and 2006), Rattey et al. (2009), Rebetzke et al. (2008), and Ruuska et al., (2006).

Data was generated for two environments from one year for the experimental lines and seven environments over three years for the released varieties. A strong trend of positive and significant correlation of WSC among all environments was observed in varieties. Correlations between the varieties in different environments ranged from 0.55 to 0.85 (Figure 3-5). The highest correlation was observed between the two Colby environments (COD and COI) in both 2016 and 2018, whereas the lowest correlation was observed between 18 COI and 16 COI. As noted for the experimental lines, high correlations were found between COD and COI in 2016. Anomalous rainfall patterns in both years complicate interpretation of the results but the fact that moisture regime resulted in very little relative change in WSC suggests that environmental factors, other than precipitation play a key role in determining WSC concentration. Correlations between environments within the same year were higher than year-to-year correlations, where correlations of WSC accumulation were stronger between 2016 and 2017 or 2017 and 2018 than between 2016 and 2018. The Spearman rank correlation also followed the same trend, with a

similar range of 0.53 to 0.88. Overall, we can conclude that the rank among varieties does not change greatly across environment and years.

Drought tolerant cultivars are expected to have a higher capacity to store and mobilize WSC and may be expected to be less productive under favorable conditions. Yield decline under terminal drought stress was found to be greater for varieties with lower WSC concentration (Blum, 1998; Dreccer et al., 2012). This could lead to the conclusion that high WSC is desirable in environments prone to terminal drought stress, even though it may compromise yield potential. Genotypes were separated into the top- and bottom-ten accumulating in each environment. Eight lines were common across the locations for each category. The eight varieties that were consistently the highest accumulating genotypes across all locations were Clara CL, Larry, SY Wolf, Gallagher, KanMark, Tiger, SY Sunrise, and Zenda. Most of these lines are considered to be at least somewhat drought tolerant, except SY Sunrise, which is marketed specifically for irrigated environments, and Zenda, which is classified as moderately susceptible to drought (Wolf et al., 2018). Similarly, eight varieties consistently among the ten varieties with the least WSC accumulation were: Brawl CL, LCS Chrome, LCS Wizard, WB Grainfield, Fuller, Iba, TAM 111, and TAM 114. TAM 111 and TAM 114. Most of these varieties are well adapted to the western part of the state and have performed well in dry environment. Cooler canopy temperatures, related to rooting depth, has been explored in some of these lines (Pradhan et al., 2014). This result suggests there may be two different drought tolerance mechanisms, reduced canopy temperature and high WSC accumulation, present in successful commercial varieties adapted to the western Great Plains. It is not clear whether both mechanisms can be effectively utilized in a single genotype.

Three varieties (Tatanka, T158, and SY Flint) had higher WSC concentration in 2016 but accumulated relatively less in 2018. This could be due to the influence of diverse years. The growing season prior to anthesis was much drier in 2018 and these genotypes may not have maintained the water status to accumulate WSC reserves. We observed significant genotype by year interaction, but the genotype by environment effect was not significant within year except for upper stem WSC accumulation in 2016 (Table 3-7). Heritability for WSC concentration in the stem was very high owing to low genotype by environment interaction. The broad sense heritability of average whole stem WSC concentration was 0.88 while heritability for the bottom portion of the stem (below the first node) was even higher at 0.9 and heritability for the top portion (first internode and peduncle) was slightly lower, at 0.78. The high heritability in our experiment is in agreement with past studies on the genotypic variation of WSC (Ruuska et al., 2006). Selection of genotypes under drought is confounded with the low heritability of drought tolerance traits. Higher heritability, significant genotypic variation, and high correlation between environments mean that selection for WSC concentration should be possible and effective.

Relationship of WSC with seed weight:

There was a consistent, albeit non-significant, relationship between WSC and yield in all environments where yield data were available (Table 3-1). WSC was positively related to yield and yield components (grain yield, seed weight, and test weight (TW)). However the relationship was significant only for seed weight. Seed weight, expressed as thousand kernel weight (TKW), was positively and significantly associated with the WSC concentration in the stem though the level of significance was different across the environments (Figure 3-7). Overall, the relationship was stronger in 2017, compared to all three locations in 2018. In 2017 at Hays, the R^2 was 0.56 and highly significant. However, in 2018, it was only marginally significant with an R^2 of 0.16

after excluding two genotypes Brawl CL and Iba. These two varieties were two of the lowest accumulating varieties in 2018 but had higher TKW, 27.7 and 27.5 g, respectively. The average range of TKW was also higher in 2017 (27-34.5g) compared to 2018 (23-28g). The two highest and lowest seed weight varieties in both years were Gallagher and LCS Chrome, respectively (Figure 3-9). The highest WSC accumulating variety, Clara CL, had a thousand kernel weight of 25.3g, which was toward the low end of the range for that trait. It seems likely there is interplay between the various yield components. Clara CL was one of the highest tillering varieties in all three locations. T158 had the highest seed weight but moderately high WSC content. There is a natural tradeoff between tillering capacity and seed size as presented in the consistent negative correlation between stems/m2 and thousand kernel weight across all locations in 2018 (Table 3-8 (a)). The highest correlation of WSC with seed weight in 2018 was observed in the Colby irrigated environment. Among the three highest WSC accumulating varieties, SY Wolf, Clara CL, and Larry, Clara CL and Larry maintained higher grain weight under irrigation at Colby, but SY Wolf was moderate in all three environments. T158, TAM 111 and TAM 114 had moderate or low WSC concentration, but the kernel weight was comparable to, or even higher than, high accumulating lines. As discussed earlier, other mechanisms to maintain seed weight and tolerate drought could be in play, aside from WSC.

The lower correlation in 2018, compared to 2017, for the same varieties would indicate the genotypes were translocating less photoassimilate to the grain to maintain grain weight. Weather is the main factor impacting yield in these areas (Barkley et al., 2014). The weather in 2018 was dry and cool through early May. The plants might not have met the required growing degree days for assimilate production and storage, and moisture deprivation might have aggravated the stress, further decreasing the assimilate production (Figure 3-1). The crop

progressed rapidly through its phenological stages after mid-May (heading, flowering, and grain filling stage), when the temperature and moisture increased greatly. This may have increased the demand for more carbohydrate consumption rather than supporting accumulation. Carbohydrate storage happens only when the assimilate is produced beyond the need and assimilate production and storage is higher only when the inputs availability (such as temperature, moisture, fertilizer, etc.) are optimum. WSC accumulation in wheat was reduced to half under moisture deprivation and was also favored by increasing carbon dioxide in earlier studies (Blum, 1998). In contrast to the expectation of terminal drought stress in this region, more stress occurred during vegetative growth in 2018 when the plant is actively involved in assimilation and storage. This could also be the reason for lower accumulation in 2018, compared to 2017 and 2016. Along with accumulation, translocation might also have been impacted due to the abnormal trend of drought this year.

In contrast to positive relation with seed weight, we didn't observe clear relation of WSC on overall yield or grain number m^{-2} area. Grain number m^{-2} were calculated from number of stems m^{-2}, seed weight, and overall yield data. WSC was positively related to grain yield in rainfed environment in Hays, no clear relation in Colby water-limited environment, whereas it was slightly negative in Colby irrigated environments (Table 3-8 (b)). We couldn't make year to year comparison because the yield data and stem data was available only for 2018 due to weather related damage to plots in 2016 and 2017.

Grain yield and quality under desiccation treatment

The direct effect of WSC on grain weight can be hard to determine and is best evaluated through the use of the desiccation treatment where all the yield components should be held constant for the treated and untreated plots. To explore the effect of terminal drought stress on

yield and quality, we applied a desiccation treatment during mid-grain filling and measured plot weight, test weight (TW), thousand kernel weight (TKW), and percent protein from plots with and without desiccation. Application of desiccant simulates drought by reducing the photosynthetic area, so the grain fill is mainly supported by mobilization of WSC reserves to the grain (Blum, 1998; Nicolas and Turner, 1993). The reduction of photosynthesis is not proportionate with the reduction in grain weight, as a result of the mobilization. The recommended rate for the desiccation treatment in 2017 had a greater than desired effect as tissue damage was also seen on spikes and yield was reduced by nearly 50%. The decline in yield was also potentially confounded by hailstorm that occurred a week before harvest. The hail appeared to have a greater impact on the desiccant-treated plots as they were more advanced in maturity compared to the control plots. Therefore, the effect of desiccation treatment is discussed using only data from 2018 at three different locations.

Overall, the effect of desiccation was more pronounced in relatively drier environments (Colby water-limited [18COD] and Hays rainfed [18Hays]) compared to Colby irrigated (18COI), as presented in the result Figures 3-8 (grain yield), 3-9 (test weight), 3-10 (thousand kernel weight), and 3-11 (grain protein %). Interestingly, the decline, as well overall yield level, was higher in the Colby dry environment compared to the two other environments. The most likely explanation is due to spatial variability in the field as the rainfed plots did not experience visual symptoms of stress at any point in the season and adequate precipitation later in the season might have favored this environment. We observed a significant decline in TKW and TW in most of the varieties, however the overall yield declined for less than half of the varieties, and protein showed mixed results. The change in protein content was inconsistent in COI but declined for all desiccant treated varieties in COD and Hays. The varieties with significantly

higher protein content under stress at COI either had slightly decreased protein or remained unchanged in the rest of the environments. The protein content was significantly lower in twelve varieties in COD, five varieties in Hays, and two varieties in COI. The average overall decline in protein concentration from the average of all varieties was 0.04 % in COI, 3% in COD, and 5% in Hays. Terminal drought stress, in conjunction with in season moisture stress, had a negative effect on protein, in spite of the overall negative relationship of protein with the overall yield related traits. The stress-related decline in yield was also not correlated with quality in the study by Stone and Nicholas (1994).

Grain yield was significantly lower in 4, 12, and 15 varieties in COI, COD, and Hays respectively. The TAM lines reputed to be drought tolerant, TAM 112 and TAM 114, were able to tolerate terminal drought only in environments where pre-flowering moisture was sufficient. They have been found to be drought tolerant based on the rooting characteristics, which might require some moisture during the growing season to become tolerant later (Pradhan et al., 2014). The desiccation treatment either marginally or significantly reduced yield of TAM 111, TAM 112 and TAM 114 in drier environments (COD and Hays) and lowered TKW and TW in all three environments.

Similar results were observed for TKW as it decreased in 64%, 80%, and 90% of the varieties in COI, COD, and Hays, respectively. However, the extent of decline was similar, ranging from 3-20% on an average. The range of decline was 5-20% in COI, 3-17% Hays, 4-20% in COI. TKW is an important component of grain yield along with grain number and the number of fertile tillers. Tatanka had high yield in all environments but had low TKW, whereas Gallagher and T158 had higher yield as well as higher TKW. Naturally, Tatanka had higher

tillers compared to these varieties. The decline in TKW was one of the reasons for lower yield under desiccation treatment in these varieties.

Test weight was also lower in all the locations under desiccation treatment, but significantly lower in all genotypes in COD, and in more than 90% of the genotypes in COI and Hays. Overall, COD had higher test weight compared to two other locations. In our study, test weight was more correlated with yield than TKW in all locations.

Role of WSC in maintaining yield under desiccation treatment

Desiccation treatment, applied as a surrogate measure of terminal drought stress causes a significant decline in yield as discussed in the last section. The decline was higher in genotypes with lower water-soluble carbohydrates, as seen in the negative correlation presented in Figure 3-12. The decline in yield with desiccant was higher in two relatively dry environments (Figure 3-12 (b) and (c)) compared to the irrigated environment (Figure 3-12 (a)). The overall yield decline under desiccant treatment was 200, 486, and 598 kg ha^{-1} in Colby Irrigated, Colby water-limited, and Hays rainfed. Past selection under terminal drought stress might have been, in part, favored indirect selection for WSC concentration due to its role in tolerance (Blum, 1998; McIntyre et al., 2012; Rebetzke et al., 2008). WSC, along with the contribution to grain filing can also serve as an important osmolytes in regulating cell turgor under drought stress in wheat (Yang et al., 2007).

Selection for high kernel weight via high WSC would be expected to decrease grain number $spike^{-1}$ or spikes unit $area^{-1}$, as these two yield-related traits are at least partially under the control of different genetic loci (Ji et al., 2010). We didn't observe a clear relationship between WSC with grains m^{-2} in our study. The correlation was slightly positive in Hays, ambiguous in COD, and slightly negative in COI. Although, the overall decline in yield under

desiccant treatment was lower in genotypes with higher WSC, the relationship of WSC with yield was dependent on environment.

Relationship between stem weight, stem number, and WSC

Stem biomass was measured on 20 individual stems, without leaves, leaf sheath, and head. Tiller numbers were counted using an 11 X 12 inch quadrats in two replicate plots and stem m^{-2} area was extrapolated. Stem weight (g) and stem number m^{-2} are negatively related in all three locations except in Hays at stem densities between 8000-10,000 stems m^{-2}, where average stem weight increased with increasing stem number (Figure 3-13, Table 3-9, Table 3-10). It could be due to more resource utilization in lower plant population, but the relationship became negative once the population was higher than 10,000 stems m^{-2}, indicating a negative effect of competition in high tillering varieties. Stem weight was slightly positively correlated to WSC concentration, however, the relationship was not significant, except in COI. Stems m^{-2} was significantly negatively correlated with WSC in the top part of the stem in COI, similar to results obtained by Dreccer et al. (2012), where the genotypes that accumulated more WSC had fewer stems. However, the relationship was not consistent across the environments in our study.

Effect of plant height and heading date on yield and WSC

Plant height

Plant height was measured only in Hays and it ranged from 92-105 cm in 2017, whereas the plants were shorter, and the range was wider 69-87 cm in 2018. This difference can be partly explained by contrasting weather (Figure 3-1) in the two different years. Rainfall is the main determinant in yield and plant phenotypes in plants growing in the rainfed environment. The growing season in 2017 was relatively moist with widespread rainfall throughout the growing season, mostly during the vegetative growth phase, whereas in 2018 the rainfall actually started

in May and generally coincided with spike emergence. Less than average precipitation occurred throughout the vegetative growth phase in 2018. Total rainfall was 388 and 318 mm in 2017 and 2018 from October to June (planting to harvesting). Even with atypical weather, plant height from the two years were significantly correlated.

Plant height was slightly negatively related to WSC concentration (Figure 3-14 and Table 3-10). The level of significance was evaluated in different scenarios, as presented in Figure 3-14. Yield, as well as WSC concentration, was negatively correlated with plant height, yet the relationship wasn't strong. Overall, there was no relationship between WSC and height in 2017 (Figure 3-14 (c)). Plant height was slightly negatively related with WSC accumualtion in the taller group (R^2 of 0.13) when varieties were separated into two categories of height: less than 98cm and more than 98cm, (20 genotypes).

Similar to the results in 2017, WSC accumulation varied with plant height except for two varieties, SY Wolf and Everest, in 2018. The average height of Everest was only 69cm in 2018, but it had moderate WSC accumulation, whereas, SY Wolf was one of the highest WSC accumulating lines, but was 81cm tall. Except in these two varieties, the plant height was significantly and negatively related to WSC as presented in Figure 3-14 (a). Short plants may have a comparative advantage in transferring a resource to the grains as opposed to tall height plants. Also, shorter genotypes had slightly better stand rating (scored shortly after germination), as opposed to taller plants (Table 3-10 and Figure 3-14 (b)).

The general convention is taller cultivars are more capable of storing large amount of reserves, but research has found mixed results (Borrell et al., 1993; Dreccer et al., 2012; Rawson and Evans, 1971). No association of WSC with plant height was observed by Rawson and Evans (1971) but the positive association with the presence of reduced plant height and dwarfing genes

was observed by Borrell et al (1993). The presence of dwarfing gene *Rht1* and *Rht2* gene reduced the height by 21% and WSC storage by 35% and 39%, respectively, in their study. Mathews et al. (2006) found that shorter plants have comparative yield advantage as compared to taller plants, except in some low yielding environments. Drought has caused significant yield losses at the locations used in this study in the past. The three years in this study were, however, higher rainfall years and yield was higher than historical levels.

Heading date

The range of heading was just four days in 2018, whereas it was eight days in 2017. It remained cold until late April and started to warm quickly in early May in 2018, as opposed to relatively uniform conditions in 2017. Considering these two contrasting weather patterns (Figure 3-1), we saw consistent, albeit non-significant, positive correlation of height and heading date in both years, meaning that taller varieties headed slightly later than shorter varieties. However, the relationship with WSC was not consistent, as well as non-significant, in both years (Table 3-10). An important implication for this study, and similar future efforts, is that as long as sampling occurs during the linear growth phase of grain fill (5-25 days after flowering), the WSC concentration values should not vary significantly. Therefore, the variation we observed is more likely to have come from the genotypic variation, as opposed to differences in phenology.

Some studies have reported a negative relationship between flowering and WSC concentration, linked to tillering opportunity (van Herwaarden et al., 2003). Late flowering provides more opportunities for vegetative growth, increases tillering and reduces WSC concentration. A large number of initiated tillers are rendered unproductive in most environments, especially those that are moisture limited (Dreccer et al., 2012). High WSC in genotypes has been reported to be associated with lower tillers m^{-2}, lower grain number m^{-2}, and

higher grain weight spike^{-1} leading to higher yield (Dreccer et al., 2012, 2008). These three components are the determinants of yield. The genetic gain in yield of wheat in UK has been attributed to the combination of increased grain number, supported by improved pre-anthesis crop growth, and an increase in grain fill capacity due to an increase in stem reserves (Shearman et al., 2005). However, we do acknowledge that the environment in UK is totally different than the environment in this study.

Deposition of photosynthetic assimilate as WSC in the stem coincides with the final stem elongation stage, so high WSC genotypes might be shorter and lower yielding under favorable environment (Dreccer et al., 2012). However, high WSC is desired in terminal drought prone environment even it compromises yield potential in favorable environments (Blum, 2011a). Although WSC was positively related with seed weight, it was negatively related with the seed number, and slightly negatively related to the overall yield in one irrigated environment in our study.

Genotyping results

Distribution of SNPs

After filtering the dataset at MAF of 1% and Heterozygosity of 10%, we retained 34,003 SNP markers on 409 genotypes. The marker polymorphism was highest on the B genome (45.2%) followed by the A (35.6%), and D (16.4%) genomes. Unanchored SNPS accounted for 2.8% of the total and were separated as 'UN'. The sparsest coverage was found on chromosomes 4B and 4D (Figure 3-15). The D genome was found to be less diverse. This is explained by the evolutionary bottleneck that occurred with the hybridization of tetraploid wheat with *Aegilops tauschii* only 8,000 years ago. Missing SNPs per genotype ranged from 1.5 to 50% and the marker coverage was dense in the telomeric regions of the genome (Figure 3-16). This

discrimination is likely due to the lower diversity in the centromeric region and/or methylation of heterochromatic region as one of the enzymes used in the GBS protocol is methylation sensitive (Poland and Rife, 2012).

Population structure analysis

A clear grouping of population structure was not observed from Bayesian Information criteria (BIC) analysis in GAPIT package (R environment), but PCA analysis separated the genotypes into two groups as presented in Figure 3-17, with some mixture. The genotypes are color coded as red, black or green for Hays breeding experimental lines, Manhattan experimental lines and released varieties, respectively. The first PC explained only about 6% of the variation while the second PC explained 3.3% of the variation. Even though the genotypes are from two different breeding programs, germplasm exchange amongst breeding programs in the Great Plains in general, and between the K-State programs in particular, is common. This is likely a major factor, leading to a lack of structure in the analysis. The kinship matrix also stratified two populations, but few genotypes showed mixed results. Some Hays genotypes were found in among the Manhattan genotypes, and some Manhattan genotypes were found with the Hays genotypes.

Genome wide association studies (GWAS)

To identify genomic regions associated with the accumulation of WSC, we conducted association mapping based on mixed linear model (MLM) with and without covariates. The use of covariate did not affect the number or position of QTLs identified. Even though a less stringent FDR of 10% was chosen, we found only two QTLs, on 1B and 7D, associated with WSC accumulation in the top and bottom part of the stem (Figure 3-18 and 3-19). Six SNPs were detected on 7D in a 12mb region. Only one SNP was found on 1B. Each of these SNP markers

explained around 4-5% of the variation in accumulation in WSC concentration (Table 3-11). The QTL in the same region 7D explained about 10% of the variation in Zhang et al., (2014). The 7D region has also been identified in several past studies (Salem et al, 2007; Rebetzke et al, 2008; Yang et al, 2007, McIntyre et al, 2012). Along with WSC accumulation, QTLs for WSC translocation have been reported in 7D, as well as 2D and 5D (Salem et al., 2007). A sucrose synthetase gene was also mapped in 7D and 7B by McIntyre et al. (2012). Dong et al, (2016) isolated and cloned a wheat 1-SST gene (*TaSST*) in chromosome 7D. The gene was validated with highly significant association with WSC content in stem among 149 Chinese wheat cultivars. The expression QTLs are co-located with the WSC accumulation QTL, and overall, more genes related to WSC synthesis are expressed and upregulated in high WSC lines compared to low WSC lines (McIntyre et al., 2012, 2012b; Ruuska et al., 2006).

Along with 7D, significant QTLs for WSC concentration have been reported in 1A, 1B, 1D, 2D, and 4A by Ovenden et al. (2007); 1A, 2D, 4A, 4B, 5D, 6B, and 7B by Salem et. al. (2007); 1B, 2B, 3D, 5B, 6B, and 7B by Rebetzke et al. (2008); 1A, 1D, 2D, 4A, 4B, and 7B by Yang et al. (2007); 1B, 2B, 3D, 4B, and 7A by Snape et al. (2007); 1D, 4A, 6B, and 7A by McIntyre et al. (2012); and 4 BS, 7AS, and 7D by Dong et al. (2015). The QTL reported on 1B was associated with 1B.1R rye translocation (Yang et al., 2007), but the SNP marker detected in our study was pericentric. Also, the lack of recombination in the translocated region should have led to the identification of markers along the entirety of 1BS if the effect were due to the 1B.1R translocation. It is likely the QTL identified here is not associated with the 1B.1R translocation and the fact that a single SNP was significant means the result may be spurious and should be interpreted with caution. The 1RS wheat rye translocation has been found to have positive effect on grain size, mostly in water-limited environments (Rattey et al., 2009; Villareal et al., 1998,

1995). One similarity among all these QTLs identified is the low genetic variation (less than 20%) explained by each of the QTL, which indicates that WSC is a quantative trait, governed by many genes of small effect. This presents a challenge for implementation of marker assisted selection in the breeding program.

We didn't observe clear relationship of heading and WSC accumulation on varieties in our study. Similar to our result, no correspondence of stem WSC with flowering time or maturity was oberved by Ovenden et al. (2017) and Salem et al. (2007), however, Rebetzke et al. (2008) saw a major flowering gene *Ppd1* co-locate with WSC accumulation and explain 28-30% variation in WSC content. QTLS for stem WSC concentration co-located with loci for tiller number, grain weight, and nitrogen use (Dreccer et al., 2012; Rebetzke et al., 2008). Also, many of the grain weight loci have been localized with WSC accumulation (Salem et al., 2007; Yang et al., 2007).

In some cases, the growing environment might also affect the accumulation of WSC (Yang et al., 2007). The WSC data for experimental lines were available from two environments in one year (Colby irrigated and rainfed in 2016). However, we observed highly significantly correlation in WSC accumulation across the varieties in seven different environments. The experiments with released varieties suggest that a greater spread in WSC occurred 2016 compared to the other years, which should have favored detection of QTL. A relaxed P-value of 0.0004, which was used in other studies (Gao et al., 2016), allowed detection of additional putative QTLs on 4B, 5A, and 6A; the QTL in 4B was identified in other studies (Salem et al., 2007; Snape et al., 2007; Yang et al., 2007).

Lines advanced in the breeding program are not directly selected for WSC concentration in the stem but some favorable alleles might have accumulated, as indirect selection for seed

weight under drought would have occurred. Such phenotypic selection would be based on the genetic variation present in specific crosses. These favorable alleles in specific crosses would be difficult to detect in a GWAS analysis if they were rare in the breeding program(s). Due to quantitative nature of this trait, even if some SNPs are modestly associated in WSC accumulation, their effect may not be strong enough to cross the $-\log_{10}p$ value threshold to be significant.

Haplotype Analysis of QTL 7DS

Haplotype analysis provide more evidence for association than a single SNP analysis from the GWAS (Barendse, 2011). 6 SNPs were significant at the 7D region were used for the haplotype analysis. Out of 412 genotypes total used in GWAS, only 171 genotypes had all six SNPs at the region of significance. The haplotype group in the region are ACCCCG, ATCTGC, GCTCCG, GTCTGC, GTTTGC (figure 3-20). Among these five groups, the most common group is GCTCCG with 112 genotypes, followed by the group ACCCCG with 41 genotypes (figure 3-20 (a)). The haplotype GCTCCG favored significant high WSC concentration and the group ACCCCG favored significantly lower WSC accumulation. On an average, there was 17% and 10% increase in top and bottom WSC concentration for GCTCCG over ACCCCG irrespective of the environment. 78% of the genotypes were from Manhattan and 17% of the genotypes were from Hays in ACCCCG haplotype, whereas, 45% of the genotypes were from Manhattan and 55% were from Hays in GCTCCG haplotype, and rest were the released varieties used in the study. The Hays genotypes are targeted for western Kansas where its relatively drier; and the Manhattan genotypes are mostly for central Kansas where it's relatively a humid and less prone to drought. Therefore, the genotypes in Hays breeding program might be indirectly selected for higher WSC haplotype group GCTCCG. Indirect selection has been already

occurring in many environments. Rebetzke et al., 2009 reviewed the increasing trend of WSC with the year of variety release in western Australian cultivars and CIMMYT genotypes. Shearman et al., 2005 also reported higher WSC in UK cultivars with the progressive year of release.

Genomic selection

The genomic prediction accuracies ranged from 0.17 to 0.6 depending on the model and training population used. The accuracy of prediction increased with increasing size of the training population (Figure 3-21). Overall, an average of the models (AVE) and Random Forest (RF) had higher accuracies compared to other models tested (rrBLUP, ELNET, and PLSR). Similar to our results, machine learning RF was superior for predicting rust response (González-Camacho et al., 2018). In contrast to our study, RF performed poorly for quality traits in Battenfield et al. (2016). Higher prediction accuracy was observed with rrBLUP and AVE in the K-State wheat breeding program for grain yield (Gaynor, 2015), and end use quality (Battenfield et al., 2016). Both of these traits are highly quantitative controlled by many genes of small effects.

RF regression has the capacity of capturing both marker with smaller effect and markers with larger effect, it's likely that both exists for WSC. The prediction accuracy was not greatly improved with incremental increases in the size of the training population. RF has performed better for traits that are governed by few major genes than the traits like yield, which is governed by genes with small effect. The efficacy of RF in this study suggests that, at least in the materials evaluated, a small number of loci with larger effect control the trait. This has implications for utilization of a drought tolerance breeding strategy focused on WSC accumulation. It may be that initial selection could be effective but, once the loci with larger effect are fixed, progress may

become slow. Further evaluation of a larger set of materials would be required to clarify long-term feasibility of improving WSC accumulation as a breeding strategy in the K-State wheat breeding programs.

Summary and Conclusions

The environment is the main hurdle to make progress in plant breeding. Out of three years of planting, phenotypic data is available from less than half of the environments. Nevertheless, high heritability and high genetic variation provide the potential for selecting genotypes with higher water-soluble carbohydrates. Although lines are not advanced in the program based on WSC measurement, selection under drought may favor alleles for WSC accumulation if they are associated with greater drought tolerance. We identified significant QTL in 7D, but identification of other significant QTLs would be necessary to support a long-term MAS strategy. Genomic selection to make predictions based on genomic estimated breeding values can be a great tool to implement in the breeding program. GS is less expensive and less labor intensive than direct phenotyping for WSC and has the potential for in-season predictions and may be a more useful strategy for improving WSC in breeding materials.

Although, we have discussed the role of WSC in maintaining grain weight under drought stress, WSC can be a buffer to grain fill under any post flowering stress that limits photosynthesis. As wheat grain filling coincides with increasing temperatures, moisture decline, and high incidence of foliar diseases, WSC can play a critical role under all these conditions. Assimilate production to meet the sink demand might be limited under normal conditions, therefore having higher WSC can provide yield stability across variable environments. The higher correlation between the top WSC and bottom WSC enables either of these parts can be

used for WSC measurement. And NIRS spectroscopy can effectively use for rapid and non-destructive measurement of WSC.

While WSC is an important trait under post anthesis drought stress, breeding strategies for highly variable areas like the Great Plains may well favor other mechanisms for drought tolerance, as WSC accumulation is likely not as effective for tolerating pre-anthesis stress. This was highlighted by the results obtained in 2018. Drought was experienced during vegetative growth, rather than during reproductive growth and WSC accumulation was decreased. In regions like the Great Plains, where weather patterns are very erratic, the timing and intensity of drought stress cannot be accurately anticipated within a given year, much less in a manner that would allow a breeding program to focus specifically on post-anthesis drought tolerance. Stress may occur post-anthesis one year, during the seedling the next and during the vegetative stage the next year. Effectively breeding for drought tolerance in the Great Plains requires development of varieties than can tolerate these various timings and intensities of stress to maintain higher yield across years. For that reason, WSC might not be effective as a tolerance strategy for the Great Plains compared to regions in the world where drought reliably occurs primarily during grain filling. Dehydration avoidance mechanisms of drought tolerance, such as osmotic adjustment and rooting characteristics, are likely to be more beneficial than a concerted effort to increase WSC reserves in the Great Plains. Such mechanisms also likely allow for higher yield in seasons when conditions are favorable. Some literature suggests that dehydration avoidance and WSC accumulation are negatively associated and may be diametrically opposed to one another. Dehydration avoidance mechanisms like early flowering, greater root depth, osmotic adjustment are reported to be more preferred than tolerance mechanism like WSC in some environments (Blum, 2011b). The presence of high levels of WSC concentration in well-

adapted varieties does, however, indicated that this trait has relevance in the Great Plains and should not be ignored. Further understanding the compatibility of improving WSC accumulation while utilizing dehydration avoidance mechanisms is of critical importance to designing the most effective approach(es) to breeding climate resilient wheat varieties for the Great Plains.

References

Acquaah, G., 2009. Principles of plant genetics and breeding. John Wiley & Sons.

Ahmadi, A., Baker, D.A., 2001. The effect of water stress on grain filling processes in wheat. J. Agric. Sci. 136, 257–269.

Barendse, W., 2011. Haplotype analysis improved evidence for candidate genes for intramuscular fat percentage from a genome wide association study of cattle. PLOS ONE 6, e29601. https://doi.org/10.1371/journal.pone.0029601

Barkley, A., Tack, J., Nalley, L.L., Bergtold, J., Bowden, R., Fritz, A., 2014. Weather, disease, and wheat breeding effects on Kansas wheat varietal yields, 1985 to 2011. Agron. J. 106, 227–235. https://doi.org/10.2134/agronj2013.0388

Battenfield, S.D., Guzmán, C., Gaynor, R.C., Singh, R.P., Peña, R.J., Dreisigacker, S., Fritz, A.K., Poland, J.A., 2016. Genomic selection for processing and end-use quality traits in the CIMMYT spring bread wheat breeding program. Plant Genome 9. https://doi.org/10.3835/plantgenome2016.01.0005

Bernardo, R., 2016. Bandwagons I, too, have known. Theor. Appl. Genet. 129, 2323–2332.

Blum, A., 2011a. Drought resistance–is it really a complex trait? Funct. Plant Biol. 38, 753–757.

Blum, A., 2011b. Plant water relations, plant stress and plant production, in: Blum, A. (Ed.), Plant Breeding for Water-Limited Environments. Springer New York, New York, NY, pp. 11–52. https://doi.org/10.1007/978-1-4419-7491-4_2

Blum, A., 1998. Improving wheat grain filling under stress by stem reserve mobilisation. Euphytica 100, 77–83.

Bonnett, G.D., Incoll, L.D., 1992. The potential pre-anthesis and post-anthesis contributions of stem internodes to grain yield in crops of winter barley. Ann. Bot. 69, 219–225.

Borrell, A.K., Incoll, L.D., Dalling, M.J., 1993. The influence of the Rht1 and Rht2 alleles on the deposition and use of stem reserves in wheat. Ann. Bot. 71, 317–326. https://doi.org/10.1006/anbo.1993.1041

Boyer, J.S., 1982. Plant productivity and environment. Science 218, 443–448.

Breiman, L., 2001. Random forests. Mach. Learn. 45, 5–32.

Covarrubias-Pazaran, G., 2016. Genome-assisted prediction of quantitative traits using the R package sommer. PloS One 11, e0156744.

Daniels, R.W., Alcock, M.B., Scarisbrick, D.H., 1982. A reappraisal of stem reserve contribution to grain yield in spring barley (Hordeum vulgare L.). J. Agric. Sci. 98, 347–355.

Dong, Y., Zhang, Yan, Xiao, Y., Yan, J., Liu, J., Wen, W., Zhang, Yong, Jing, R., Xia, X., He, Z., 2016. Cloning of TaSST genes associated with water-soluble carbohydrate content in bread wheat stems and development of a functional marker. Theor. Appl. Genet. 129, 1061–1070. https://doi.org/10.1007/s00122-016-2683-5

Dowell, F.E., Ram, M.S., Seitz, L.M., 1999. Predicting scab, vomitoxin, and ergosterol in single wheat kernels using near-infrared spectroscopy. Cereal Chem. 76, 573–576.

Dreccer, M.F., Chapman, S.C., Ogbonnaya, F.C., Borgognone, M.G., Trethowan, R.M., 2008. Crop and environmental attributes underpinning genotype by environment interaction in synthetic-derived bread wheat evaluated in Mexico and Australia. Aust. J. Agric. Res. 59, 447–460.

Dreccer, M.F., Chapman, S.C., Rattey, A.R., Neal, J., Song, Y., Christopher, J. (Jack) T., Reynolds, M., 2012. Developmental and growth controls of tillering and water-soluble carbohydrate accumulation in contrasting wheat (Triticum aestivum L.) genotypes: can we dissect them? J. Exp. Bot. 64, 143–160.

Ehdaie, B., Alloush, G.A., Madore, M.A., Waines, J.G., 2006. Genotypic variation for stem reserves and mobilization in wheat. Crop Sci. 46, 2093–2103.

Ehdaie, B., Alloush, G.A., Waines, J.G., 2008. Genotypic variation in linear rate of grain growth and contribution of stem reserves to grain yield in wheat. Field Crops Res. 106, 34–43.

Endelman, J.B., 2011. Ridge regression and other kernels for genomic selection with R package rrBLUP. Plant Genome J. 4, 250. https://doi.org/10.3835/plantgenome2011.08.0024

Friedman, J., Hastie, T., Tibshirani, R., 2009. glmnet: Lasso and elastic-net regularized generalized linear models. R Package Version 1.

Gao, L., Turner, M.K., Chao, S., Kolmer, J., Anderson, J.A., 2016. Genome wide association study of seedling and adult plant leaf rust resistance in elite spring wheat breeding lines. PLOS ONE 11, e0148671. https://doi.org/10.1371/journal.pone.0148671

Gaynor, R.C., 2015. Genomic selection for Kansas wheat (PhD Thesis). Kansas State University.

Gebbing, T., 2003. The enclosed and exposed part of the peduncle of wheat (Triticum aestivum)–spatial separation of fructan storage. New Phytol. 159, 245–252.

González-Camacho, J.M., Ornella, L., Pérez-Rodríguez, P., Gianola, D., Dreisigacker, S., Crossa, J., 2018. Applications of machine learning methods to genomic selection in breeding wheat for rust resistance. Plant Genome.

Guzman, C., Peña, R.J., Singh, R., Autrique, E., Dreisigacker, S., Crossa, J., Rutkoski, J., Poland, J., Battenfield, S., 2016. Wheat quality improvement at CIMMYT and the use of genomic selection on it. Appl. Transl. Genomics 11, 3–8. https://doi.org/10.1016/j.atg.2016.10.004

Haley, S.D., Quick, J.S., 1993. Early-generation selection for chemical desiccation tolerance in winter wheat. Crop Sci. 33, 1217–1223.

Hayes, B.J., Visscher, P.M., Goddard, M.E., 2009. Increased accuracy of artificial selection by using the realized relationship matrix. Genet. Res. 91, 47–60. https://doi.org/10.1017/S0016672308009981

Hayes, M.J., 2010. What is drought? National Drought Mitigation Center, University of Nebraska, Lincoln.

Heffner, E.L., Sorrells, M.E., Jannink, J.-L., 2009. Genomic Selection for Crop Improvement. Crop Sci. 49, 1–12. https://doi.org/10.2135/cropsci2008.08.0512

Housley, T.L., Kanabus, J., Carpita, N.C., 1989. Fructan synthesis in wheat leaf blades. J. Plant Physiol. 134, 192–195.

Jarquín, D., Lemes da Silva, C., Gaynor, R.C., Poland, J., Fritz, A., Howard, R., Battenfield, S., Crossa, J., 2017. Increasing genomic-enabled prediction accuracy by modeling genotype × environment interactions in Kansas wheat. Plant Genome 10. https://doi.org/10.3835/plantgenome2016.12.0130

Ji, X., Shiran, B., Wan, J., Lewis, D.C., Jenkins, C.L.D., Condon, A.G., Richards, R.A., Dolferus, R., 2010. Importance of pre-anthesis anther sink strength for maintenance of grain number during reproductive stage water stress in wheat. Plant Cell Environ. 33, 926–942. https://doi.org/10.1111/j.1365-3040.2010.02130.x

Keeling, P.L., Bacon, P.J., Holt, D.C., 1993. Elevated temperature reduces starch deposition in wheat endosperm by reducing the activity of soluble starch synthase. Planta 191, 342–348. https://doi.org/10.1007/BF00195691

Korte, A., Farlow, A., 2013. The advantages and limitations of trait analysis with GWAS: a review. Plant Methods 9, 29. https://doi.org/10.1186/1746-4811-9-29

Langmead, B., Salzberg, S.L., 2012. Fast gapped-read alignment with Bowtie 2. Nat. Methods 9, 357.

Liaw, A., Wiener, M., 2002. Classification and regression by randomForest. R News 2, 18–22.

Mathews, K.L., Chapman, S.C., Trethowan, R., Singh, R.P., Crossa, J., Pfeiffer, W., Van Ginkel, M., DeLacy, I., 2006. Global adaptation of spring bread and durum wheat lines near-isogenic for major reduced height genes. Crop Sci. 46, 603–613.

McIntyre, C.L., Seung, D., Casu, R.E., Rebetzke, G.J., Shorter, R., Xue, G.P., 2012. Genotypic variation in the accumulation of water soluble carbohydrates in wheat. Funct. Plant Biol. 39, 560–568.

Meuwissen, T.H.E., Hayes, B.J., Goddard, M.E., 2001. Prediction of total genetic value using genome-wide dense marker maps. Genetics 157, 1819–1829.

Musick, J.T., Jones, O.R., Stewart, B.A., Dusek, D.A., 1994. Water-yield relationships for irrigated and dryland wheat in the US Southern Plains. Agron. J. 86, 980–986.

Nicolas, M.E., Turner, N.C., 1993. Use of chemical desiccants and senescing agents to select wheat lines maintaining stable grain size during post-anthesis drought. Field Crops Res. 31, 155–171.

Ovenden, B., Milgate, A., Wade, L.J., Rebetzke, G.J., Holland, J.B., 2017. Genome-wide associations for water-soluble carbohydrate concentration and relative maturity in wheat using SNP and DArT marker arrays. G3 Genes Genomes Genet. g3–117.

Piaskowski, J.L., Brown, D., Campbell, K.G., 2016. Near-infrared calibration of soluble stem carbohydrates for predicting drought tolerance in spring wheat. Agron. J. 108, 285–293. https://doi.org/10.2134/agronj2015.0173

Plaut, Z., Butow, B.J., Blumenthal, C.S., Wrigley, C.W., 2004. Transport of dry matter into developing wheat kernels and its contribution to grain yield under post-anthesis water deficit and elevated temperature. Field Crops Res. 86, 185–198. https://doi.org/10.1016/j.fcr.2003.08.005

Poland, J., Rutkoski, J., 2016. Advances and challenges in genomic selection for disease resistance. Annu. Rev. Phytopathol. 54, 79–98.

Poland, J.A., Rife, T.W., 2012. Genotyping-by-Sequencing for Plant Breeding and Genetics. Plant Genome 5, 92–102. https://doi.org/10.3835/plantgenome2012.05.0005

Pradhan, G.P., Xue, Q., Jessup, K.E., Rudd, J.C., Liu, S., Devkota, R.N., Mahan, J.R., 2014. Cooler canopy contributes to higher yield and drought tolerance in new wheat cultivars. Crop Sci. 54, 2275–2284. https://doi.org/10.2135/cropsci2013.11.0788

Prakash, P., Kumari, A., Singh, D.V., Pandey, R., Sharma-Natu, P., Ghildiyal, M.C., 2009. Starch synthase activity and grain growth in wheat cultivars under elevated temperature: a comparison of responses. Indian J Plant Physiol 14, 364–369.

Prasad, P.V.V., Staggenborg, S.A., Ristic, Z., 2008. Impacts of drought and/or heat stress on physiological, developmental, growth, and yield processes of crop plants. Response Crops Ltd. Water Underst. Model. Water Stress Eff. Plant Growth Process. 301–355.

Rattey, A., Shorter, R., Chapman, S., Dreccer, F., van Herwaarden, A., 2009. Variation for and relationships among biomass and grain yield component traits conferring improved yield and grain weight in an elite wheat population grown in variable yield environments. Crop Pasture Sci. 60, 717–729.

Rawson, H.M., Evans, L.T., 1971. The contribution of stem reserves to grain development in a range of wheat cultivars of different height. Aust. J. Agric. Res. 22, 851–863.

Rebetzke, G.J., Van Herwaarden, A.F., Jenkins, C., Weiss, M., Lewis, D., Ruuska, S., Tabe, L., Fettell, N.A., Richards, R.A., 2008. Quantitative trait loci for water-soluble carbohydrates and associations with agronomic traits in wheat. Aust. J. Agric. Res. 59, 891–905.

Reynolds, M., Manes, Y., Izanloo, A., Langridge, P., 2009. Phenotyping approaches for physiological breeding and gene discovery in wheat. Ann. Appl. Biol. 155, 309–320.

Roberts, C.A., Workman, J., Reeves, J.B., 2004. Near-infrared spectroscopy in agriculture. American Society of Agronomy Madison.

Rutkoski, J., Benson, J., Jia, Y., Brown-Guedira, G., Jannink, J.-L., Sorrells, M., 2012. Evaluation of genomic prediction methods for fusarium head blight resistance in wheat. Plant Genome 5, 51–61. https://doi.org/10.3835/plantgenome2012.02.0001

Rutkoski, J.E., Poland, J., Jannink, J.-L., Sorrells, M.E., 2013. Imputation of unordered markers and the impact on genomic selection accuracy. G3 Genes Genomes Genet. 3, 427–439.

Rutkoski, J.E., Poland, J.A., Singh, R.P., Huerta-Espino, J., Bhavani, S., Barbier, H., Rouse, M.N., Jannink, J.-L., Sorrells, M.E., 2014. Genomic selection for quantitative adult plant stem rust resistance in wheat. Plant Genome 7. https://doi.org/10.3835/plantgenome2014.02.0006

Ruuska, S.A., Rebetzke, G.J., Herwaarden, A.F. van, Richards, R.A., Fettell, N.A., Tabe, L., Jenkins, C.L.D., 2006. Genotypic variation in water-soluble carbohydrate accumulation in wheat. Funct. Plant Biol. 33, 799–809. https://doi.org/10.1071/FP06062

Salem, K., Röder, M., Börner, A., 2007. Identification and mapping quantitative trait loci for stem reserve mobilisation in wheat (Triticum aestivum L.). Cereal Res. Commun. 35, 1367–1374.

Schnyder, H., 1993. The role of carbohydrate storage and redistribution in the source-sink relations of wheat and barley during grain filling—a review. New Phytol. 123, 233–245.

Shearman, V.J., Sylvester-Bradley, R., Scott, R.K., Foulkes, M.J., 2005. Physiological processes associated with wheat yield progress in the UK. Crop Sci. 45, 175–185.

Snape, J.W., Foulkes, M.J., Simmonds, J., Leverington, M., Fish, L.J., Wang, Y., Ciavarrella, M., 2007. Dissecting gene x environmental effects on wheat yields via QTL and physiological analysis. Euphytica 154, 401–408.

Stone, P.J., Nicolas, M.E., 1994. Wheat cultivars vary widely in their responses of grain yield and quality to short periods of post-anthesis heat stress. Funct. Plant Biol. 21, 887–900. https://doi.org/10.1071/pp9940887

Tack, J., Barkley, A., Nalley, L.L., 2014. Heterogeneous effects of warming and drought on selected wheat variety yields. Clim. Change 125, 489–500. https://doi.org/10.1007/s10584-014-1185-1

Tang, Y., Liu, X., Wang, J., Li, M., Wang, Q., Tian, F., Su, Z., Pan, Y., Liu, D., Lipka, A.E., 2016. GAPIT version 2: an enhanced integrated tool for genomic association and prediction. Plant Genome 9.

Thomson, M.J., 2014. High-throughput SNP genotyping to accelerate crop improvement. Plant Breed. Biotechnol. 2, 195–212. https://doi.org/10.9787/PBB.2014.2.3.195

Tian, B., Talukder, S.K., Fu, J., Fritz, A.K., Trick, H.N., 2018. Expression of a rice soluble starch synthase gene in transgenic wheat improves the grain yield under heat stress conditions. Vitro Cell. Dev. Biol. - Plant 54, 216–227. https://doi.org/10.1007/s11627-018-9893-2

Trethowan, R., Pfeiffer, W.H., 2000. Challenges and future strategies in breeding wheat for adaptation to drought stressed environments: A CIMMYT wheat program perspective. Mol. Approaches Genet. Improv. Cereals Stable Prod. Water-Ltd. Environ. 21–25.

van Herwaarden, A., Richards, R., Angus, J.F., 2003. Water soluble carbohydrates and yield in wheat, in: Proceedings of the 11th Australian Agronomy Conference'.(The Australian Society of Agronomy: Geelong).

Villareal, R.L., Bañuelos, O., Mujeeb-Kazi, A., Rajaram, S., 1998. Agronomic performance of chromosomes 1B and T1BL.1RS near-isolines in the spring bread wheat Seri M82. Euphytica 103, 195–202. https://doi.org/10.1023/A:1018392002909

Villareal, R.L., Toro, E. del, Mujeeb-Kazi, A., Rajaram, S., 1995. The 1BL/1RS chromosome translocation effect on yield characteristics in a Triticum aestivum L. cross. Plant Breed. 114, 497–500. https://doi.org/10.1111/j.1439-0523.1995.tb00843.x

Wang, Z., Liu, X., Li, R., Chang, X., Jing, R., 2011. Development of near-infrared reflectance spectroscopy models for quantitative determination of water-soluble carbohydrate content in wheat stem and glume. Anal. Lett. 44, 2478–2490. https://doi.org/10.1080/00032719.2011.551859

Wardlaw, I.F., Willenbrink, J., 2000. Mobilization of fructan reserves and changes in enzyme activities in wheat stems correlate with water stress during kernel filling. New Phytol. 148, 413–422.

Wardlaw, I.F., Willenbrink, J., 1994. Carbohydrate storage and mobilisation by the culm of wheat between heading and grain maturity: the relation to sucrose synthase and sucrose-phosphate synthase. Funct. Plant Biol. 21, 255–271.

Wehrens, R., Mevik, B.-H., 2007. The pls package: principal component and partial least squares regression in R.

Wolf, E.D.D., Lollato, R., Whitworth, R.J., 2018. Wheat variety disease and insect ratings 2018 (No. MF991). K-State Research and Extension.

Xue, G.-P., McIntyre, C.L., Jenkins, C.L., Glassop, D., van Herwaarden, A.F., Shorter, R., 2008. Molecular dissection of variation in carbohydrate metabolism related to water-soluble carbohydrate accumulation in stems of wheat. Plant Physiol. 146, 441–454.

Yang, D.-L., Jing, R.-L., Chang, X.-P., Li, W., 2007. Identification of quantitative trait loci and environmental interactions for accumulation and remobilization of water-soluble carbohydrates in wheat (Triticum aestivum L.) stems. Genetics.

Yemm, E.W., Willis, A.J., 1954. The estimation of carbohydrates in plant extracts by anthrone. Biochem. J. 57, 508.

Zadoks, J.C., Chang, T.T., Konzak, C.F., 1974. A decimal code for the growth stages of cereals. Weed Res. 14, 415–421.

Figure 3-1 Weather showing average of monthly maximum temperature (Tmax in ºC), minimum temperature (Tmin in ºC), sum of monthly precipitation (Pcp in mm), and normal monthly precipitation is from 1981 to 2010 in Colby (top) and Hays (bottom).

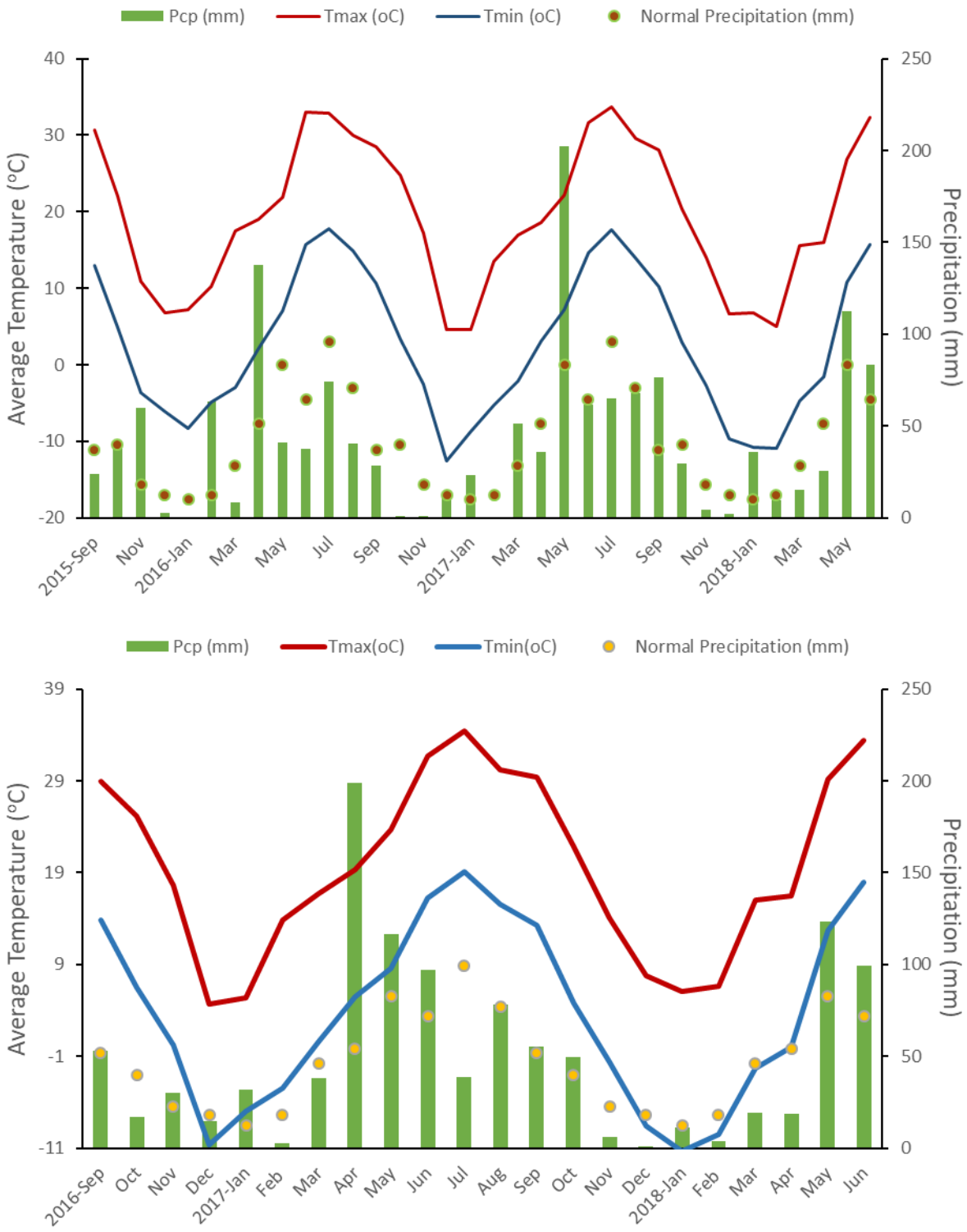

Figure 3-2 Standard curve to determine the sugar concentration in samples using glucose as a standard. Standard curve was prepared in each microplate and these three (a), (b), and (c) randomly chosen to display very low plate to plate variation among them. Each data point is an average of four readings in microplate from two technical replicates.

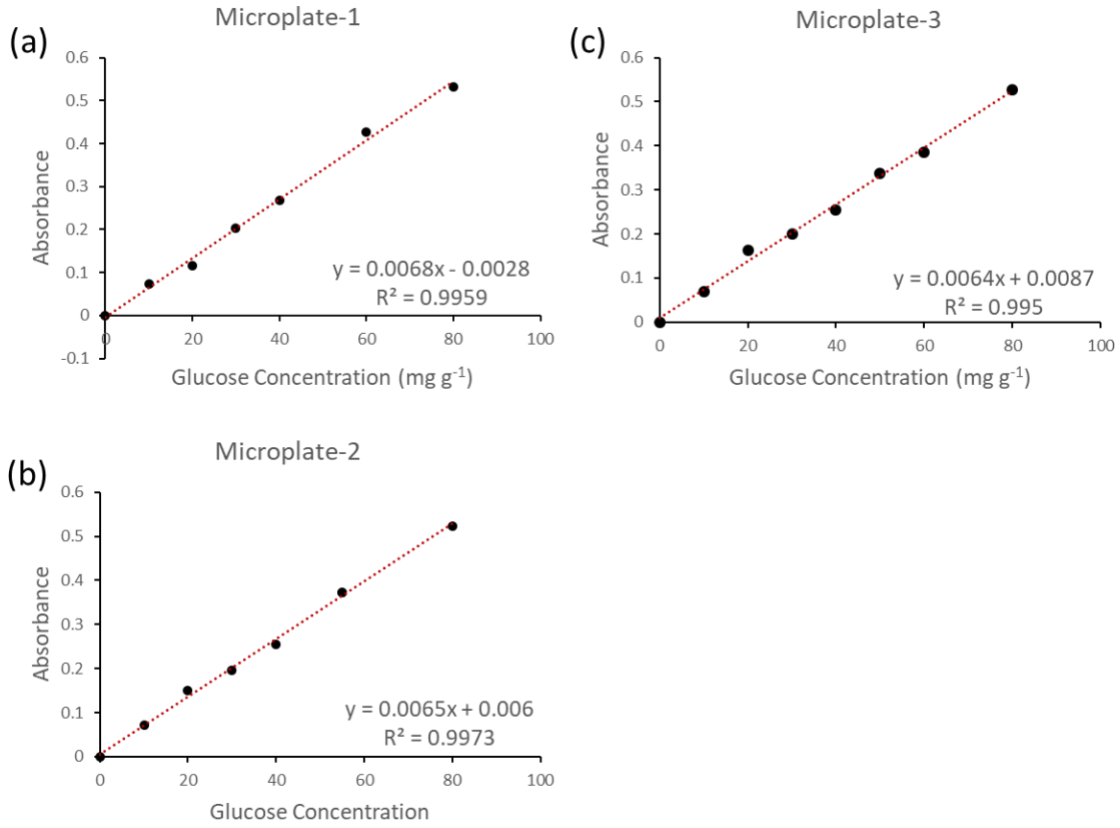

Figure 3-3 The correlation diagram between the predicted values of WSC from the model and actual values measured from the lab analysis in 2016. Each data point represents individual sample of diverse breeding lines or varieties grown under irrigated or water-limited environments.

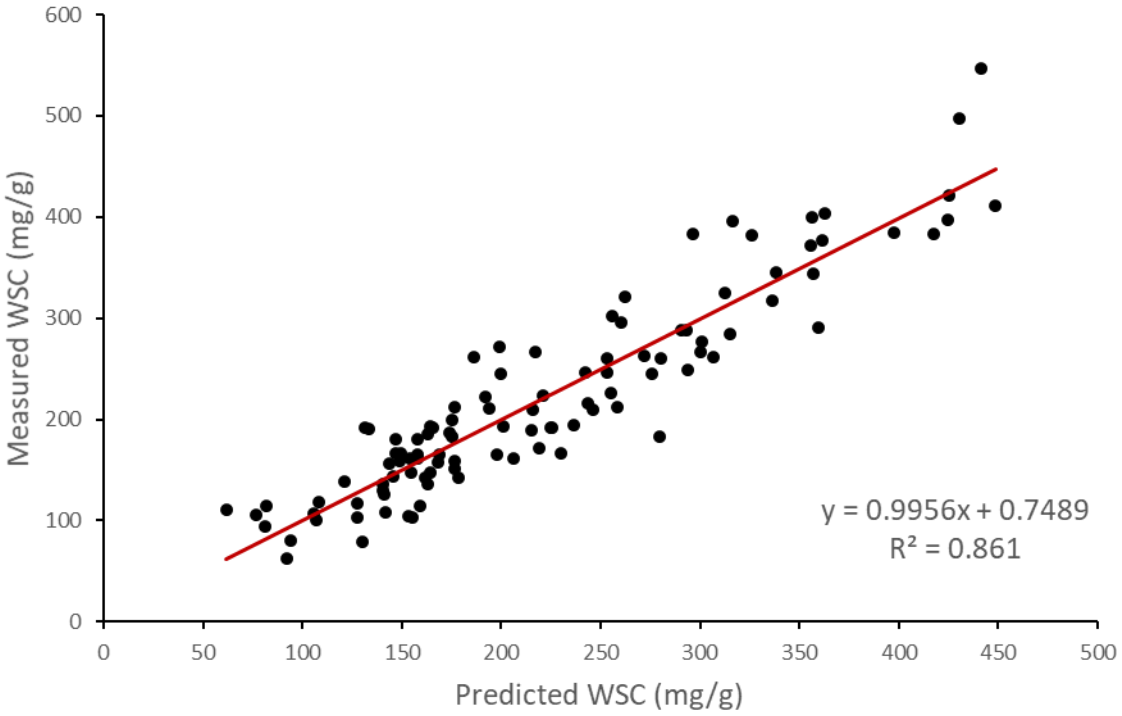

Figure 3-4 (a) Average WSC concentration on 400 diverse winter wheat genotypes and 30 varieties evaluated from top (peduncle and top internode) and bottom (below top internode) from 1512 plots planted in 2016. (b) Relationship between bottom and top WSC concentration. The genotypes were harvested 15 days after mid-flowering period. Triple asterisks (***) indicates the significance at <0.001 level of probability.

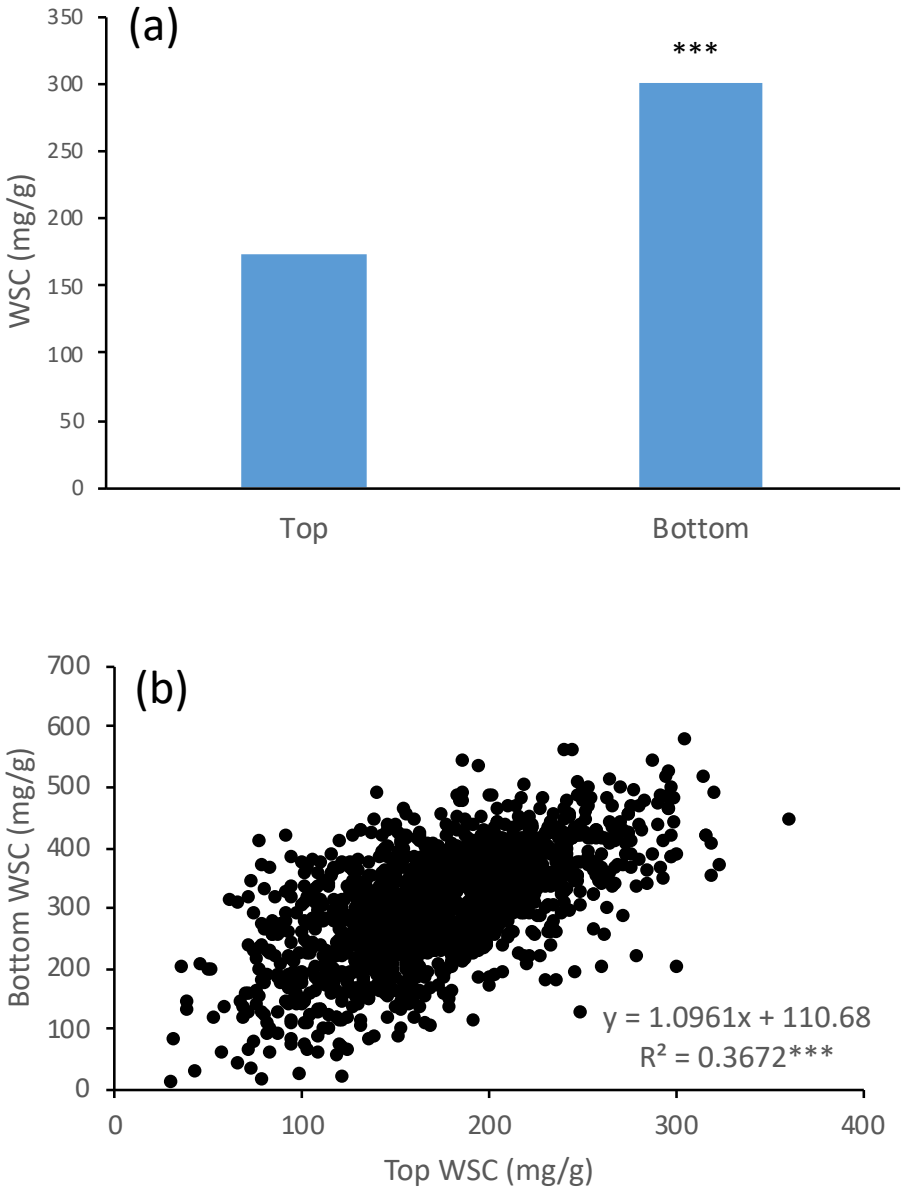

Figure 3-5 Correlation scatterplot of Pearson Correlation between WSC calculated across seven different environments in three years 2016, 2017, and 2018. From bottom right 2016 Colby irrigated (16coi) and Colby water-limited (16cod), 2017 Colby irrigated (17coi) and hays rainfed (17hays), 2018 Colby irrigated (18coi), Colby water-limited (18cod), and Hays rainfed (18hays). Each point is an average of four replicates for that year and location. Correlation value is presented on the top and the bottom is the scatterplot with the fitted line. Single (*), double (**) or Triple asterisks (***) indicates the significance at 0.05, 0.01 or <0.001 level of probability.

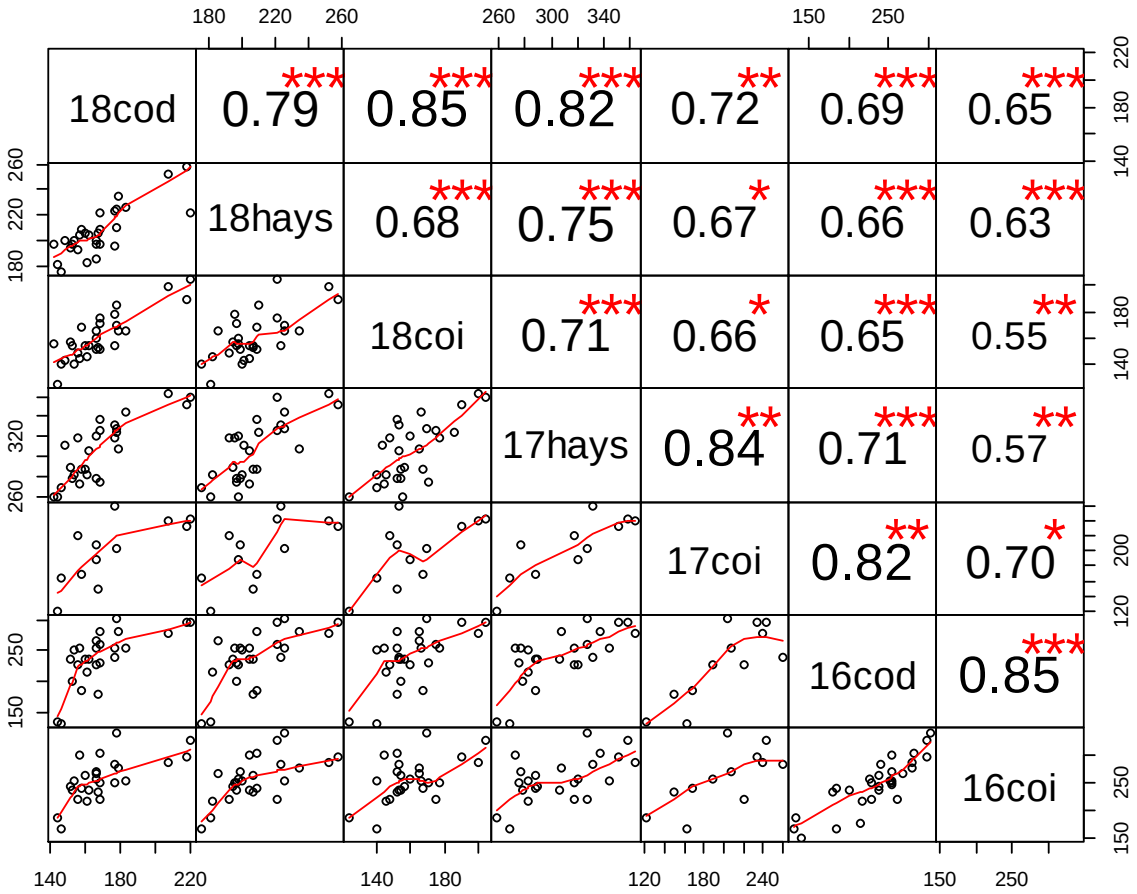

Figure 3-6 Relationship between WSC concentration on 400 diverse winter wheat genotypes and 30 varieties evaluated in irrigated and water-limited environment in 2016. The genotypes were harvested 15 days after mid-flowering period. Triple asterisks (***) indicates the significance at <0.001 level of probability.

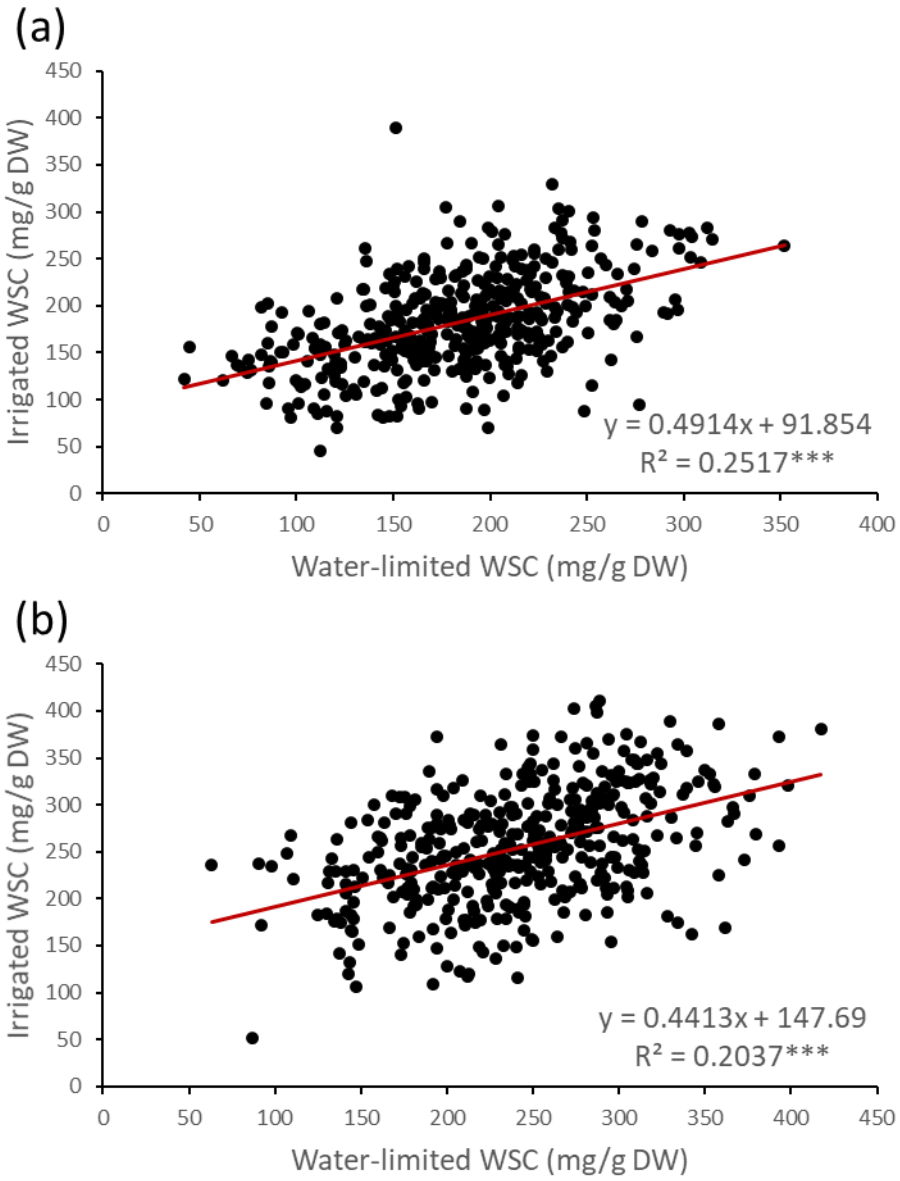

Figure 3-7 Relationship between thousand kernel weight (TKW[g]), and water-soluble carbohydrates (WSC) concentration in (a) Hays 2017 and (b) Hays 2018; WSC content/stem in (c) Colby irrigated 2018 and (d) Colby water-limited 2018. The single (*), double (**) or Triple asterisks (***) indicates the significance at <0.05, <0.01 or <0.001 level of probability, respectively. † indicates marginally significant (<0.1 level of probability).

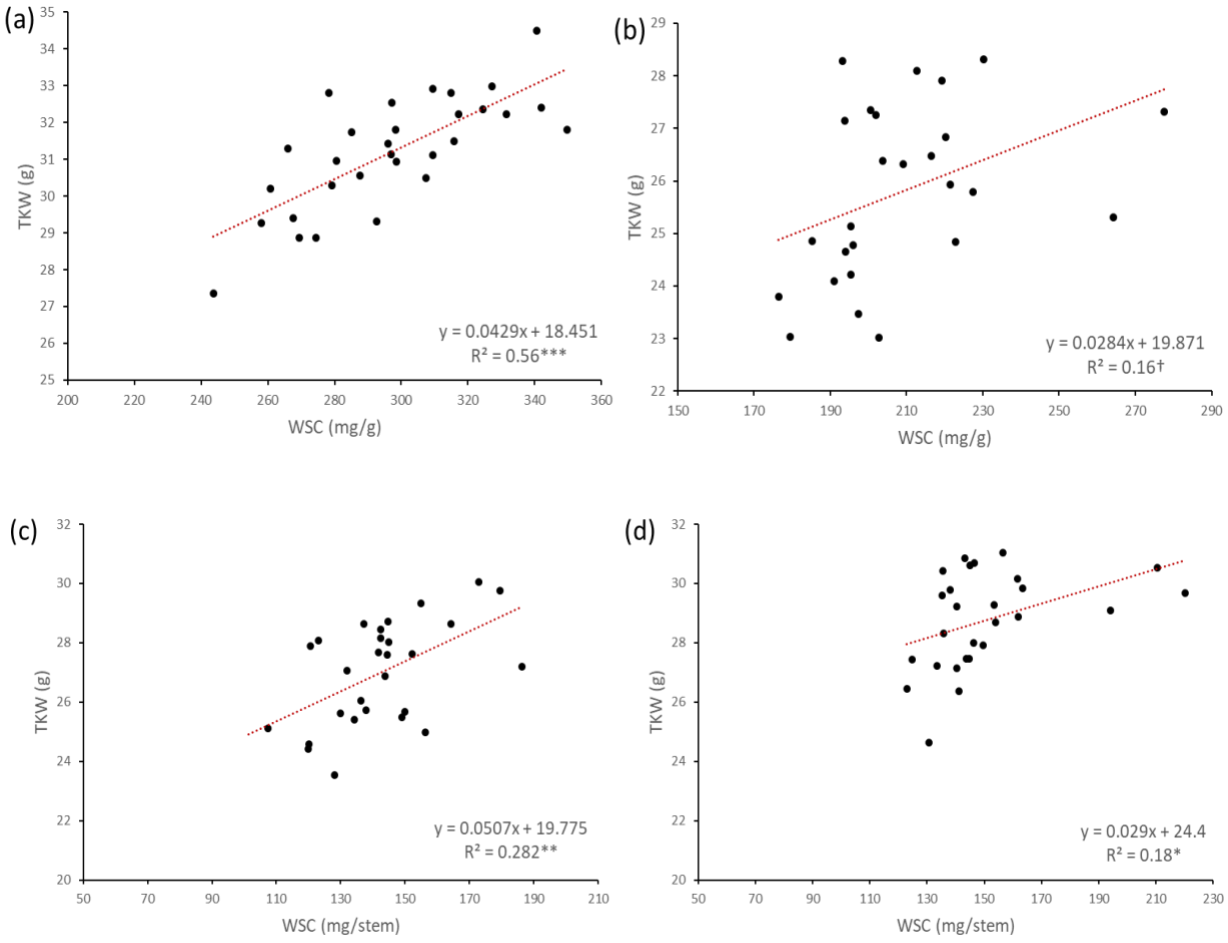

Figure 3-8 Grain yield (tonnes ha^{-1}) under control and terminal drought stress in 2018 (a) Colby irrigated, (b) Colby water-limited, and (c) Hays rainfed. The single (*), double (**) or Triple asterisks (***) indicates the significance at <0.05, <0.01 or <0.001 level of probability, respectively. The number preceding asterisks indicates average percent decline in yield for that genotype under desiccation treatment compared to control.

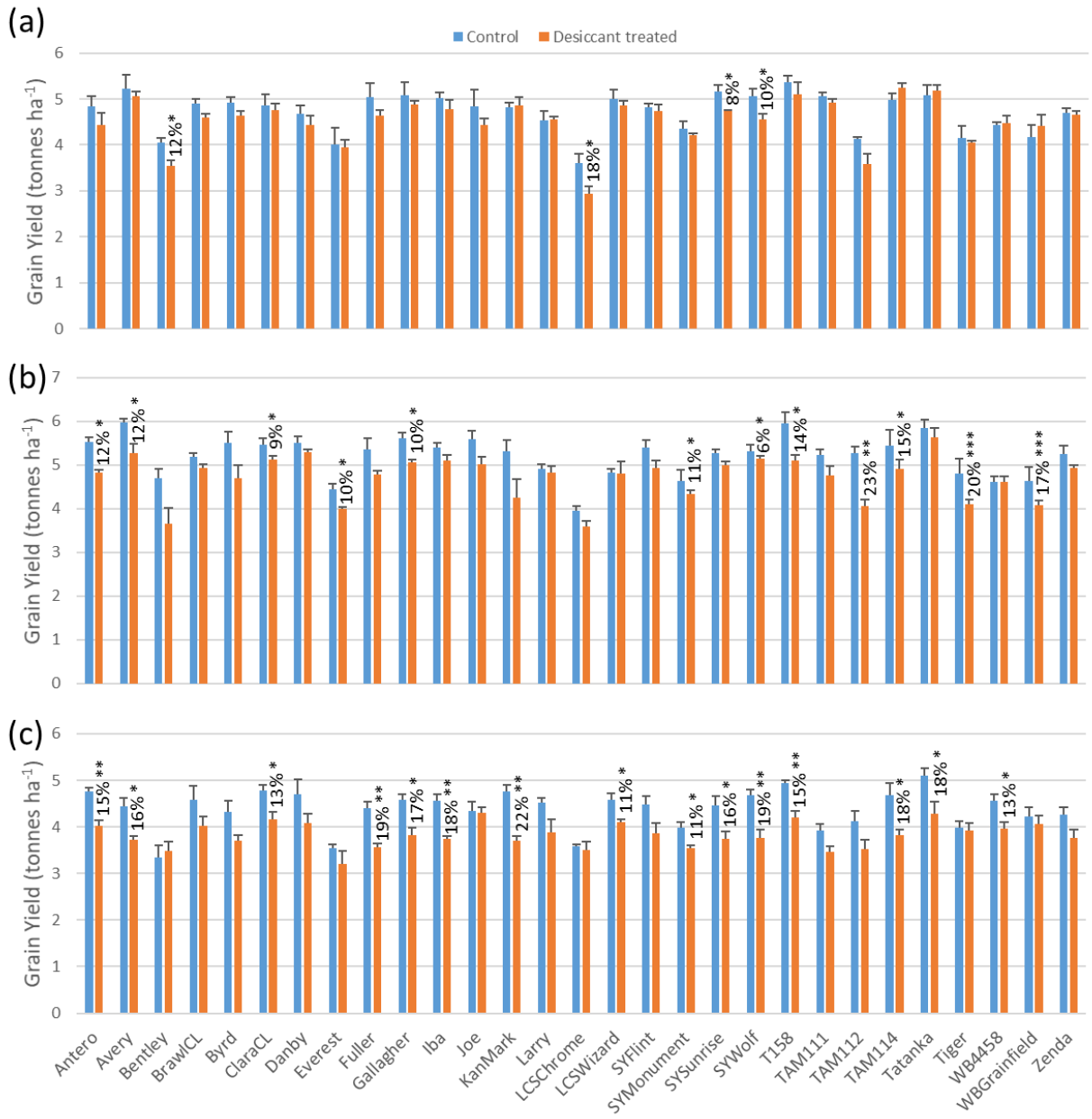

Figure 3-9 Thousand Kernel Weight (TKW [g]) under control and desiccation treatment in 2018 (a) Colby irrigated, (b) Colby water-limited, and (c) Hays rainfed.

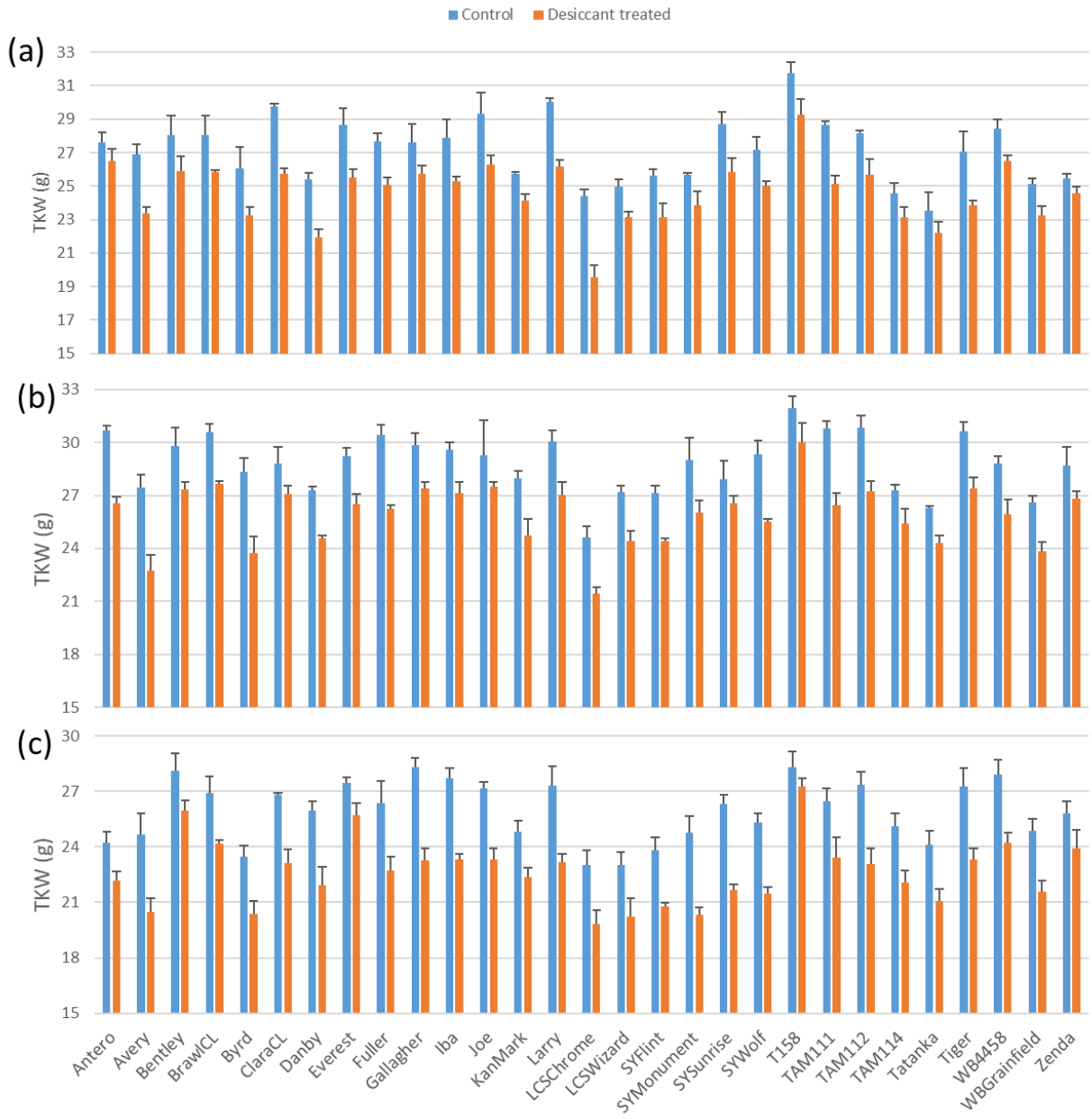

Figure 3-10 Test weight (kg) under control and desiccation treatment in 2018 (a) Colby irrigated, (b) Colby water-limited, and (c) Hays rainfed.

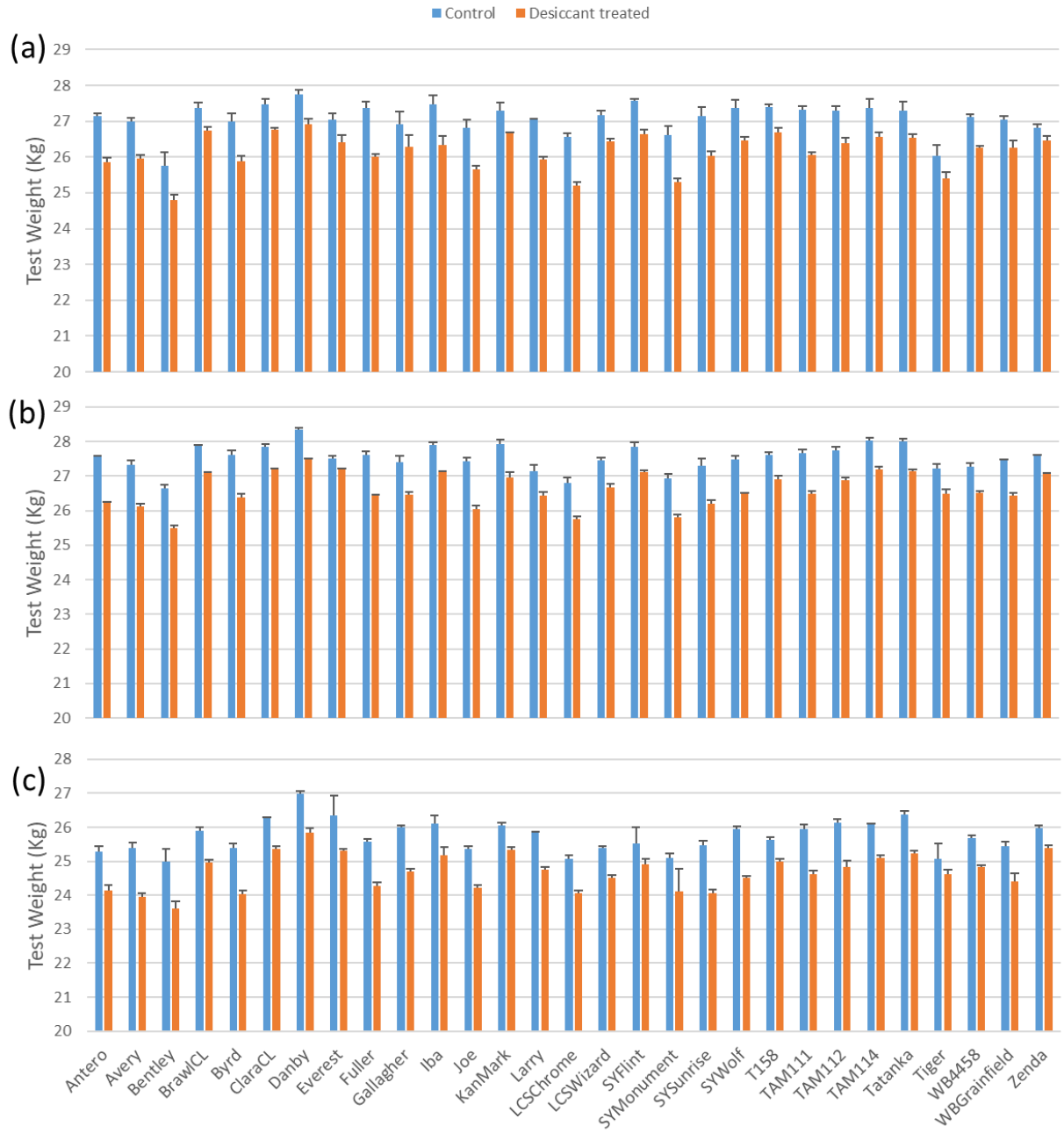

Figure 3-11 Protein (%) under control and desiccation treatment in 2018 (a) Colby irrigated, (b) Colby water-limited, and (c) Hays rainfed.

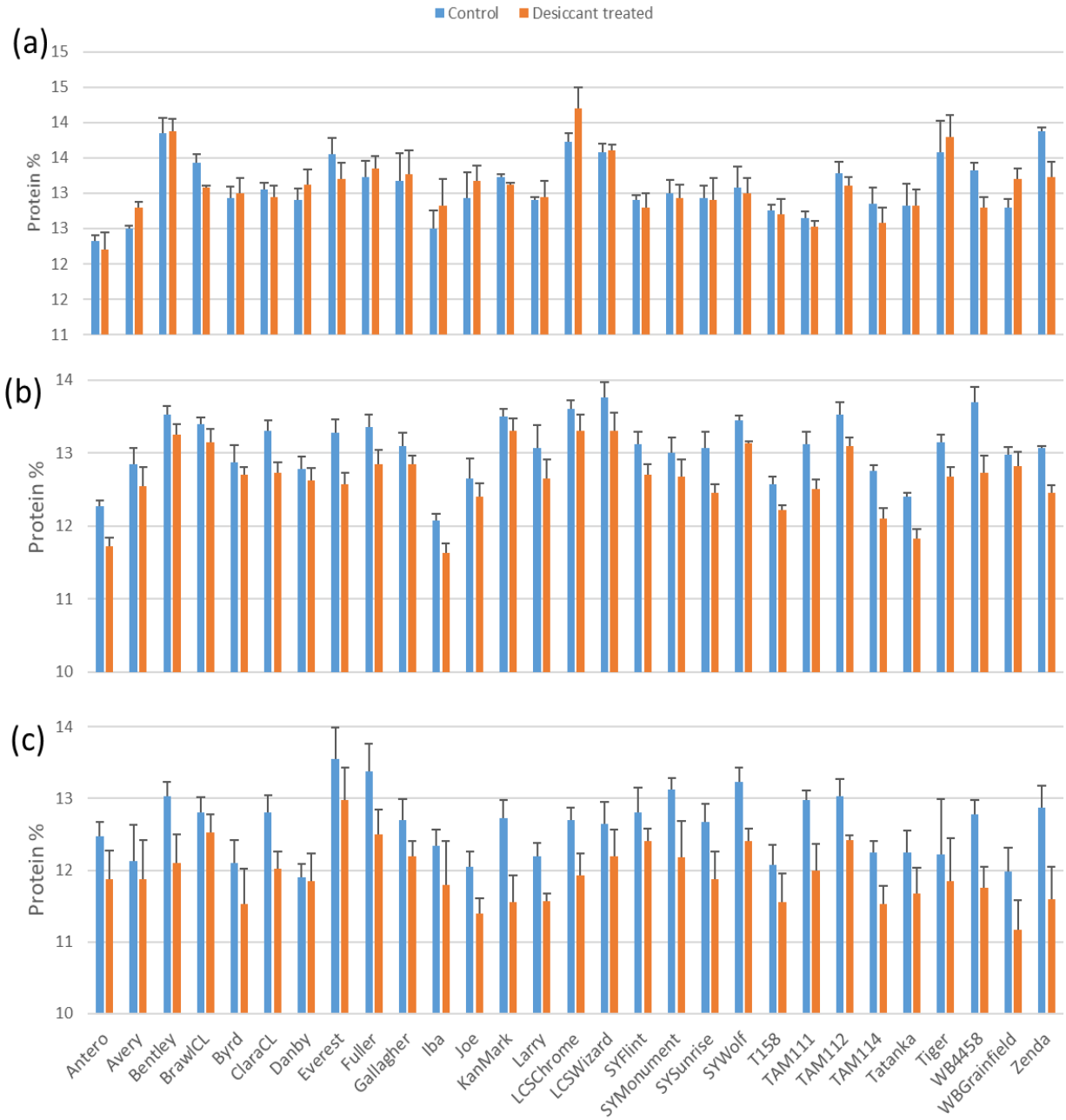

Figure 3-12 Role of WSC in maintaining grain yield in 2018 (a) COI (b) COD (c) Hays. Y-axis represent average decline in grain weight (kg ha^{-1}) under desiccation treatment and X-axis is the average WSC concentration (mg/g). The single (*) and double asterisks (**) indicates the significance at <0.05 and <0.01 level of probability, respectively.

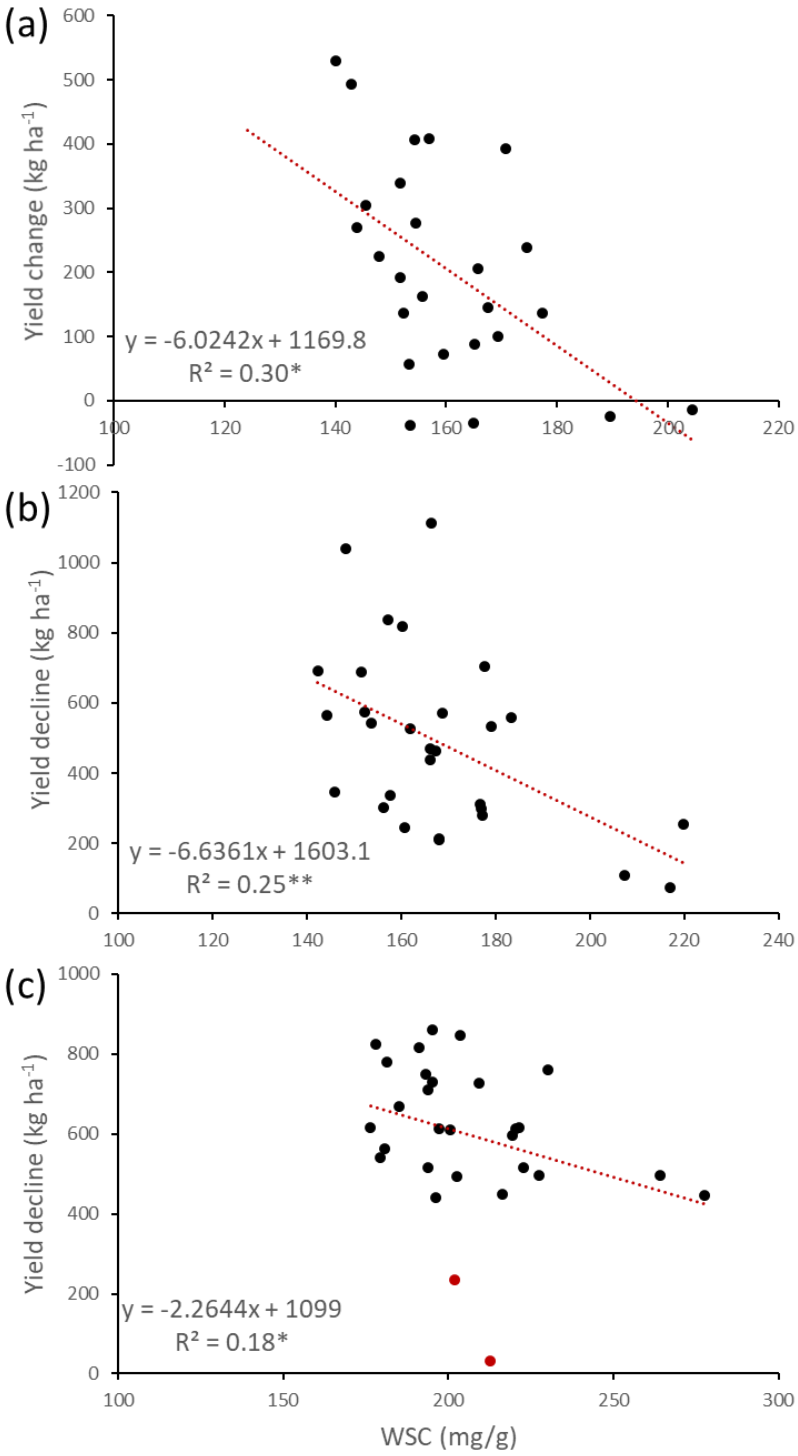

Figure 3-13 Relationship between stem number per m^2 and individual stem weight (g) in varieties from location (a) COI (b) COD, and (c) Hays. The single (*), double (**) or Triple asterisks (***) indicates the significance at <0.05, <0.01 or <0.001 level of probability, respectively.

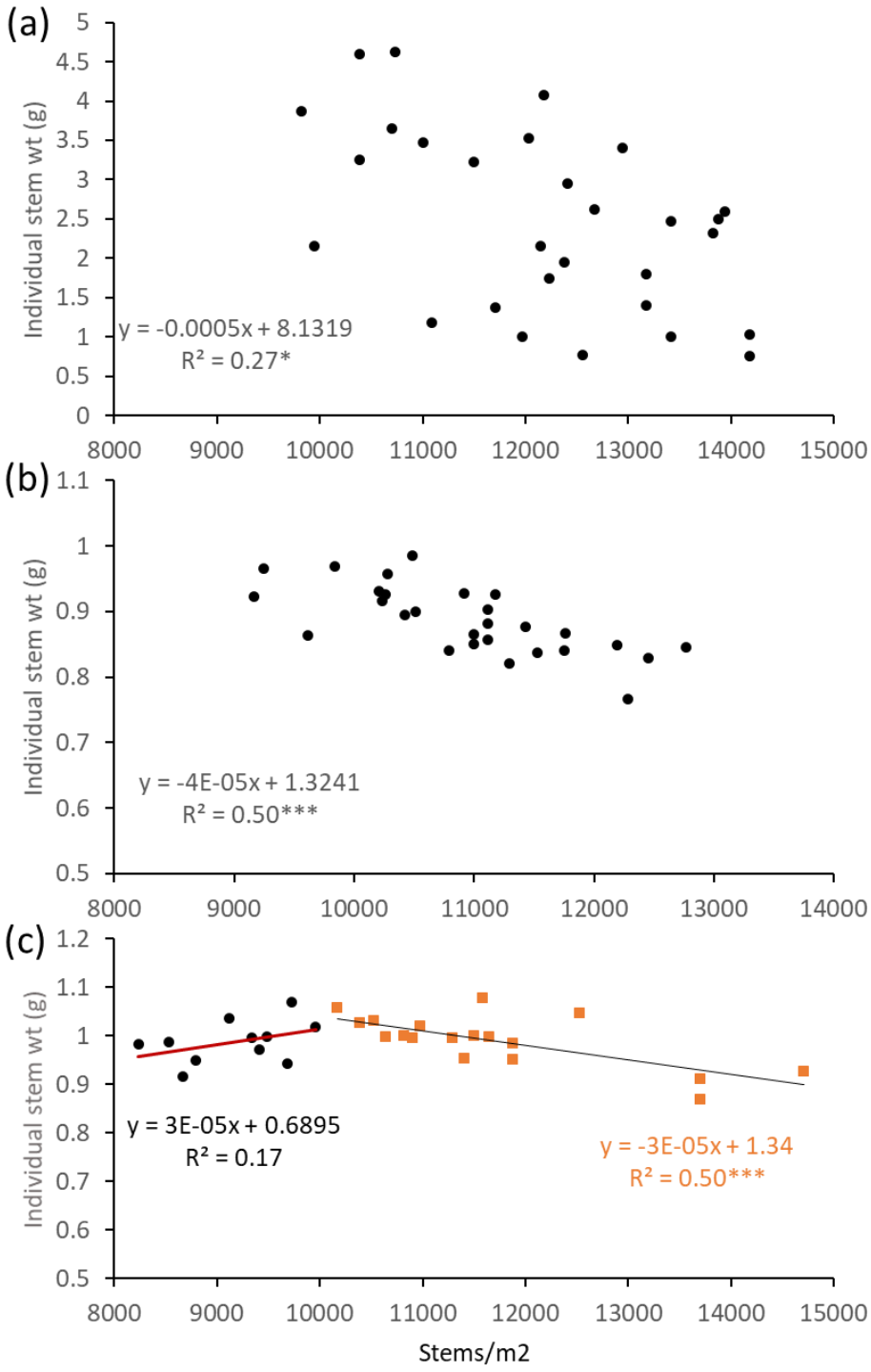

Figure 3-14 Relationship between average WSC concentration (mg/g) with (a) Plant height (cm) in Hays 2018, (b) Stand rating in Hays 2018, (c) Plant height (cm) in Hays 2017, and (d) Plant height (cm) of tallest 20 plants in Hays 2017. The single (*), double (**) or Triple asterisks (***) indicates the significance at <0.05, <0.01 or <0.001 level of probability, respectively.

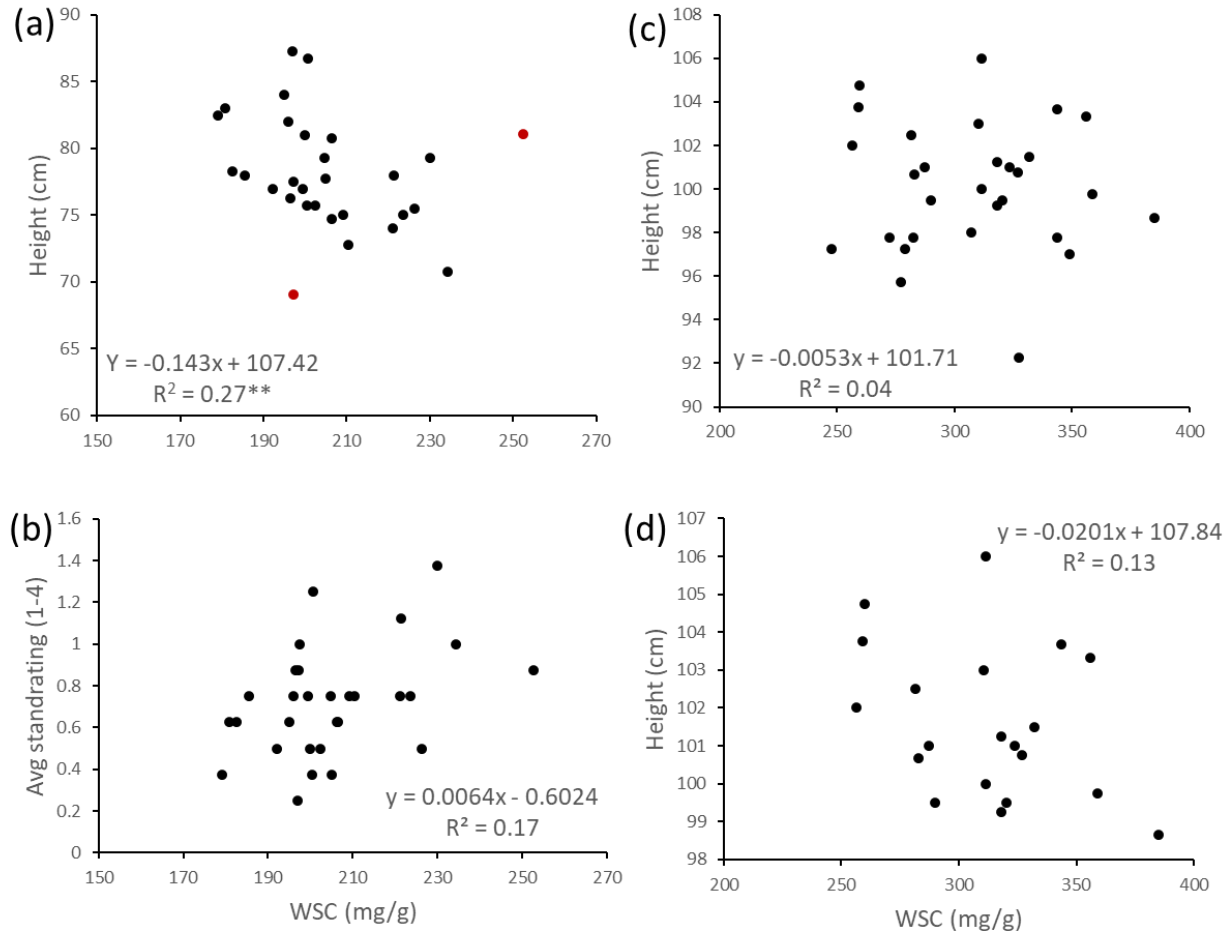

Figure 3-15 SNP markers distribution across chromosome. The y-axis represent marker counts and X-axis represent the physical position in the wheat genome for 409 genotypes and 34,000 markers.

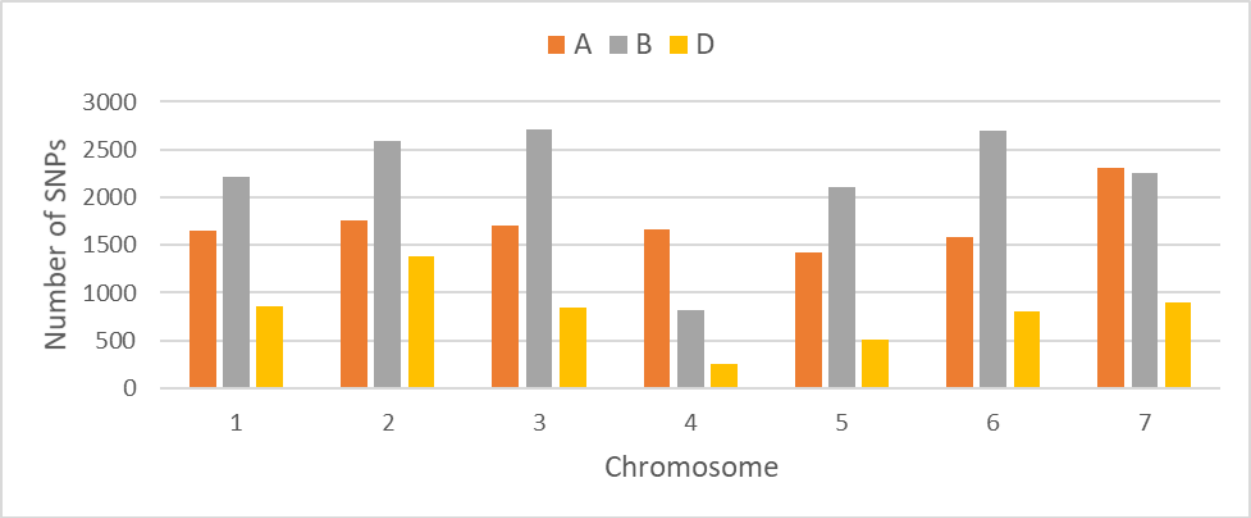

Figure 3-16 SNP density in each wheat chromosome.

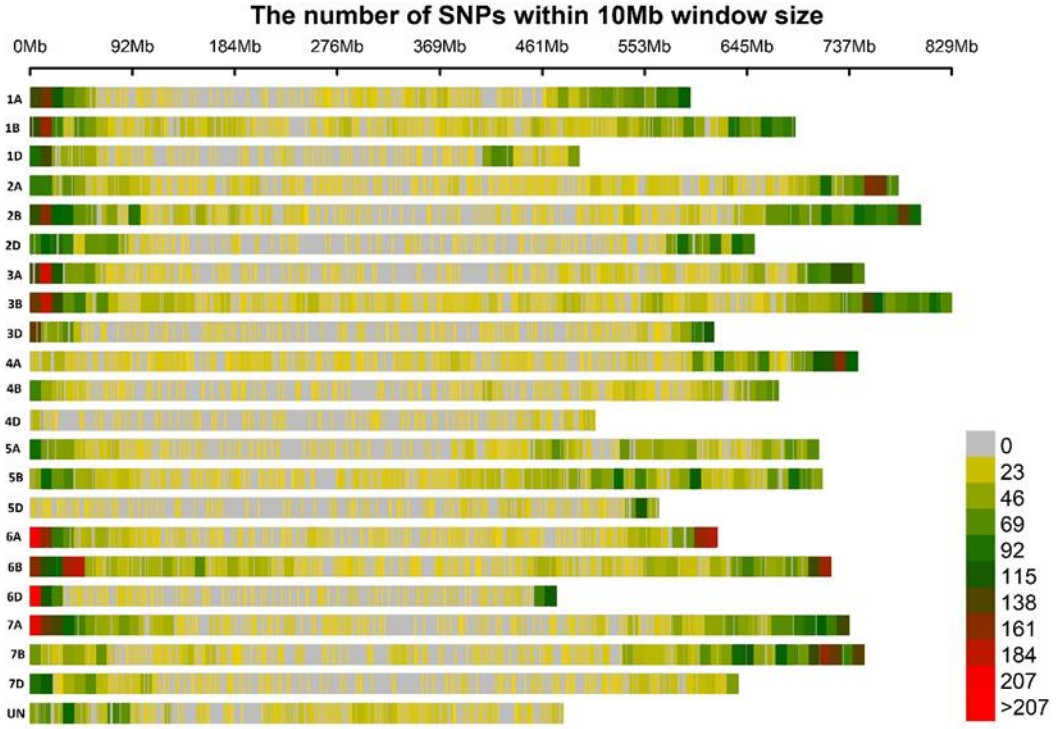

Figure 3-17 Principal components analysis of a wheat association panel based on 34,000 SNP markers tested on 2016. The black and red dot represent breeding lines from Manhattan and Hays wheat breeding program, and the green dots are the varieties.

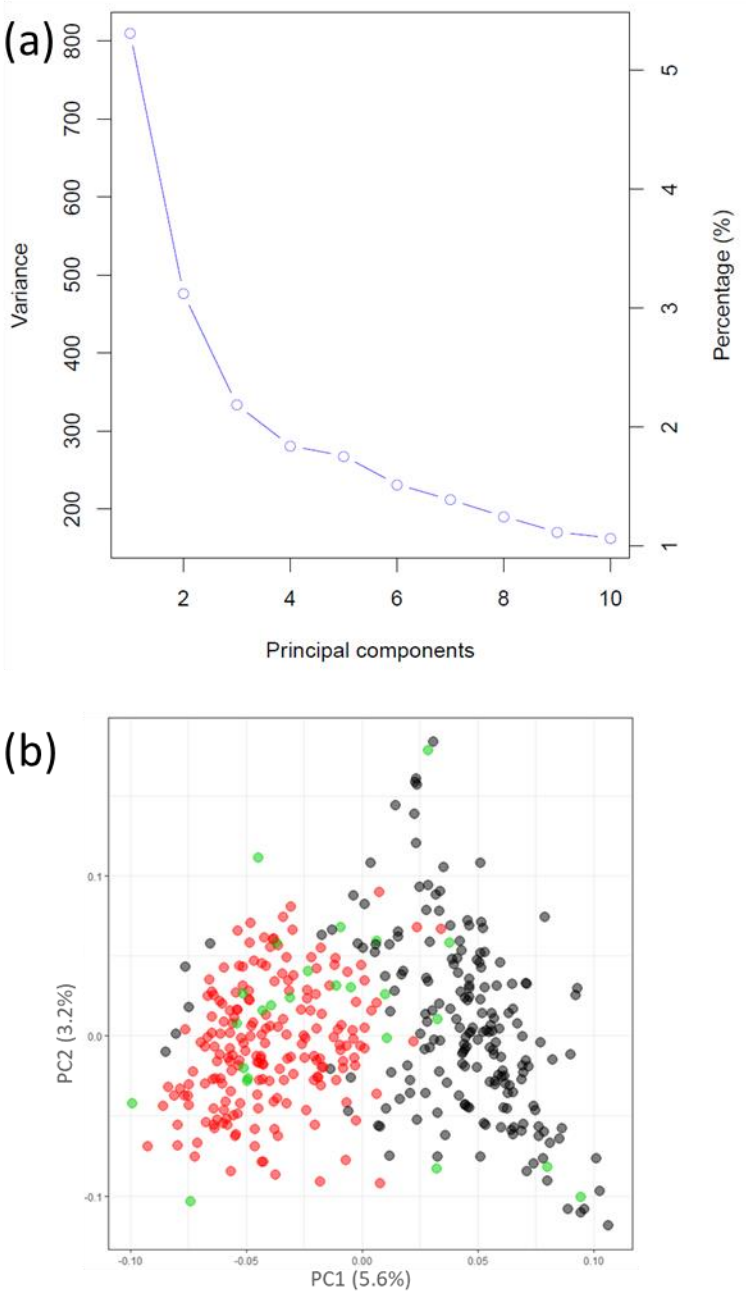

Figure 3-18 Manhattan plot showing association from the results of average WSC concentration in the stem, WSC concentration in the top (Twsc), and bottom (Bwsc) part of the stem from diverse wheat breeding lines based on 34,000 SNP markers. The x-axis represents physical position of SNPs in the wheat genome and y-axis represents $-\log_{10}$ of P-values. Top solid line at FDR 10%, and bottom dotted line at 0.0004 level of probability.

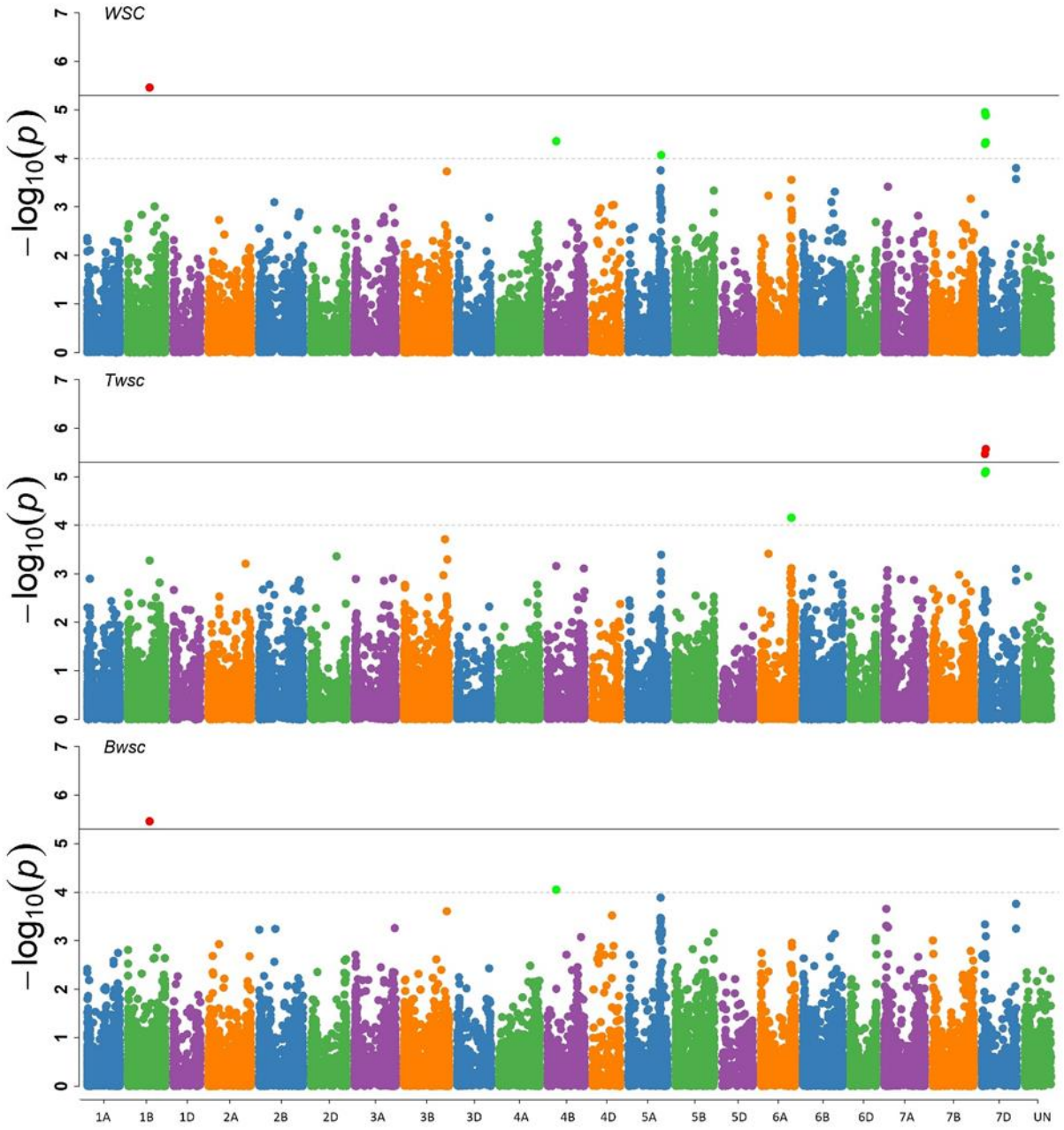

Figure 3-19 Combined Manhattan plot showing association results of average WSC concentration in the stem, WSC concentration in the top (Twsc), and bottom (Bwsc) part of the stem from diverse wheat breeding lines based on 34,000 SNP markers. The x-axis represents physical position of SNPs in the wheat genome and y-axis represents $-\log_{10}$ of P-values. Top solid line represents FDR 10% and bottom dotted line at 0.0004 level of probability.

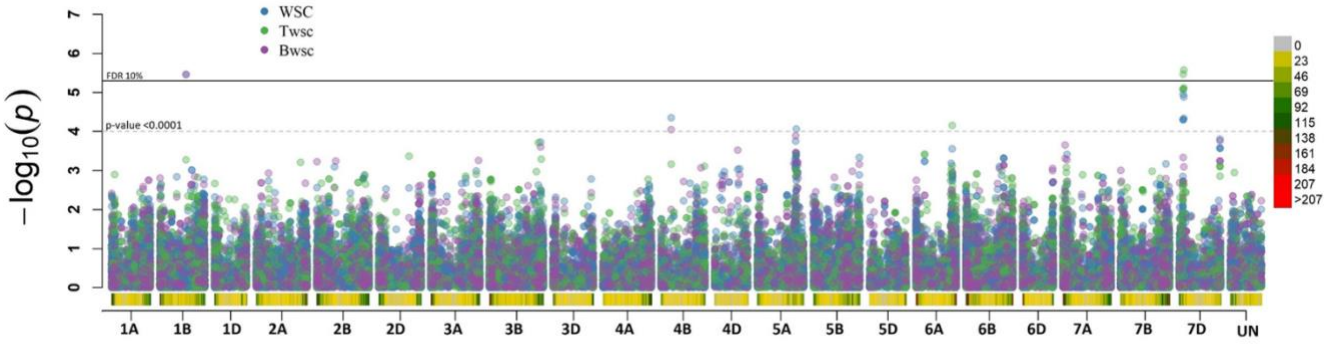

Figure 3-20 Haplotype analysis of QTL 7DS. (a) The five haplotype group and the number of genotypes without any missing SNPs at the region analyzed (b) Top WSC (TWSC) concentration, and (c) Bottom WSC (BWSC) concentration in genotypes having two most common haplotic group ACCCCG and GCTCCG. The double (**) or Triple asterisks (***) indicates the significant difference in WSC between two haplotype groups at <0.01 or <0.001 level of probability, respectively.

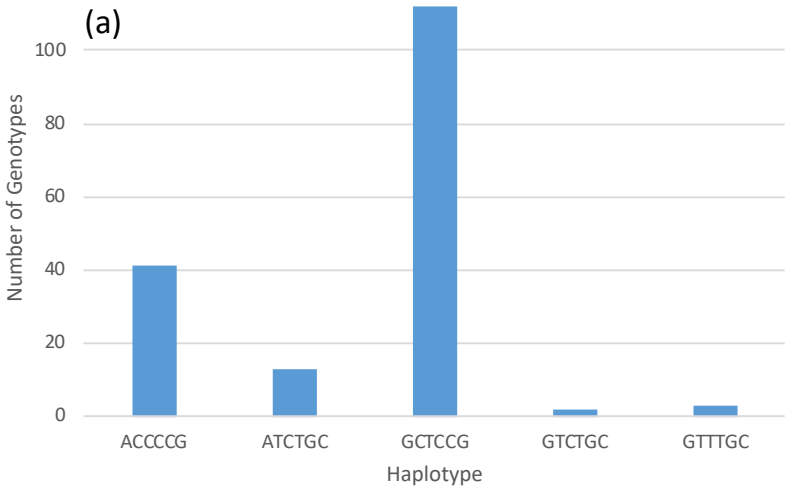

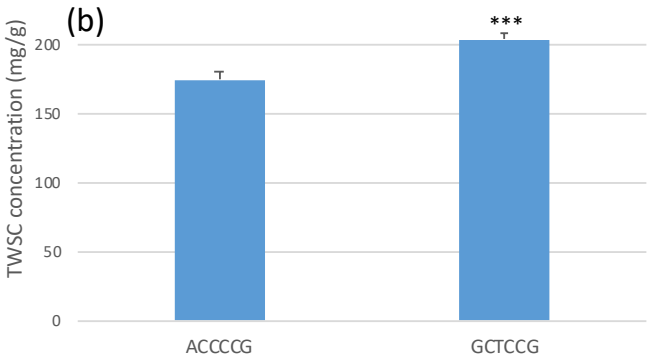

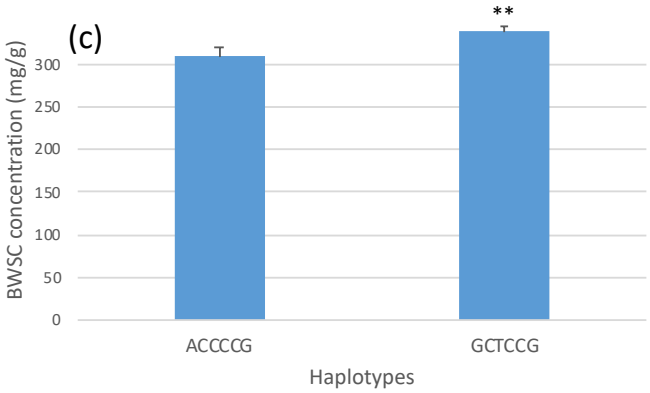

Figure 3-21 Prediction accuracies in diverse winter wheat genotypes using four genomic selection models: RRBLUP: Ridge regression best linear unbiased predictor, RF: Random Forest, PLSR: Partial Least Square Regression, ELNET: Elastic net, and AVE: average prediction across all four GS models. The model was randomly iterated 100 times.

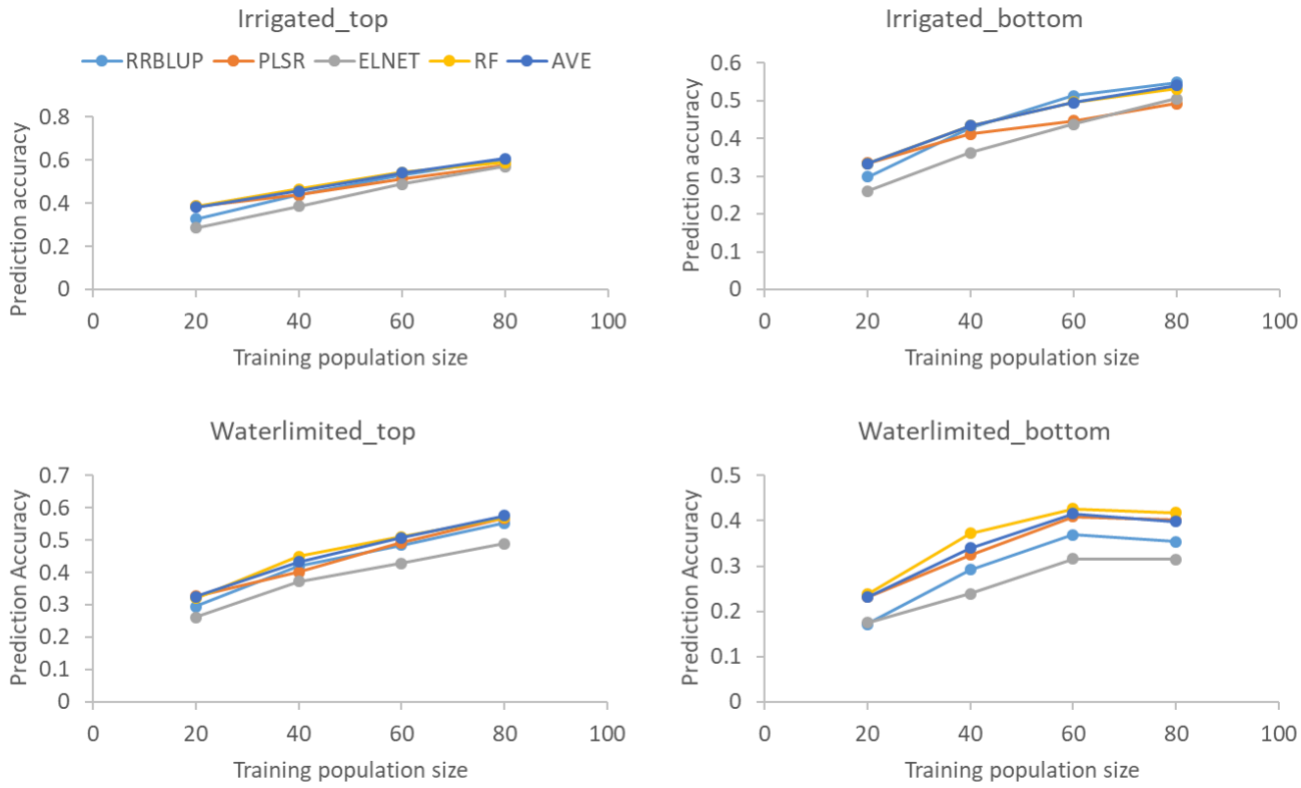

Table 3-1 List of 30 winter wheat varieties planted in three wheat growing seasons 2015/2016, 2016/2017 and 2017/2018 in western Kansas. Four varieties were different in the second two years because of not having enough seed. The different varieties in two years are marked in bold.

2015/2016	**2016/17 & 2017/18**
Antero	Antero
Armour	**Avery**
Bill Brown	**Bentley**
Billings	**SY Grit**
Brawl CL	Brawl CL
Byrd	Byrd
Clara CL	Clara CL
Danby	Danby
Everest	Everest
Fuller	Fuller
Gallagher	Gallagher
Iba	Iba
Joe	Joe
KanMark	KanMark
Tatanka	Tatanka
Larry	Larry
LCS Chrome	LCS Chrome
LCS Wizard	LCS Wizard
Santa Fe	**SY Sunrise**
SY Flint	SY Flint
SY Monument	SY Monument
SY Wolf	SY Wolf
T158	T158
TAM 111	TAM 111
TAM 112	TAM 112
TAM 114	TAM 114
Tiger	Tiger
WB 4458	WB 4458
WB Grainfield	WB Grainfield
Zenda	Zenda

Table 3-2 Planting and harvesting information of varieties where COD is Coly dry and COI is Colby Irrigated. COI* only 10 varieties were harvested from COI in 2017.

Year	Varieties	Replications	Environments planted	Environments harvested (wsc)	Environments harvested (yield)	Plot dimensions
2016	30	6	2	2 (COD and COI)	None	3-row (0.84m x 2.44m)
2017	30	4	3	2 (Hays and COI*)	3 (Hays, COD, and COI)	6-row (1.68m x 3.81m)
2018	30	4	5	3 (COD, COI, and Hays)	3 (COD, COI, and Hays)	6-row (1.68m x 3.81m)

Table 3-3 Timing and amount of irrigation application in Colby irrigated environment (COI) in three different wheat growing years.

	2015/2016	**2016/2017**	**2017/2018**
Fall			
Oct/Nov	38.1	38.1	25.4
Spring			
Mar	Na	38.1	25.4
Apr	Na	38.1	12.7
May	Na	Na	50.8
Total	**38.1**	**114.3**	**114.3**

Na= Not applied

Table 3-2 Minimum, maximum, and mean WSC concentration from actual values measured in the lab and predicted WSC concentration. AE is an average of absolute error in the lab measured and predicted samples, and P-value is from t-test on two groups predicted and actual measured. NS is non-significant at 0.05 level of probability.

	Min	Max	Mean	AE	P-value
Actual	62.44	496.78	218.77	-0.23	0.94^{NS}
Predicted	61.82	448.65	219.71		

Table 3-3 Summary of water-soluble carbohydrate concentration (mg/g) in 30 varieties in six different environments from three years. The number preceding location code (COI-Colby irrigated, COD-Colby Water-limited, and Hays) represents the data from that year.

	18COD	18COI	18Hays	17Hays	16COD	16COI
Minimum	142.4	124.2	175.8	258.9	131.0	151.7
Maximum	219.8	204.5	258.4	363.6	301.4	340.6
Mean	168.2	160.8	209.0	306.1	233.5	247.3

Table 3-4 Summary of water-soluble carbohydrate (WSC) concentration (mg/g) in diverse winter wheat genotypes in 2016.

	Water-limited WSC COD (mg/g)			Irrigated WSC COI (mg/g)		
	Top	Bottom	Average	Top	Bottom	Average
Minimum	41.9	67.2	63.0	45.6	51.9	51.9
Maximum	352.1	523.1	417.4	389.0	555.7	411.1
Mean	182.8	301.3	241.7	180.9	325.8	253.3

Table 3-5 Mean squares from the joint and individual year analysis on Top WSC, Bottom WSC, and average WSC in three different wheat growing years. Single (*), double (**), or Triple asterisks (***) indicates the significance at 0.05, 0.01, or <0.001 level of probability.

Year	Source of Variation	Degrees of freedom	Top WSC	Bottom WSC	WSC
2015/2016	Genotype	29	14476.3***	37502***	22522.9***
	Env	1	1333.6	48570**	16842**
	Block	5	3924**	44555***	17180.4***
	Genotype:Env	29	1651*	3551	1832.3
	Residuals	276	1036.1	4522	1911
2016/2017	Genotype	29	2452.2***	9366.3***	4115.7***
	Block	3	3659.1**	12611.6***	1414.1
	Residuals	87	767.7	2042.5	1009.4
2017/2018	Genotype	28	2334.1***	6454***	3542***
	Env	2	10249.6***	199128***	75059***
	Block	3	1552.1	1708*	1000
	Genotype:Env	56	529.7	477	346
	Residuals	243	601.2	591	397
Combined	Genotype	25	10212***	35635***	20014***
	Env	2	234072***	87880***	139654***
	Year	2	353345***	1280200***	656014***
	Block	5	3031**	27902***	10911***
	Env:Year	1	678	67209***	21617***
	Genotype:Year	50	3574***	5552***	3271***
	Env:Year:Block	17	2753***	25497***	8082***
	Genotype:Env:Year	75	952	1625	836
	Residuals	520	792	2031	1029

Table 3-8 (a) Pearson correlation between tillering (Stems/m^2) and Thousand Kernel Weight (b) Pearson correlation between WSC (mg/g) with Stems/m^2, yield/m^2, and grains/m^2.

(a)

Locations	r
Hays	-0.13
COD	-0.13
COI	-0.17

(b)

Locations	Stems/m^2	Yield/m^2	Grains/m^2
Hays	0.27	0.11	0.22
COD	0.15	0.05	-0.03
COI	-0.19	-0.19	-0.27

Table 3-9 Results from Pearson correlation between stem number per m^2, individual stem weight (g), and WSC (Top, Bottom, and average) concentration (mg/g) in two different environments in Colby 2018. Correlation from Colby water-limited (COD) environment is presented in the lower triangle, and Colby irrigated (COI) environment is presented in the upper triangle. The bold number indicates significant at 0.05 level of probability.

	Stems/m2	Stem wt	Twsc	Bwsc	WSC
Stems/m2		**-0.58**	**-0.33**	0.05	-0.19
Stem wt	**-0.31**		**0.33**	0.15	**0.30**
Twsc	0.12	0.11		**0.45**	**0.86**
Bwsc	0.12	0.10	**0.41**		**0.85**
WSC	0.15	0.12	**0.85**	**0.83**	

Table 3-10 Pearson correlations between stand rating (0-4), height (cm), stems number per m^2, individual stem weight (g), and average WSC concentration (mg/g) from the location hays in 2018 (lower triangle) and 2017 (upper triangle). The bold number indicates significant at 0.05 level of probability.

	Standrating	Height	Heading	Stems/m^2	Stem wt	WSC
Standrating		NA	NA	NA	NA	NA
Height	-0.32		0.25	NA	NA	-0.04
Heading	-0.04	0.21		NA	NA	0.00
Stems/m2	-0.17	0.05	0.24		NA	NA
Stem wt	0.29	**0.48**	0.13	-0.29		NA
WSC	**0.47**	-0.26	0.22	0.26	0.25	

Table 3-6 Details of the single nucleotide polymorphism (SNPs) significantly associated with the WSC accumulation in the stem as detected by the enhanced mixed linear model at FDR of 10%.

SNP	Chromosome	Position	MAF	%variation
S7D_PART1_71569531	7D	71569531	0.462	5%
S7D_PART1_59538630	7D	59538630	0.274	5%
S7D_PART1_71628885	7D	71628885	0.455	4%
S7D_PART1_59538604	7D	59538604	0.265	4%
S7D_PART1_59538617	7D	59538617	0.265	4%
S7D_PART1_59538610	7D	59538610	0.265	4%
S1B_PART1_399534182	1B	4E+08	0.088	5%

MAF = minor allele frequency, %variation is the variation explained by each marker

Chapter 4 - Application of aerial imaging to study genotypic response in diverse winter wheat genotypes

Introduction

With the current trends of population rise, high demand for food and energy, and limited availability of land, water, and other resources, agriculture production needs to be increased relative to the current rate (Alexandratos, 2009; Ray et al., 2013; Reynolds et al., 2009a). The genetic gain in most of the cultivated crops has been below 1%, which is lower than what is needed to meet the projected demand (Ray et al., 2013; Rife, 2016; Tester and Langridge, 2010). Further, extremities in temperature and variability in precipitation due to global climate change are likely to complicate the process, presenting a key challenge for the new generation of researchers addressing food security.

The triumph of "next generation" sequencing and genotyping technologies are rapidly reducing the cost of genotyping but it's applicability is constrained with limited phenotyping capability (Poland, 2015). Conventional phenotyping methods are mostly destructive, time consuming, subjective, and labor intensive, as a result, they can be acquired only a few times during the growing season. Some phenotyping progress has been made in controlled environment conditions, however huge variability in the field due to weather, topography, and soil, makes it harder to extrapolate the field phenotype from the response in the controlled environment (Araus and Cairns, 2014; Dhondt et al., 2013; Fiorani and Schurr, 2013; Yang et al., 2007). Therefore, field based phenotyping is the only way to capture this variation and link the phenotype with the genotype (Araus and Cairns, 2014; White et al., 2012).

Realizing the importance and need of field based phenotyping, an increasing number of scientists are turning to the use of different remote sensing platforms for plant phenotyping such

as satellite imagery, imagery captured using manned or unmanned aircrafts, ground based phenotyping platforms and so on. These platforms are becoming helpful to identify yield, biomass, height, insect and disease infestation, crop stress signals, and many more. Satellite imagery could be an important resource as images are freely available. However, they suffer from issues with resolution, cloudiness, timeliness, and readiness in availability (Rango et al., 2009). Imagery using manned aircrafts can be up to date and generate higher resolution data, but the cost per acre is higher and might not be accessible for every location or breeding program. One way to accommodate these shortcomings is by using a ground based phenotyping platform, as they can provide higher resolution, multiple angles and can be operated at various time points (Gago et al., 2015). However, there are disadvantages of ground-based phenotyping including the longer time for data collection, lower temporal resolution, appropriate sensor requirement, portability and associated vehicle cost, increased human intervention, inability to phenotype wet fields, and potential crop damage due to vehicles running in the field. Therefore, unmanned air vehicles (UAVs) are preferred as they can mitigate the limitations from satellite and ground based phenotyping and have distinct advantages relative to satellite imaging (Poland, 2015; Tattaris et al., 2016). In general, UAVs are practical, accessible and come in different size and cost ranges, so the user can choose the platform based on resources available (Gago et al., 2015; Myers et al., 2015; Poland, 2015).

UAV based platform uses proximal sensors with higher spatial and temporal resolution. They can be fully or partially automated and can be operated with little or no human involvement. These platforms have been successfully implemented in predicting yield, biomass and/or plant height (Haghigharttalab et al., 2016; Wang, 2017). They have also been used for fertilizer recommendations (Lorence and Asebedo, 2017), weed management (Rasmussen et al.,

2013), plant protection (Garcia-Ruiz et al., 2013) species monitoring in ecological and conservational studies (Lu and He, 2017), rangeland ecosystem management (Rango et al., 2009) and studying soil properties (Acevo-Herrera et al., 2009). The height of the flight can be adjusted depending on the need as the distance between the sensor and the target is negatively correlated with the spatial resolution. The flight at higher altitude provides a wider view where the flights at lower altitude can provide greater resolution. The payload of the aircraft can range from different spectral range from RGB, NIR bands to thermal, infrared and microwave bands. Temporal resolution can be maximized on demand. Therefore, the UAV can be of critical importance in breeding programs by providing accurate and timely measurement and capturing real time field variation in the form of images.

UAVs can be an efficient phenotyping platform to assist the breeder in making decisions for selection, however, obtaining meaningful information out of myriad data points is a challenge. The evaluation of hundreds or thousands of genotypes every year in the breeding program demands a more efficient phenotyping platform as opposed to traditional phenotyping methods. At the same time, phenotyping should be at the canopy level to predict plant performance based on efficiency of capturing resources and mobilizing them to produce yield (Reynolds et al., 2012, 2009b). Yield is the main trait for selection in wheat breeding program.

Lodging is another important traits for selection in the wheat breeding program. The displacement of plant from its vertical position results lodging which can happen due to failure of root anchorage, or by weak stem strength. Lodging resistant varieties can tolerate higher plant densities and get more responsive to nitrogen fertilizer for obtaining higher yield. Ideal genotypes should be able to maximize partitioning to the grain while maintaining stalk or root strength (Foulkes et al., 2011; Piñera-Chavez et al., 2016). Lodging can have a negative effect in

yield and quality and can decrease up to 80% of the harvestable yield in wheat (Berry et al., 2004; Berry and Spink, 2012; Reynolds et al., 2012). Therefore, increased harvest index to maximize yield should take lodging into account (Austin et al., 1980; Foulkes et al., 2011; Reynolds et al., 2012).

The main purpose of this study was to implement aerial imaging as a plant breeding tool to detect genotypic response and assist breeders in making selection of genotypes in Kansas State winter wheat breeding program. This study was based on images captured in VIS-NIR region. The canopy light properties in the VIS and NIR region can define the plant photosynthetic characteristics. NDVI, along with other indices measuring the reflected light in these regions, has been proposed as a method of estimating plant performance in terms of chlorophyll content, leaf area index, biomass accumulation, yield in wheat (Babar et al., 2006a, 2006c, 2006b; Haboudane et al., 2004; Royo et al., 2003; Wright Jr et al., 2005). Chlorophyll and associated pigments (such as carotenoid and xanthophyll) in leaves absorb light in the VIS region (400-700nm), whereas the light in the NIR (700-1300) range gets scattered by the leaf tissues. Therefore, the healthy leaf reflects more in the near infrared region whereas the stressed leaf will have a lower reflectance in the NIR region and relatively higher reflectance in the VIS region. These mechanisms can be captured in the form of vegetative indices (VIs). Using basic physiology in plants, we present an affordable approach to identify the genotypic response at different stages in wheat. The objective of this study was to examine the suitability of aerial imaging to detect genotypic response and help breeders in selection, examine how the response changes with stage of crop growth, and study the relationship of vegetative index to yield and lodging in different stages of wheat growth.

Materials and Methods

Experimental details

The experiment material consisted of four hundred diverse winter wheat experimental lines from Manhattan and Hays wheat breeding program at Kansas State University and 30 released winter wheat varieties from Great Plains (Table 4-1). Two hundred experimental lines from preliminary yield nursery (PYN) or advance yield nursery (AYN) from each of the two K-State breeding programs were evaluated.

The experimental lines and varieties were planted in 2015/2016 and 2016/2017 growing seasons in Colby, Kansas under two moisture regimes (well irrigated and limited irrigation). All management factors (fertilizers, pesticide, fungicide, tillage, etc.) in the two environments were similar, except irrigation, in both years. A total of three supplementary irrigations of 114.3 mm was supplied 2017 (38 mm in the fall and 76.2 mm in the spring) and only one supplementary irrigation 38 mm was supplied in the fall of 2016 in well irrigated environments on top of seasonal rainfall (Figure 4-1). A pre-germination irrigation of 25.4 mm was supplied in both environments to ensure uniform germination and plant stand. The soil type in both environments was a Keith silt loam, buried soil phase, fine-silty, mixed, superactive, mesic Aridic Argiustolls.

The experimental lines were planted in type II modified augmented design, where 'WB Grainfield' was used as a central check, and 'Joe' and 'SY Monument' were used as sub-plot checks. These three winter wheat varieties are commonly planted varieties in western Kansas and are also included in broader set of varieties tested. The layout for augmented design is presented in Figure 4-2. The varieties were planted in a randomized complete block design (RCBD) embedded with the experimental lines in 2016 and separate blocks in 2017 (Figure 4-3). Four varieties used in 2016 were not available in 2017 and were replaced (Table 4-1). The plots were

planted in three row paired plots (two adjacent plots together) in 2016 and changed to six rows in 2017. Detail about planting is presented in Table 4-2.

Image acquisition

A commercially available Canon S100 (S/N 322030001417) camera was modified by LDP LLC, Carlstadt, NJ 07072, USA, (www.MaxMax.com) was used for image capture. A filter was removed from the camera, a modification resulting in output of green-red- near-infrared image layers (8 byte) in the 490-760 nm range, effectively replacing the blue band was a near infrared band. The CMOS (complementary metal oxide semiconductor) sensor dimensions were 7.44 mm x 5.58 mm. The camera was mounted on a DJI S900 hexacopter (DJI® Science and Technology, Co., Ltd. Shenzhen, China) with two axis gimbal (GAUI, Crane III) to maintain a nadir orientation during the flight for capturing images. The camera focal length was set to an equivalence to 28 mm (relative to a 35mm frame) and exposure time of 1/1600; images were acquired at ~2 s acquisition intervals. Autonomous flight control was established by DJI Ground Station, datalink (LK900) communications with PC, and a Wookong 'M' avionics controller. The images were captured between 9:00 to 15:00 CST and stored as raw and jpeg formats.

With weather permitting, date of imaging was planned to capture crop growth at approximately two-week intervals throughout the spring growing season, though the dates of image acquisition in 2016 and 2017 were different.

Ground control points

Ground control points (GCPs) were established at the corners of study areas. The light almond and dark green 5.08 cm × 10.16 cm boards were used as GCPs as well as reflectance calibration standards. UTM coordinates were measured for each board in the field.

Image preprocessing

Image pre-processing followed similar steps outlined in An et al. (2016). The steps, including color correction and optical distortion adjustment, were conducted by the K-State NWREC Crops Research Program (Aiken, pers comm.). A hyperspectral radiometer (GER 1500, Spectral Vista Corporation, NY) was used to obtain reflectance spectra in red, green, and near-infrared wavebands. A reflectance calibration procedure was developed to relate these spectra to digital number (DN, 0-255) values obtained from the modified S100 digital camera.

Orthomosaic generation

The images captured in three bands (red, green, and near infrared) were merged using Agisoft Photoscan package to output single orthomosaic image.

Field plot extraction

The plots were manually extracted in arcGIS ArcMap 10.5 following a field map-based plot extraction, where a polygon was manually drawn inside the plot (Figure 4-4). A set of manually drawn plots were geo-referenced for the same blocks at subsequent dates using 'georeference' tool in ArcGIS for geo-referenced orthomosaics. Once geo-referenced, the plot location for each plot at one date could be used for the same block for rest of the dates in that year. All polygon were monitored before processing to make sure that they align properly inside the plots.

The vegetative index for analysis was calculated as a normalized difference vegetative index (NDVI). NDVI is a measure of the the ratio of the difference of pixel brightness value in near-infrared and red to the sum of the values in near infrared and red (NDVI = NIR-RED/NIR+RED). We used zonal statistics plugin in ArcGIS to calculate NDVI. Early stage images were confounded with soil layer in between the rows, so we classified the NDVI into two

groups “vegetation group” and “non-vegetation group”. The index based classification was also adopted in earlier studies (An et al., 2016; Haghighattalab et al., 2016). First, the threshold that separates these two groups were identified based on the NDVI values measured in representative sample pixels inside the plot. The threshold ranged from 0.2-0.3 depending on the crop stage. The pixels covered with wheat plants (NDVI > (0.2-0.3) classified as Vegetation group, and soil between the rows classified as non-vegetation group (NDVI < (0.2-0.3). Using this threshold, a clause in ArcGIS was added using ‘set null’ tool which removed the pixel with NDVI equal to or below the threshold value, such that only pixels classified as vegetation were included in the analysis. The NDVI was then calculated from the resulting raster, which contained pixels from the vegetative group only. This was found to be more helpful when the canopy coverage is not established during early growth stages or when the soil was exposed due to lodging.

For every plot, we calculated plot area, pixel count, minimum, maximum, range, mean, standard deviation, and the the sum of NDVI for vegetative pixel, where we used mean NDVI value for additional comparison and analysis. The data was exported and merged to respective plot id, entry number, row, and range number in R (R core team, 2018).

Visual observation for lodging and canopy greenness

The lodging was scored during heading and mid-grain filling stages in 60 plots of irrigated blocks. The score was assigned as 0%, 50%, or 90% lodged indicating upright plants, partial lodging, or 90% plants in the plot lying on the ground. One additional visual assessment was carried out during mid-grain filling for either lodged or not-lodged indicating more than 50% upright plants or more than 50% of the plots lying on the ground, respectively. Canopy greenness was calculated as percentage of green leaves from visual observation during mid-grain filling stage.

Statistical analysis

Experimental design

The experimental lines were planted in type II modified augmented design (Figure 4-2). The augmented design is used mostly in breeding programs due to the need of evaluation of a large number of lines, limited land availability, and limited seed supply per line. The random arrangement of checks in the design may not be adequate to describe soil/field variability, so, Lin and Pouchinsky (1985) proposed the type II modified augmented design for rectangular plots with the systematic placement of control plots. The design is structured in the split plot, within the whole plot arranged in rows and columns. The subplots inside the whole plots are designed in odd numbers (5,7, or 9), so the central plot is always the check plot. The check plot in the center of the whole plot is used to adjust for the soil heterogeneity and obtain the measure of experimental error for genotype comparisons in subplots. To estimate the subplot error, two secondary check varieties are assigned in randomly selected whole plots, and the remaining subplots are assigned to test genotypes. The trial was designed in Agrobase Generation II (Agronomix software Inc., Winnipeg, Canada).

The number of rows, columns, and whole plots were different in the two years, but the subplots within in the whole plots were seven in both years. The six subplots were assigned to test genotypes or secondary checks (Joe and SY Monument), and the central subplot was always the primary check (WB Grainfield).

Experimental analysis

To determine the method of adjustment, we performed Analysis of variance on the control plot NDVI data to know row and column variation and method of adjustment using SAS 9.3 (SAS Institute, Cary NC). Row, column, and row-column interaction (whole plot error) effect

were calculated from whole plot controls. Subplot error was calculated from the subplot controls and whole plot control from the whole plots containing subplot checks. The degrees of freedom for subplot error was (3-1) m, where m is the number of subplots. No adjustment was needed if the source of variation row, column or row column interaction was not significant, suggesting homogenous spatial variation. However, adjustment is required if any of the sources of variation are significant. The method of adjustment depends on the direction of heterogeneity.

Three methods (1, 2, or 3) are proposed for adjusting the soil variation, but based on the lower efficiency reported by Lin and Pouschinsky (1985) and Lin and Voldeng (1989) on Method 2, we only compared method 1 and method 3.

Method 1 uses the design structure (row and column correction factors) and disregards the presence of secondary checks whereas method 3 uses the regression analysis between primary and secondary checks (Lin and Poushinsky, 1985; Snijders, 2002).

Method 1: Adjusted $Y_{ijk} = Y_{ij(k)} - R_i - C_j$

Where, $R_i = \overline{x_{i.}} - \overline{x_{..}}$ *and* $C_j = \overline{x_{.J}} - \overline{x_{..}}$

Method 3: Adjusted $Y_{ijk} = Y_{ij(k)} - b(x_{ij} - \overline{x_{..}})$

Where b = slope of primary and average of secondary checks

Examples of adjustment of one the genotype present in 2nd row 3rd column or wholeplot (WP) 4:

Method 1: $\text{Adjusted\_G1}_{\text{Row(R)2 Column(C)3}} = \text{RawG1}_{\text{R2C3}} - (\text{Check1}_{\text{AvgR2}} - \text{Check}_{\text{Avg}}) - (\text{Check1}_{\text{AvgC3}} - \text{Check1}_{\text{Avg}})$

Method 3: $Adjusted\_G1_{WholePlot(wp)4} = RawG1_{wp4} - slope*(Check1_{wp4} - Check1_{Avg})$

where the slope is the regression line slope of check1 and average of two secondary checks.

If the spatial heterogeneity is in one or both directions (row, column, or both), the additive model can describe the variation and method 1 can be used. However, if the interaction term is significant, the non-additive model is required to explain the variation, and thus, method 3 is used for adjustment. Both adjustments were carried out using a custom script in R (R Core Team, 2018).

Results and Discussions

Weather Conditions

The daily mean minimum and maximum temperatures during the growing season (Oct-June) in western Kansas were -8/33 ^{o}C in 2016 and -12/32 ^{o}C in 2017 (Fig. 4-1). The precipitation was higher than normal precipitation in both years 2016 and 2017. The total precipitation was 390 mm in 2016 (2015 Oct- 2016 Jun) and 388 mm in 2017 (2016 Oct- 2017 June), whereas the normal rainfall in this area is 321 mm only. The rainfall was uniformly distributed in 2016 compared to 2017, where more than half of the precipitation was on May, 2017. The rainfall in both years were compounded with strong winds. The higher incidence of precipitation, along with hail, and heavy winds caused severe lodging mostly in genotypes that had weak straw strength. Because of this reason, the breeding lines couldn't be harvested in both 2016 and 2017, and only the varieties were harvested in 2017.

Image processing data

To evaluate the potential use of aerial imaging in detecting genotypic differences in wheat, we analyzed images captured by a consumer grade camera mounted on a low-cost UAV

platform in two environments, well irrigated and limited irrigation (Figure 4-3). The camera captured images in the VIS-NIR region, and VI was calculated as NDVI from the red and near infrared bands. Plot data were extracted separately for each block (Figure 4-4) from orthmosaic generated at multiple time points. The date of image capture was different in 2016 and 2017 for both experimental lines and varieties. However, in both years, dates of image capture were frequent during vegetative and reproductive stages. The NDVI values are expressed on the basis of date of image capture, displayed as days of the year and year. The dates and the general stage of crop development are presented in the Table 4-3.

NDVI adjustment for experimental lines based on the control plots

Uniformity is reasonably the exception, rather than the rule, in field research. Therefore the observation of experimental lines needs to be adjusted based on the spatial variation. In this case, the checks in the augmented design were used to correct for spatial variability. First, we ran an ANOVA to test if there was a significant effect of the row, column, and interaction. The ANOVA result showed significant row column interaction in all analyses, therefore method 3 was used for adjustment, as suggested by Lin and Pouschinsky (1985). Method 3 uses all available primary and secondary check values for adjustment, as given in equation in method section. It can account for variation in large and small scale as opposed to method 1 which can only account for smaller scale variation. Snijders (2002) also observed higher relative efficiency with method 3 adjustment compared to method 1. The control plots of WB Grainfield and subplot control plots of Joe and SY Monument data were used to adjust for spatial heterogeneity and obtain a measure of experimental error for NDVI.

NDVI over the years

The correlation analysis showed mixed result; positive, negative, and no relation between the NDVI values calculated at different time points in both years. Table 4-4 includes correlation coefficients of NDVI captured at multiple time points in 2016 for 400 experimental lines and 30 varieties in rainfed or irrigated environment. The correlation of experimental lines from 2017 are displayed in Table 4-5. The time points are expressed as days of the year of 2016 and 2017 for winter wheat growing seasons 2015/2016 and 2016/2017. The correlation ranged from -0.6 to 0.6. Overall, we saw higher correlation among the dates in 2017 compared to 2016 in both environments. The correlation was higher among closely spaced dates (144 and 159 days in 2017 and 104 and 116 days in 2016), as opposed to NDVI calculated over a large interval (like 67 and 162 days in 2016 and 73 and 159 days in 2017). Therefore, NDVI at an earlier vegetative stage might not be a good predictor of NDVI at the reproductive, which is also in agreement with Crain (2015).

The fractional canopy cover (calculated from the ratio of the pixels classified as vegetation group to total pixels (vegetation + non-vegetation group) in each plot) was not well established at the earlier vegetative stage. It ranged from 80-100% at earlier vegetative stage images depending on the genotype. Along with the genotype differences, plant physiology during the reproductive stage is impacted by several environmental factors. Plant height can be another confounding factor, as it can directly impact lodging if the straw strength is not strong enough to support during rain and wind.

The relationship between the NDVI, yield, and factors impacting yield

To get the relationship between yield and NDVI calculated from aerial imaging, we ran a correlation analysis on average yield, test weight and NDVI from images captured on 047, 061,

073, 110, 123, 144, 159, and 179th day of the year 2017 (Figure 4-5). The yield data were available only in varieties in 2017 as the breeding lines from both years and varieties from 2016 couldn't be harvested due to adverse weather in both years. The dates are presented as NDVI followed by the DOY, and the first three dates are vegetative stages followed by the reproductive stages. We saw significant correlation of NDVI with yield across the growing season with a maximum positive correlation of 0.83 at 159th day (June 9th), followed by the 144th day (May 24th) with a correlation of 0.72 (Figure 4-5). The 144th and 159th day correspond to the late flowering and grain filling stages of winter wheat in western Kansas (Table 4-3). The higher correlation during grain filling is consistent with previous studies (Babar et al., 2006a; Crain, 2016; Reynolds et al., 2012; Royo et al., 2003). Along with yield, earlier studies showed that the biomass also increased to maximum in grain filling stage, with maximum correlation with NDVI (Babar et al., 2006a). The positive correlation with biomass and yield is likely the main reason behind the significant positive correlation of NDVI with yield, however we couldn't test the relation on our study. The yield was negatively correlated with NDVI measured at the early green up stage (047th, 061st, 073rd day of 2017), suggesting that varieties that greened up earlier in the season yielded less than late season varieties.

The trend of negative correlation with yield earlier in the season holds true of varieties grown under both irrigated and limited water environments. However, the trend was stronger in rainfed, compared to the irrigated environment (Figure 4-6). The genotypes that broke dormancy earlier in the season possibly used up available moisture on early season growth, as the weather in early 2017 was relatively dry (Figure 4-1). This may have negatively affected their growth later in the season as they may have sloughed tillers early in season due to moisture stress created by excessive early growth. A similar pattern in NDVI measurement was observed for

experimental lines where the NDVI at earlier dates were negatively correlated to NDVI measured later in the growing season (Table 4-4 and 4-5).

The negative relationship between NDVI and yield during early green up stage under both environments implies that the relationship isn't solely based on early season water status. Some other factors must simultaneously impact this relationship. The minimum daily temperature for winter wheat growth is 5^{o}C but it should be around 15-20^{o}C for optimum growth and tillering (Porter and Gawith, 1999). Occasional cold snaps during the Spring of 2017 could have damaged plants that broke dormancy earlier. Spring frost or chilling weather can have a more negative impact on the actively growing crop in early spring, compared to the one during the winter. Along with spring frost, the data could have been compounded with some disease pressure and severe lodging due to heavy rainfall and a late-season snowstorm later in the crop cycle (Figure 4-1).

The lower correlation with yield at 179th day (Figure 4-5 and 4-6) was due to the differential rate of senescence, leading to the variable rate of loss of chlorophyll, decline in photosynthetic activity, and remobilization of the assimilate to the grains (Vijayalakshmi et al., 2010). Plant phenology changes greatly from the vegetative stage to reproductive, therefore, early vegetative stage and late senescence might not be able to explain the relationship of NDVI and yield. Lopes and Reynolds (2007) also suggested measuring stay green to predict yield during mid grain filling stage.

The relationship of lodging with NDVI and yield

Lodging was more severe in irrigated blocks compared to rainfed, therefore, we scored 60 plots of irrigated blocks as 0%, 50%, or 90% lodged indicating upright plants, partial lodging, or 90% plants in the plot lying flat in the ground a week after the first snowstorm in May of

2017. Also, we took another visual assessment of lodging during mid grain filling (DOY 153), where the observer rated the plot as lodged or not lodged, irrespective of the genotype. Lodging was also reflected in the images captured later in the season (DOY 144, 159, and 179), where 99% of the plots marked as lodged from the visual observation matched with the plots identified as lodged from the image (data not shown). Because of the heavier rainfall throughout the heading, flowering, and grain filling period (Figure 4-1, precipitation bar for 2017- May, June, and July), 12% of the plots marked as upright during heading stage were marked as lodged during grain filling period. Loss from lodging can be greater on those plots where lodging occurs after flowering (Berry and Spink, 2012). Higher wind, heavy rain coupled with timely irrigation in irrigated blocks might have weaken plant anchorage in the soil leading to severe lodging in the irrigated blocks compared to the water-limited.

Yield was significantly lower in lodged plots compared to upright, non-lodged plots, irrespective of the genotype (Figure 4-7 (a)). Lodging during heading stage was able to explain more than 50% variation in grain yield (Figure 4-8 (a)). Similar effect of lodging was also observed in the studies by Berry and Spink (2012), where they observed 54% yield loss due to lodging. A similar relationship between lodging and yield was observed in NDVI measurements (Figure 4-7 (b) and figure 4-8 (b)). NDVI was calculated from the images captured from the top of the canopy, which was able to get the signal from the displacement of the plant on the ground due to lodging. Plant position might have changed flag leaf orientation, which greatly impacts light interception (Inoue et al., 2004). Flag leaf is a predominant light receptor and can contribute up to 50% of the photosynthesis in wheat (Al-Tahir, 2014). The study by Al-Tahir (2014) showed a high correlation of grain yield with flag leaf area, fresh weight of flag leaf and total chlorophyll content. Because of the plant position on the ground due to lodging, the original top

canopy (top canopy before lodging) may not be exposed in an orientation for maximum solar radiation interception. Lower leaves, bottom stems, or plant parts that are not as efficient in capturing solar radiation would likely have contributed signficantly to the reflectance measurement, resulting in lower NDVI and yield in lodged plants.

Visual observation of canopy greenness *vs* UAV measured NDVI

NDVI as a measure of stay green can be regarded as a stress adaptive trait under abiotic or biotic stress (Joshi et al., 2007; Lopes and Reynolds, 2012). Some stripe rust pressure was present in 2017, therefore the greenness was confounded not just by the genotypic character, but by the foliar disease infection. Visual scores were recorded as the percentage of green leaves in plants and ranged from 0-100%, where 0 means no any green leaves and 100 means all leaves are green. Visual observation was conducted in an irrigated environment during the grain filling period (DOY 160; June 9, 2017) and imaging was captured within the same week. As expected, the visual observation is subjective and ranged from 0-95%, where the NDVI range was within a 10% range.

There was a significant positive relationship between visually scored greenness and NDVI calculated from images (Figure 4-9). More importantly, the NDVI calculated from images explained more variation in yield (53%) compared to the visually scored greenness (27%), as presented in Figure 4-10. The NDVI value is continuous as opposed to visual screening and is more sensitive to small change in the top canopy. The visual assessment is impacted by the observer's view of the lower canopy which plays a smaller role in light interception. Image capture more information from the top canopy, area of light interception and yield is the function of light interception, radiation use efficiency and harvest index (Reynolds et al., 2012, 2009b), resulting in higher correlation with the sensor measurement than the visual assessment. Also,

hyperspectral imaging can capture spike photosynthesis, which is very difficult to measure, and this could have resulted higher correlation between yield and NDVI measurement after spike emergence (Tambussi et al., 2007). This suggests that physiological criteria like NDVI can be used as an indirect breeding approach to predict grain yield which has also been reported in earlier studies (Babar et al., 2006a; Lopes and Reynolds, 2012; Prasad et al., 2007). Indirect breeding approach or indirect selection becomes more important when the trait under evaluation is difficult to measure, like yield (Falconer and Mackay, 1996).

Lopes and Reynolds (2012) showed that NDVI could explain 30% of the variation in yield, and also can give an additional insight about plant health. NDVI can also be used as a potential tool to differentiate genotypes for yield growing under irrigated and water limited environments (Reynolds et al., 2012; You et al., 2013). This suggests it can be used to identify stress tolerance in genotypes. In our study, we saw a strong relationship between NDVI and yield in the water-limited water environment compared to the irrigated environment, which has also been reported by You et al. (2013) and Reynolds et al. (2013). However, the reason for lower correlation in their study might be different than our study, as our limited water environment, was not severely moisture deprived. The limited water environment received 390 and 388 mm of water from rainfall during the wheat growing season (Oct-Jun) in 2016 and 2017 respectively, whereas the normal rainfall in this area is 321 mm only based on 30 years average. In 2017, the precipitation was more towards the reproductive development stages with snow and hail later in the spring, whereas in 2016 it was throughout the wheat growth period. Notably, they were not moisture limited during critical growth stages as most of the rainfall occurred after heading (Figure 4-1).

The 2016 growing year was favorable for wheat production, producing double the average yield across the state, while 2017 was drier earlier in the season, followed by heavy moisture after the heading stage, leading to higher disease pressure. This disease response could have been reflected in the NDVI measurement, as reported in the study by Joshi et al. (2007).

Genetic Analysis of NDVI

Genome wide association studies (GWAS) on NDVI calculated during early vegetative, heading, and mid-grain filling stage did not find any marker significantly associated with the NDVI. It could be that the effect is controlled by many genes with small effect and we didn't have enough power to detect them. Nevertheless, accurate phenotyping using aerial imaging in conjunction with genomic selection (GS) might be able to predict grain yield more accurately. Accurate phenotyping is a very important aspect for linking genotype with the phenotype as demonstrated in a modelling study by Lamsal et al. (2018). Unlike GWAS, GS uses the effect of all markers to calculate Genomic Estimated Breeding Values. The integration of HTP and GS has the potential to increase the rate of genetic gain by increasing accuracy of selection and reducing time per breeding cycle. This may be accomplished by providing more accurate yield estimates and increasing confidence in the breeding value of a line allowing elite genotypes to be identified earlier in the breeding cycle and this, in turn, allows for more rapid cycling of the breeding material compared to conventional approaches.

Summary and Conclusions

The genetic gain in winter wheat is around 1%, much lower than the required gain to sustain the current trend of genetic population growth. We showed that the aerial phenotyping can have the capacity to detect genotypic differences in yield, lodging and canopy greenness and can be more effective than manual selection. Phenotyping for traits in the breeding program

mainly includes field scouting, which is very time consuming, labor intensive, and subjective, therefore, the application of aerial imaging can be helpful in increasing the efficiency, accuracy, and precision in selecting genotypes.

Aerial phenotyping provides broader insight to breeders for selection compared to conventional methods of selection. Human error can be minimized and the likelihood of identifying genetically superior individuals can be improved in the context of the breeding program. This is expected to be beneficial especially in earlier stages of the selection process where a large number of genotypes are to be considered and should allow the breeder to focus on the stronger candidates for future release.

While the UAV platform is efficient in capturing variation in the canopy, the main limitation is payload and flight time associated with the batteries used in the system. At the same time, the requirement of sensor calibration and image processing are still limitations for taking full advantage of this platform. User-friendly software, as well as efficient and standardized procedures to process images for a given crop are needed to be addressed as areas of future research.

References

Acevo-Herrera, R., Aguasca, A., Bosch-Lluis, X., Camps, A., 2009. On the use of compact L-band dicke radiometer (ARIEL) and UAV for soil moisture and salinity map retrieval: 2008/2009 field experiments, in: Geoscience and Remote Sensing Symposium, 2009 IEEE International, IGARSS 2009. IEEE, pp. IV–729.

Alexandratos, N., 2009. World food and agriculture to 2030/50: Highlights and views from mid-2009. FAO, in: Economic and Social Development Dept., Expert Meeting on How to Feed the World.

Al-Tahir, F.M., 2014. Flag leaf characteristics and relationship with grain yield and grain protein percentage for three cereals. J. Med. Plants Stud. 2, 01–07.

An, N., Palmer, C.M., Baker, R.L., Markelz, R.J.C., Ta, J., Covington, M.F., Maloof, J.N., Welch, S.M., Weinig, C., 2016. Plant high-throughput phenotyping using photogrammetry and imaging techniques to measure leaf length and rosette area. Comput. Electron. Agric. 127, 376–394. https://doi.org/10.1016/j.compag.2016.04.002

Araus, J.L., Cairns, J.E., 2014. Field high-throughput phenotyping: the new crop breeding frontier. Trends Plant Sci. 19, 52–61.

Austin, R.B., Bingham, J., Blackwell, R.D., Evans, L.T., Ford, M.A., Morgan, C.L., Taylor, M., 1980. Genetic improvements in winter wheat yields since 1900 and associated physiological changes. J. Agric. Sci. 94, 675–689.

Babar, M.A., Reynolds, M.P., Van Ginkel, M., Klatt, A.R., Raun, W.R., Stone, M.L., 2006a. Spectral reflectance to estimate genetic variation for in-season biomass, leaf chlorophyll, and canopy temperature in wheat. Crop Sci. 46, 1046–1057.

Babar, M.A., Reynolds, M.P., Van Ginkel, M., Klatt, A.R., Raun, W.R., Stone, M.L., 2006b. Spectral reflectance indices as a potential indirect selection criteria for wheat yield under irrigation. Crop Sci. 46, 578–588.

Babar, M.A., Van Ginkel, M., Klatt, A.R., Prasad, B., Reynolds, M.P., 2006c. The potential of using spectral reflectance indices to estimate yield in wheat grown under reduced irrigation. Euphytica 150, 155–172.

Berry, P. M., & Spink, J. 2012. Predicting yield losses caused by lodging in wheat. Field Crops Research, 137, 19-26.

Berry, P. M., Sterling, M., Spink, J. H., Baker, C. J., Sylvester-Bradley, R., Mooney, S. J., ... & Ennos, A. R. 2004. Understanding and reducing lodging in cereals. Advances in Agronomy, 84(04), 215-269.

Crain, J.L., 2016. Leveraging the genomics revolution with high-throughput phenotyping for crop improvement of abiotic stresses (PhD Thesis). Kansas State University.

Dhondt, S., Wuyts, N., Inzé, D., 2013. Cell to whole-plant phenotyping: the best is yet to come. Trends Plant Sci. 18, 428–439. https://doi.org/10.1016/j.tplants.2013.04.008

Falconer, D.S., Mackay, T.F., 1996. Introd. Quant. Genet.

Fiorani, F., Schurr, U., 2013. Future scenarios for plant phenotyping. Annu. Rev. Plant Biol. 64, 267–291. https://doi.org/10.1146/annurev-arplant-050312-120137

Foulkes, M.J., Slafer, G.A., Davies, W.J., Berry, P.M., Sylvester-Bradley, R., Martre, P., Calderini, D.F., Griffiths, S., Reynolds, M.P., 2011. Raising yield potential of wheat. III. Optimizing partitioning to grain while maintaining lodging resistance. J. Exp. Bot. 62, 469–486.

Gago, J., Douthe, C., Coopman, Re., Gallego, Pp., Ribas-Carbo, M., Flexas, J., Escalona, J., Medrano, H., 2015. UAVs challenge to assess water stress for sustainable agriculture. Agric. Water Manag. 153, 9–19.

Garcia-Ruiz, F., Sankaran, S., Maja, J.M., Lee, W.S., Rasmussen, J., Ehsani, R., 2013. Comparison of two aerial imaging platforms for identification of Huanglongbing-infected citrus trees. Comput. Electron. Agric. 91, 106–115.

Haboudane, D., Miller, J.R., Pattey, E., Zarco-Tejada, P.J., Strachan, I.B., 2004. Hyperspectral vegetation indices and novel algorithms for predicting green LAI of crop canopies: Modeling and validation in the context of precision agriculture. Remote Sens. Environ. 90, 337–352. https://doi.org/10.1016/j.rse.2003.12.013

Haghighattalab, A., González Pérez, L., Mondal, S., Singh, D., Schinstock, D., Rutkoski, J., Ortiz-Monasterio, I., Singh, R.P., Goodin, D., Poland, J., 2016. Application of unmanned aerial systems for high throughput phenotyping of large wheat breeding nurseries. Plant Methods 12, 35. https://doi.org/10.1186/s13007-016-0134-6

Inoue, T., Inanaga, S., Sugimoto, Y., An, P., Eneji, A.E., 2004. Effect of drought on ear and flag leaf photosynthesis of two wheat cultivars differing in drought resistance. Photosynthetica 42, 559–565.

Joshi, A.K., Kumari, M., Singh, V.P., Reddy, C.M., Kumar, S., Rane, J., Chand, R., 2007. Stay green trait: variation, inheritance and its association with spot blotch resistance in spring wheat (Triticum aestivum L.). Euphytica 153, 59–71.

Lamsal, A., Welch, S.M., White, J.W., Thorp, K.R., Bello, N.M., 2018. Estimating parametric phenotypes that determine anthesis date in Zea mays: Challenges in combining ecophysiological models with genetics. PLOS ONE 13, e0195841. https://doi.org/10.1371/journal.pone.0195841

Lin, C.-S., Poushinsky, G., 1985. A modified augmented design (type 2) for rectangular plots. Can. J. Plant Sci. 65, 743–749.

Lin, C.S., Voldeng, H.D., 1989. Efficiency of type 2 modified augmented designs in soybean variety trials. Agron. J. 81, 512–517.

Lopes, M.S., Reynolds, M.P., 2012. Stay-green in spring wheat can be determined by spectral reflectance measurements (normalized difference vegetation index) independently from phenology. J. Exp. Bot. 63, 3789–3798.

Lorence, A., Asebedo, A., 2017. Evaluation of optical sensor technologies to optimize winter wheat (Triticum aestivum L.) management (PhD Thesis). Kansas State University.

Lu, B., He, Y., 2017. Species classification using Unmanned Aerial Vehicle (UAV)-acquired high spatial resolution imagery in a heterogeneous grassland. ISPRS J. Photogramm. Remote Sens. 128, 73–85.

Myers, D., Ross, C.M., Liu, B., 2015. A review of unmanned aircraft system (UAS) applications for agriculture, in: 2015 ASABE Annual International Meeting. American Society of Agricultural and Biological Engineers, p. 1.

Poland, J., 2015. Breeding-assisted genomics. Current opinion in plant biology, 24, pp.119-124.

Poland, J.A., Rife, T.W., 2012. Genotyping-by-Sequencing for Plant Breeding and Genetics. Plant Genome 5, 92–102. https://doi.org/10.3835/plantgenome2012.05.0005

Porter, J.R., Gawith, M., 1999. Temperatures and the growth and development of wheat: a review. Eur. J. Agron. 10, 23–36.

Prasad, B., Carver, B.F., Stone, M.L., Babar, M.A., Raun, W.R., Klatt, A.R., 2007. Potential use of spectral reflectance indices as a selection tool for grain yield in winter wheat under great plains conditions. Crop Sci. 47, 1426–1440.

Rango, A., Laliberte, A., Herrick, J.E., Winters, C., Havstad, K., Steele, C., Browning, D., 2009. Unmanned aerial vehicle-based remote sensing for rangeland assessment, monitoring, and management. J. Appl. Remote Sens. 3, 033542.

Rasmussen, J., Nielsen, J., Garcia-Ruiz, F., Christensen, S., Streibig, J.C., 2013. Potential uses of small unmanned aircraft systems (UAS) in weed research. Weed Res. 53, 242–248.

Ray, D.K., Mueller, N.D., West, P.C., Foley, J.A., 2013. Yield trends are insufficient to double global crop production by 2050. PloS One 8, e66428.

Reynolds, M., Foulkes, J., Furbank, R., Griffiths, S., King, J., Murchie, E., Parry, M., Slafer, G., 2012. Achieving yield gains in wheat. Plant Cell Environ. 35, 1799–1823.

Reynolds, M., Foulkes, M.J., Slafer, G.A., Berry, P., Parry, M.A., Snape, J.W., Angus, W.J., 2009a. Raising yield potential in wheat. J. Exp. Bot. 60, 1899–1918.

Reynolds, M., Manes, Y., Izanloo, A., Langridge, P., 2009b. Phenotyping approaches for physiological breeding and gene discovery in wheat. Ann. Appl. Biol. 155, 309–320.

Rife, T.W., 2016. Utilizing a historical wheat collection to develop new tools for modern plant breeding (PhD Thesis). Kansas State University.

Royo, C., Aparicio, N., Villegas, D., Casadesus, J., Monneveux, P., Araus, J.L., 2003. Usefulness of spectral reflectance indices as durum wheat yield predictors under contrasting Mediterranean conditions. Int. J. Remote Sens. 24, 4403–4419.

Snijders, C.H.A., 2002. Field evaluation of type 2 modified augmented designs for non-replicated yield trials in the early stages of a wheat breeding program. na.

Tambussi, E.A., Bort, J., Guiamet, J.J., Nogués, S., Araus, J.L., 2007. The photosynthetic role of ears in C3 cereals: metabolism, water use efficiency and contribution to grain yield. Crit. Rev. Plant Sci. 26, 1–16.

Tattaris, M., Reynolds, M.P., Chapman, S.C., 2016. A direct comparison of remote sensing approaches for high-throughput phenotyping in plant breeding. Front. Plant Sci. 7, 1131.

Tester, M., Langridge, P., 2010. Breeding technologies to increase crop production in a changing world. Science 327, 818–822.

Vijayalakshmi, K., Fritz, A.K., Paulsen, G.M., Bai, G., Pandravada, S., Gill, B.S., 2010. Modeling and mapping QTL for senescence-related traits in winter wheat under high temperature. Mol. Breed. 26, 163–175.

Wang, H., 2017. Crop assessment and monitoring using optical sensors (PhD Thesis). Kansas State University.

White, J. W., Andrade-Sanchez, P., Gore, M. A., Bronson, K. F., Coffelt, T. A., Conley, M. M., ... & Jenks, M. A. 2012. Field-based phenomics for plant genetics research. Field Crops Research, 133, 101-112.

Wright Jr, D.L., Rasmussen Jr, V.P., Ramsey, R.D., 2005. Comparing the use of remote sensing with traditional techniques to detect nitrogen stress in wheat. Geocarto Int. 20, 63–68.

Yang, D.-L., Jing, R.-L., Chang, X.-P., Li, W., 2007. Identification of quantitative trait loci and environmental interactions for accumulation and remobilization of water-soluble carbohydrates in wheat (Triticum aestivum L.) stems. Genetics.

You, X., Meng, J., Zhang, M., Dong, T., 2013. Remote sensing based detection of crop phenology for agricultural zones in China using a new threshold method. Remote Sens. 5, 3190–3211.

Figure 4-1 Weather during 2015/2016 and 2016/2017 wheat growing season. The green bar is the sum of monthly precipitation and the dot with the bar is normal precipitation from 1988 to 2015 for that month. Red and blue lines are the average maximum and minimum temperature, respectively.

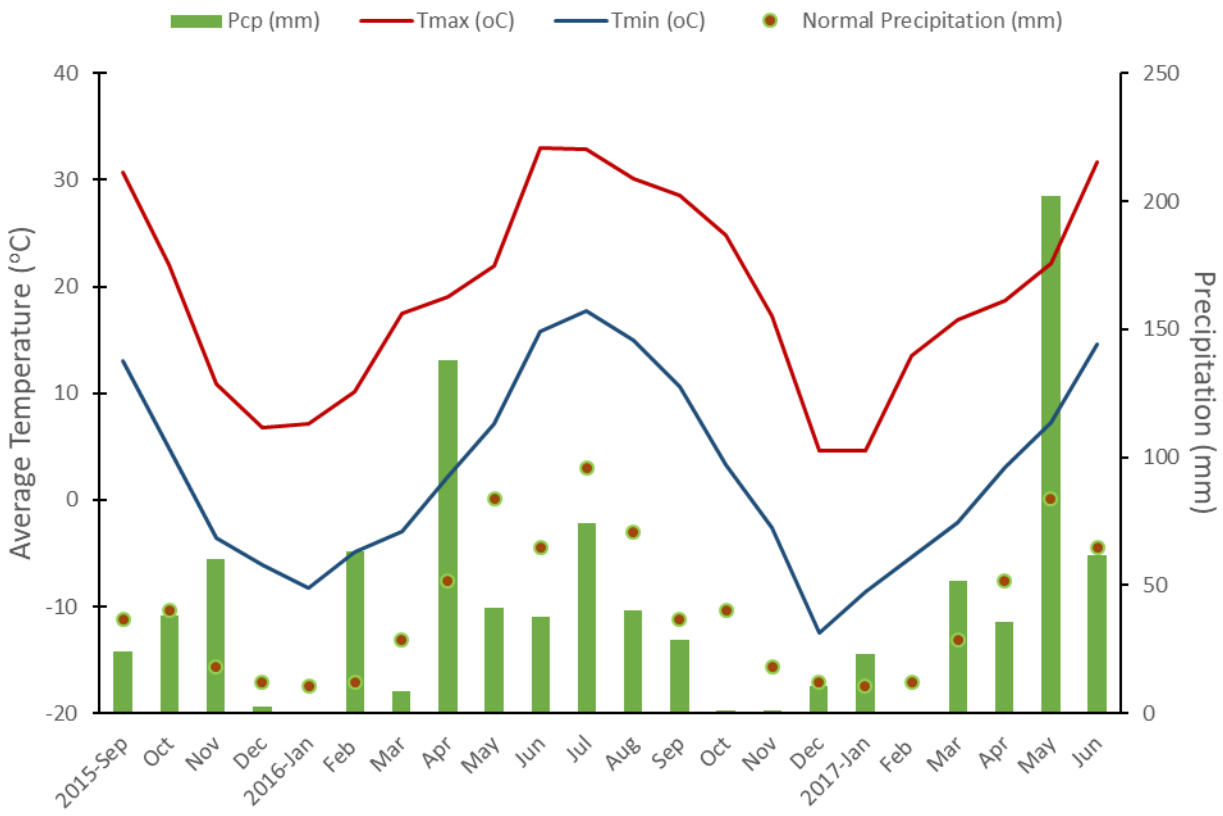

Figure 4-2 Type II modified augmented design layout where the field is divided into row and columns. The row and column combination is a whole plot (WP). Each whole plot has seven subplots, and the center one is always a control check. Subplot checks are randomly assigned in selected whole plots.

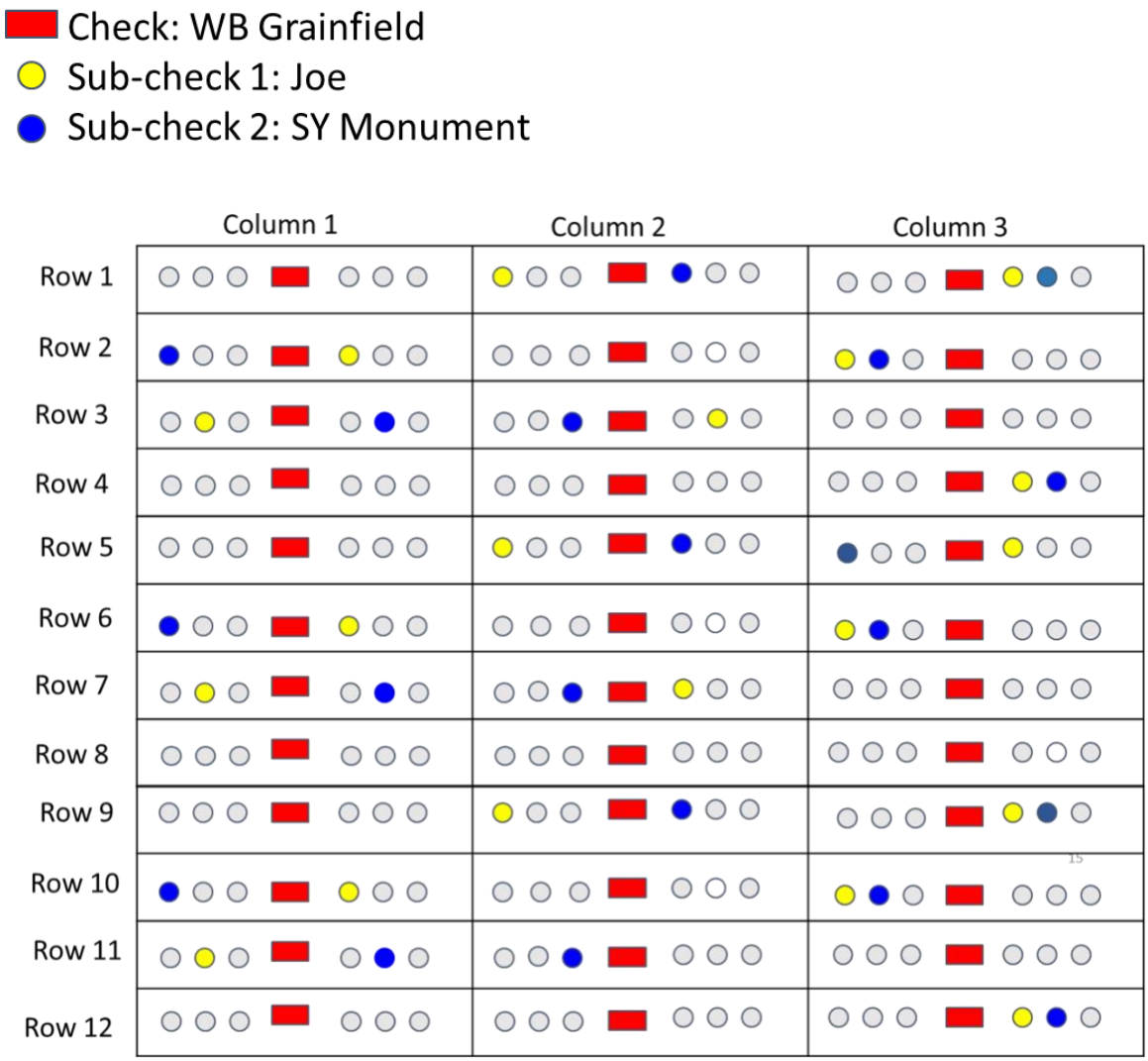

Figure 4-3 Field layout around a central pivot in 2016/2017 (top) and 2015/2016 (bottom) from the aerial image taken on April 20, 2017, and Nov 10, 2015, respectively. The varieties are labeled as V and Experimental lines as L. The number after the letter corresponds to the block number and irrigated environment are denoted in bold. The labels are oriented in planting direction from bottom left of each block.

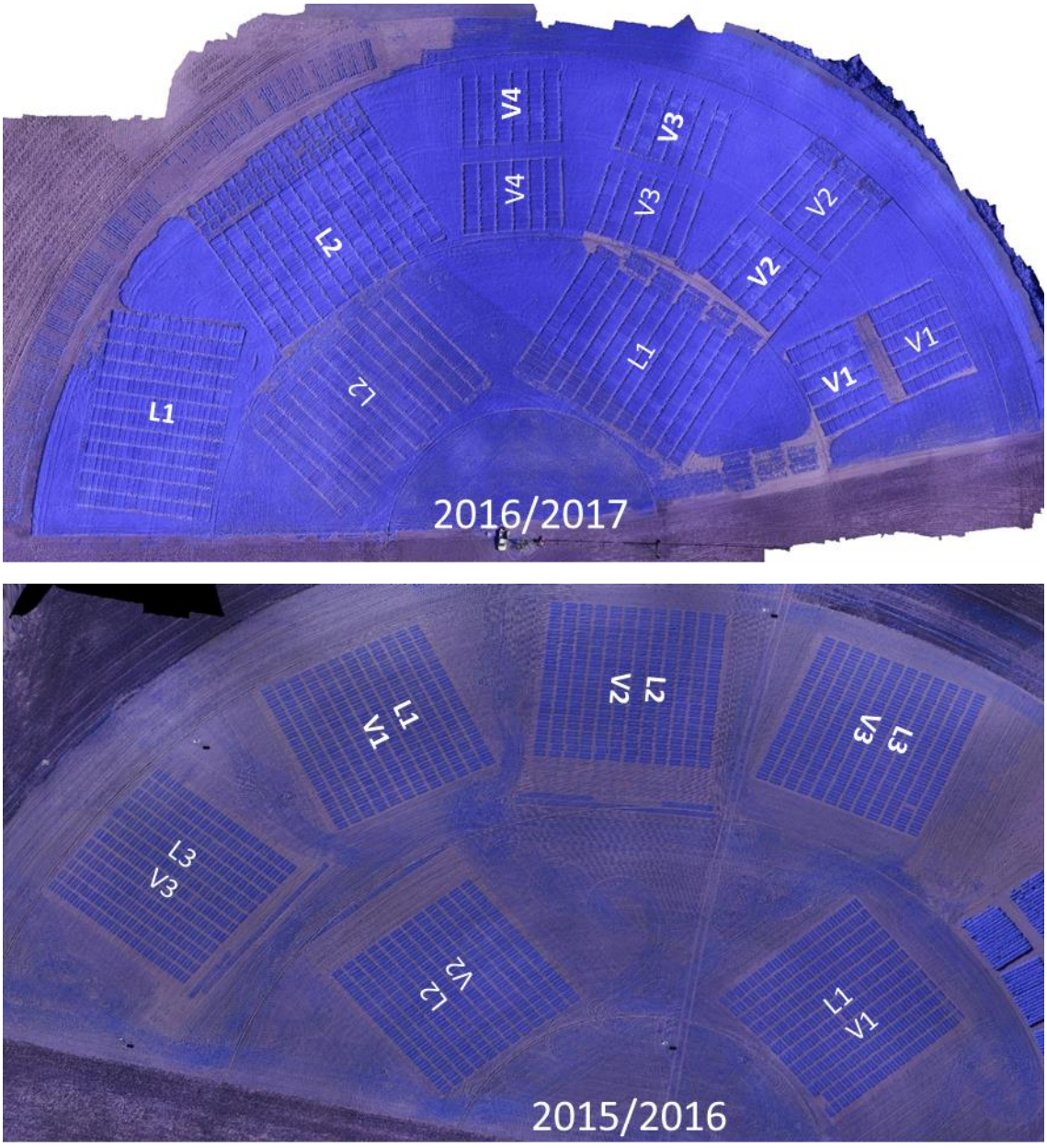

Figure 4-4(a) Raw image of B1 captured in the 073rd day of 2017 by a UAV. The white rectangular box represents individual plot boundaries. Ground plot dimension is 4.5' x 12.5' (b) NDVI of B1 in the 073rd day of 2017.

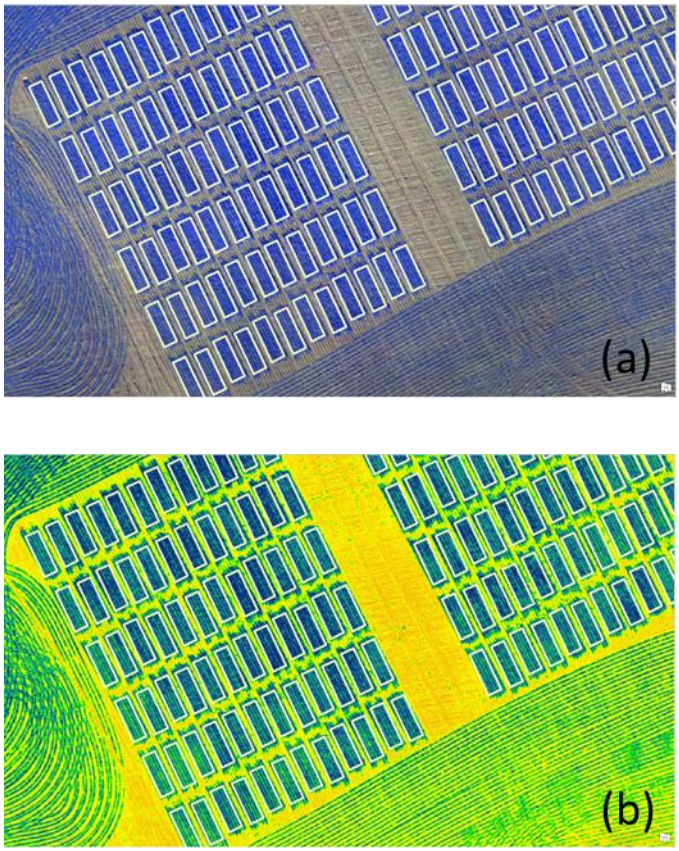

Figure 4-5 Correlation scatterplot of Pearson Correlation between Test weight (Tstwght), Yield (lb A^{-1}) and NDVI measured at different days of 2017, 47th day (NDVI047), 61st day (NDVI061), 73rd day (NDVI073), 110th day (NDVI110), 123rd day (NDVI123), 144th day (NDVI144), 159th day (NDVI159) of 2017. Correlation value is presented on the top half and the bottom is the scatterplot with a red fitted line. Single (*), double (**), or Triple asterisks (***) indicates the significance at 0.05, 0.01 or <0.001 level of probability.

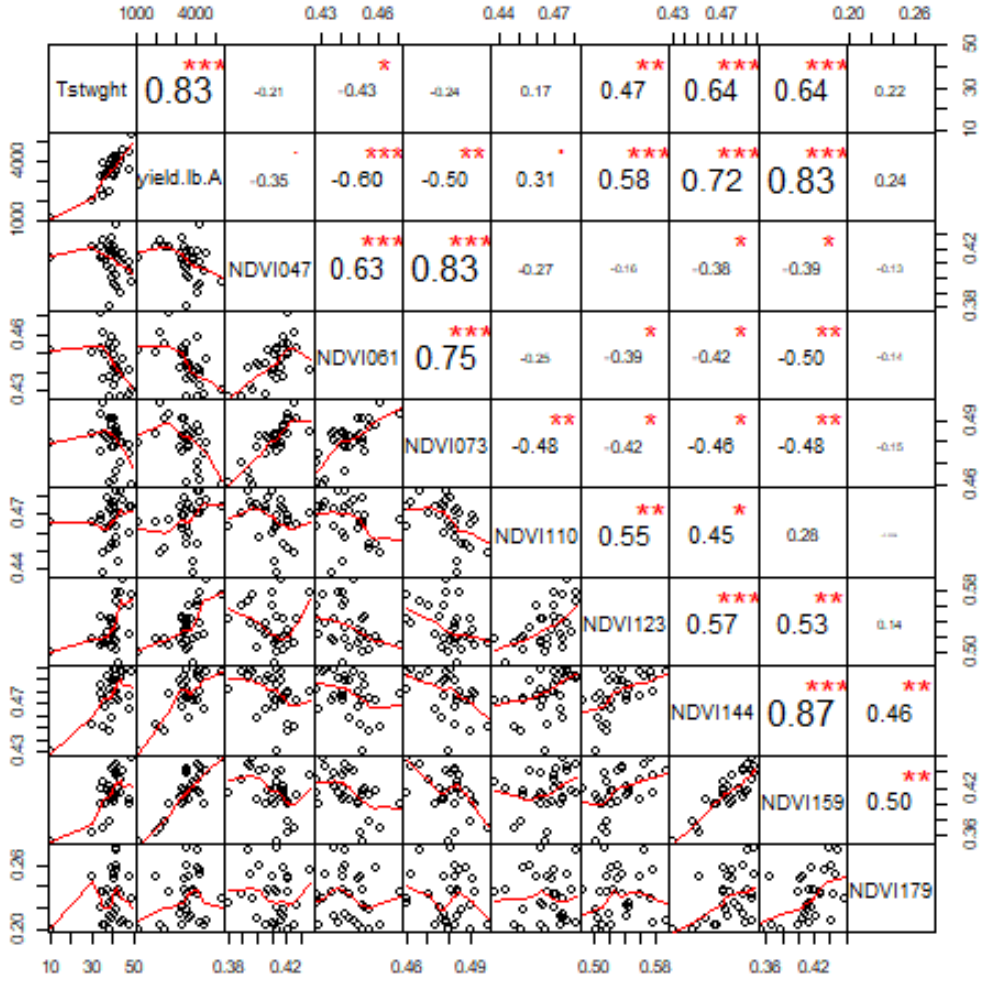

Figure 4-6 Correlation scatterplot of Pearson Correlation between Test weight (Tstwght), Yield (lb A^{-1}) and NDVI measured at different days of 2017, 47th day (NDVI047), 61st day (NDVI061), 73rd day (NDVI073), 110th day (NDVI110), 123rd day (NDVI123), 144th day (NDVI144), 159th day (NDVI159) of 2017 for an (a) Irrigated environment and (b) water-limited environment. Correlation value is presented on the top half and the bottom is the scatterplot with a red fitted line. Single (*), double (**), or Triple asterisks (***) indicates the significance at 0.05, 0.01 or <0.001 level of probability.

(a)

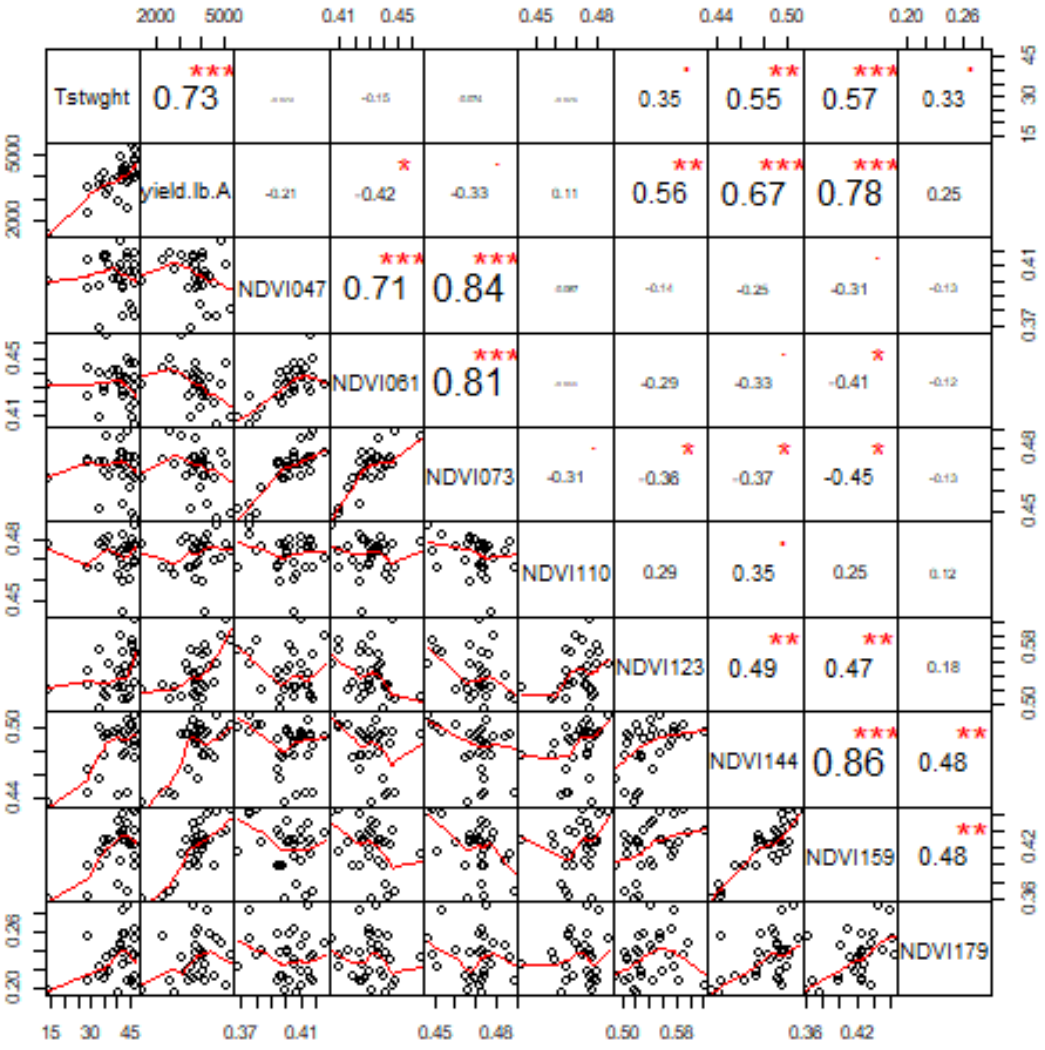

(b)

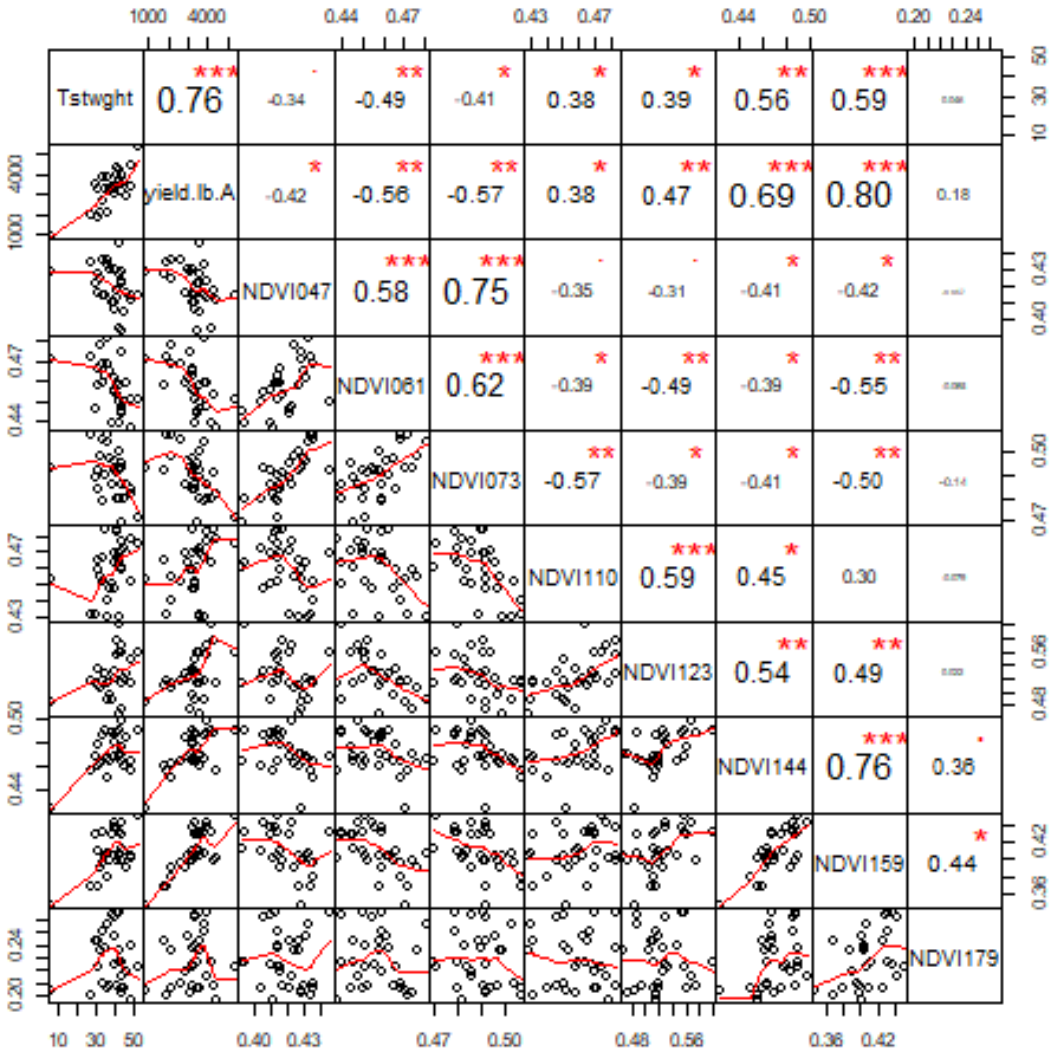
Tstwght
yield.lb.A
NDVI047
NDVI061
NDVI073
NDVI110
NDVI123
NDVI144
NDVI159
NDVI179

Figure 4-7 Yield (lb A^{-1}) and (b) NDVI between lodged and not lodged plots, lodging was assessed during mid grain filling period as severely lodged and standing upright plants in 30 varieties in western Kansas. Triple asterisks (***) indicates the differences at the <0.001 level of probability.

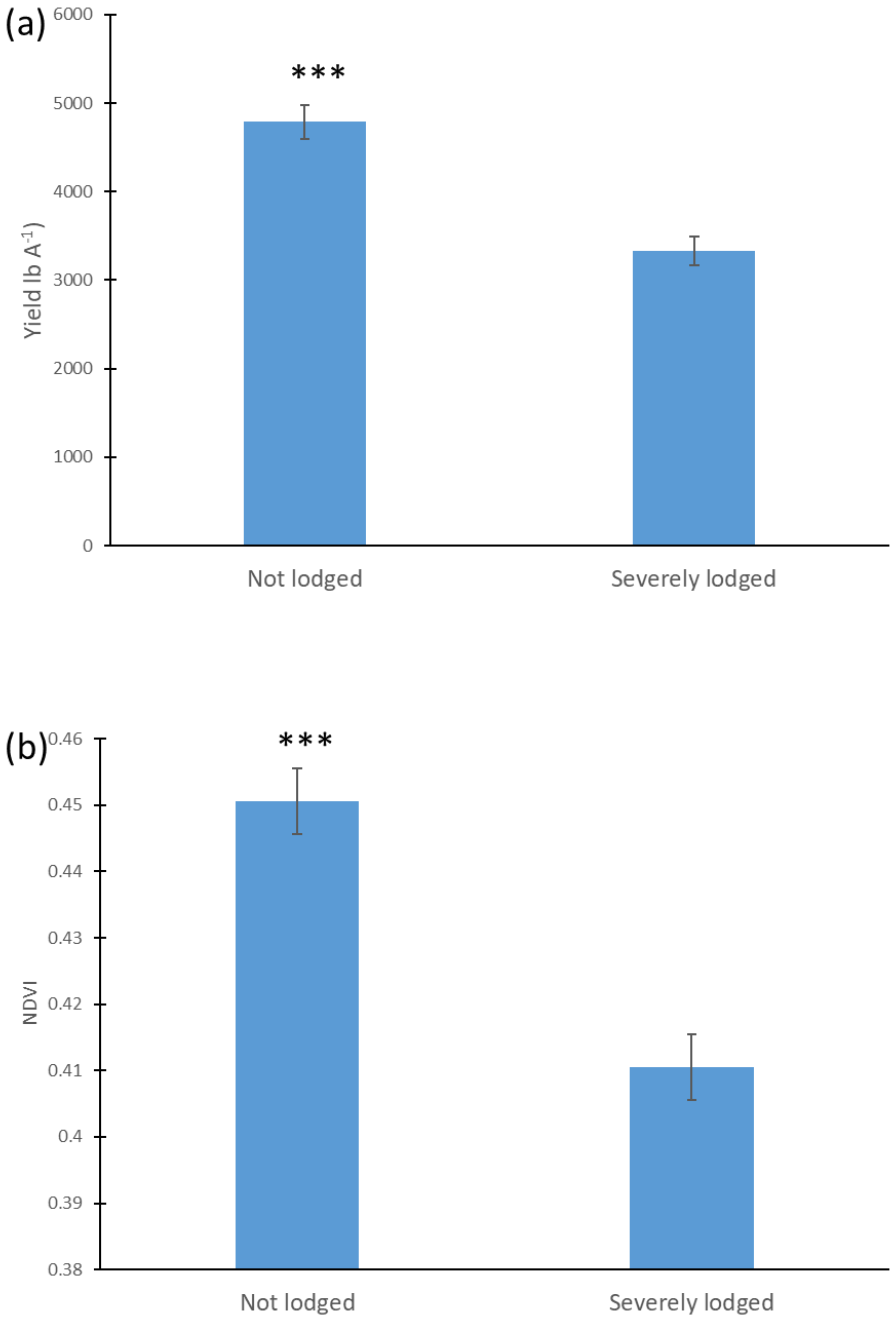

Figure 4-8 Correlation between Yield and NDVI with lodging in western Kansas. (a) Relationship between yield (lb A^{-1}) and % lodging scored after first snowstorm/ rainfall (b) Relationship between NDVI measured during grain filling and % lodging scored after the first week of a snowstorm/heavy rainfall. Triple asterisks (***) indicates the significance at the <0.001 level of probability.

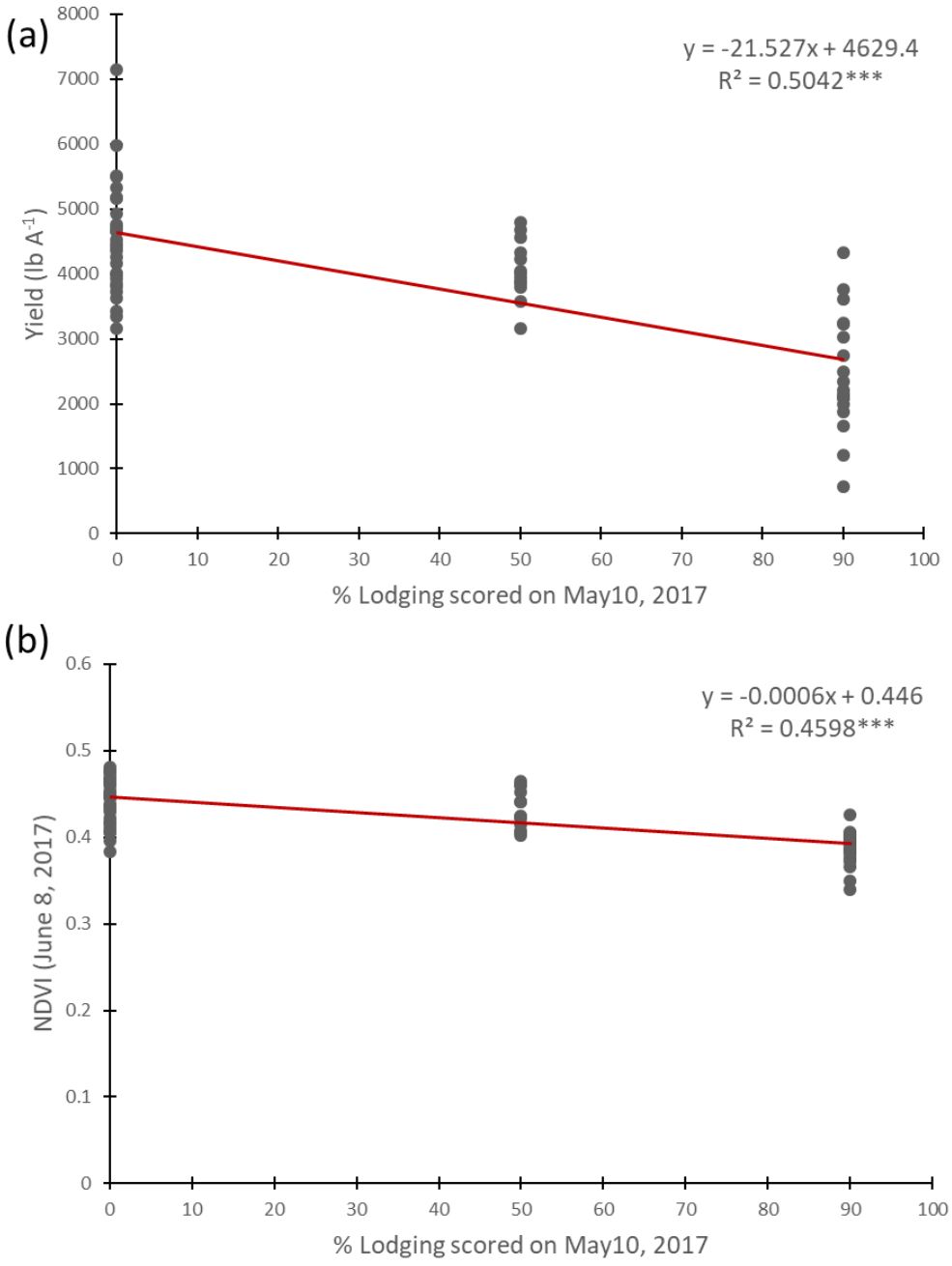

Figure 4-9 Relationship between stay green calculated from the image as NDVI and manually scored stay green (percentage of green leaves) during mid-grain filling. Triple asterisks (***) indicates the significance at the <0.001 level of probability.

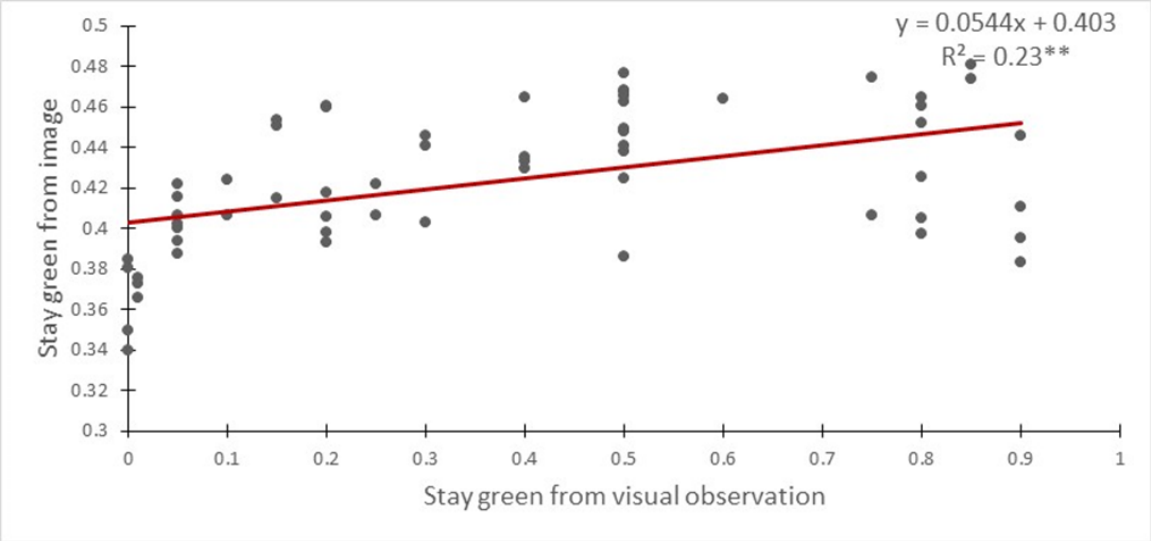

Figure 4-10 Correlation between Yield and stay green calculated as NDVI from the image and visual scoring (a) Relationship between yield (lb A^{-1}) and NDVI measured during the mid-grain filling period on June 8, 2017 (b) Relationship between yield (lb A^{-1}) and manually scored percentage of green leaves during the mid-grain filling period. Triple asterisks (***) indicates the significance at the <0.001 level of probability.

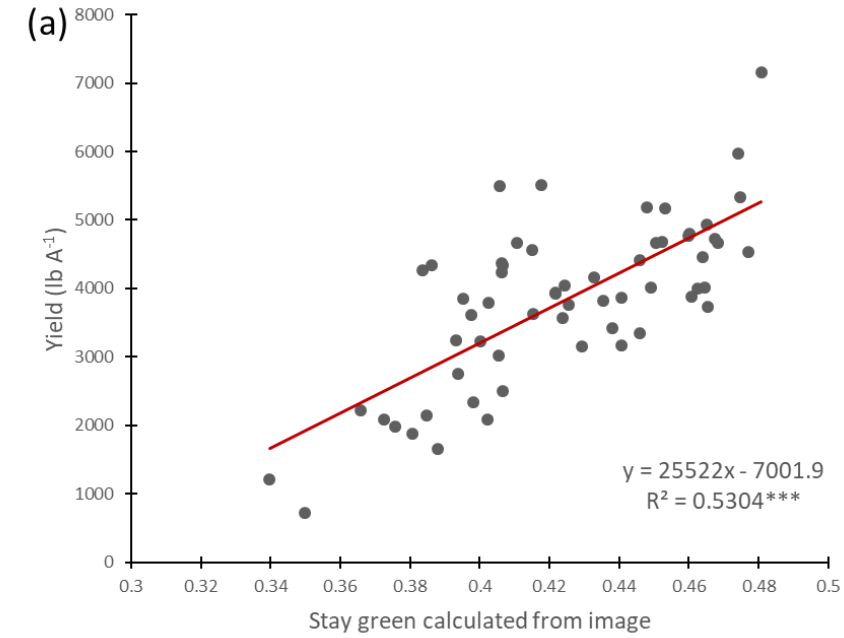

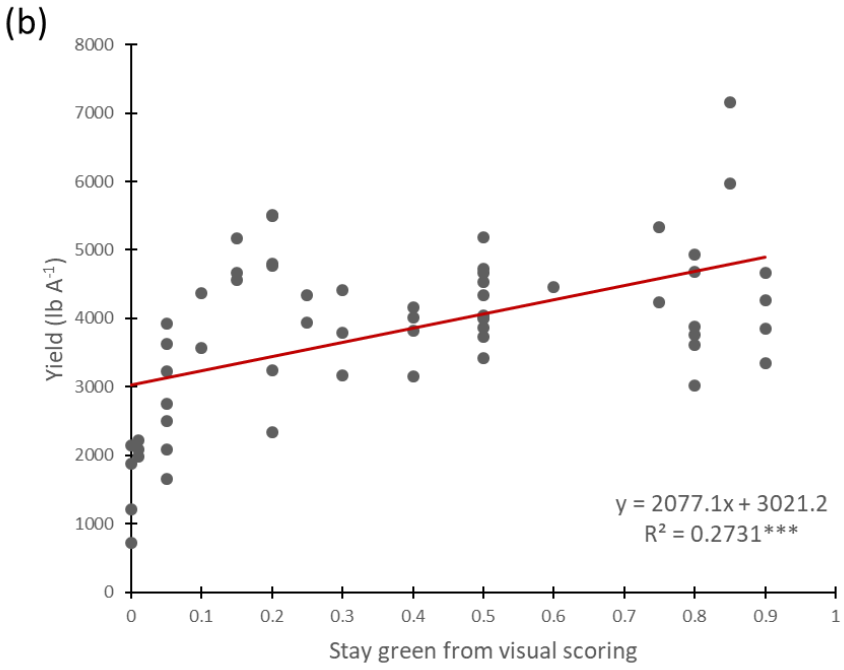

Table 4-1 List of 30 winter wheat varieties planted in 2015/2016 and 2016/2017 wheat growing season in western Kansas. Four varieties were different in two years because of the lack of seed. The different varieties in two years are marked in bold.

2015/2016	**2016/2017**
Antero	Antero
Armour	**Avery**
Bill Brown	**Bentley**
Billings	**SY Grit**
Brawl CL	Brawl CL
Byrd	Byrd
Clara CL	Clara CL
Danby	Danby
Everest	Everest
Fuller	Fuller
Gallagher	Gallagher
Iba	Iba
Joe	Joe
KanMark	KanMark
Tatanka	Tatanka
Larry	Larry
LCS Chrome	LCS Chrome
LCS Wizard	LCS Wizard
Santa Fe	**SY Sunrise**
SY Flint	SY Flint
SY Monument	SY Monument
SY Wolf	SY Wolf
T158	T158
TAM 111	TAM 111
TAM 112	TAM 112
TAM 114	TAM 114
Tiger	Tiger
WB 4458	WB 4458
WB Grainfield	WB Grainfield
Zenda	Zenda

Table 4-2 Planting details of experimental lines and varieties.

Year	Experimental lines	Varieties	Environments	Varieties Replications	Plot size
2016	400 (paired plots)	30 (paired plots)	2	6	3-row (0.84m x 2.44m)
2017	400	30 (paired plots)	2	4	6-row (1.68m x 3.81m)

Table 4-3 Images date available and general crop stages in western Kansas.

	2017			**2016**	
DOY	**Date**	**Crop stage**	**DOY**	**Date**	**Crop stage**
47	16-Feb	Prejointing			
61	2-Mar	Prejointing			
73	14-Mar	Jointing	67	7-Mar	Jointing
110	20-Apr	Early green up	99	8-Apr	Early green up
123	3-May	Early heading	104	13-Apr	Early green up
144	24-May	Late heading	116	25-Apr	Preheading
159	8-Jun	Mid-grainfill	153	1-Jun	Mid-grainfill
179	28-Jun	Senescence	162	10-Jun	Late grainfill

Table 4-4 Pearson correlation between NDVI measured at different days of year 2016 in 400 diverse wheat breeding lines and 30 released varieties. Correlation of water-limited environment are presented in the lower triangle and irrigated environment are in the upper triangle. Numbers in bold are statistically significant at 0.05 level of probability.

DOY	67	99	104	116	153	162
67		0.036	NA	**-0.25**	**-0.11**	**-0.2**
99	NA		NA	NA	**0.33**	**0.28**
104	**-0.28**	NA			NA	NA
116	**-0.21**	NA	**0.44**		**0.36**	**0.27**
153	0.01	NA	**0.14**	**0.32**		**0.29**
162	**-0.19**	NA	**0.15**	0.021	**0.19**	

Table 4-5 Pearson correlation between NDVI measured at different days of year 2017 in 400 diverse wheat breeding lines. Correlation of water-limited environment are presented in the lower triangle and irrigated environment are in the upper triangle.

DOY	73	110	144	159
73		-0.13423	-0.52324	-0.16027
110	-0.68355		0.563366	0.308146
144	-0.56351	0.64809		0.412388
159	-0.26494	0.271934	0.362714	